

School of Agriculture, Engineering and Science



**UNIVERSITY OF
KWAZULU-NATAL**

**INYUVESI
YAKWAZULU-NATALI**

**Design and Analysis of a Multi-Trailer System for the Durban
Container Terminal**

Theo Govender - 209508046

In fulfilment of the MSc-Eng. Degree in Mechanical Engineering

March 2018

Supervisor: Dr. Michael Brooks

Co-Supervisor: Dr. Clinton Bemont

Preface

The research contained in this *Design and Analysis of a Multi-Trailer System for the Durban Container Terminal* was completed by the candidate whilst based in the Discipline of Mechanical Engineering, School of Agriculture, Engineering and Science, University of KwaZulu-Natal, Howard College, South Africa.

The contents of this work have not been submitted in any form to another university and, except where the work of others is acknowledged in the text, the results reported are derived from investigations undertaken by the candidate.

As the candidate's Supervisor, I agree to the submission of this thesis;

Signed: Dr. M Brooks

Date:

Declaration - Plagiarism:

I, **Theo Govender** declare that:

- (i) The research reported in this dissertation is my original work, except where otherwise indicated.
- (ii) This dissertation has not been submitted for any degree or examination at any other university.
- (iii) This dissertation does not contain other persons' data, pictures, graphs or other information, unless specifically acknowledged.
- (iv) This dissertation does not contain another persons' writing, unless specifically acknowledged:
 - a) Where other written sources have been quoted, their words have been re-written but the general information attributed to them has been referenced.
 - b) Where exact words are used, the writing is placed inside quotation marks, and referenced.
- (v) Where I have reproduced a publication of which I am the author, co-author or editor, I have indicated in detail which part of the publication was written by myself alone and have fully referenced the publication.
- (vi) This dissertation does not contain text, graphics or tables copied and pasted from the Internet, unless specifically acknowledged.

Signed:

Date:

Place:

Acknowledgements

I wish to thank my supervisors, Dr Michael Brooks and Dr Clinton Bemont, for their continuous guidance and support which enabled me to complete this study. Your experience and expertise has been invaluable throughout this journey.

I also extend my sincere gratitude to the following people:

The operational staff at the Durban Container Terminal, who were ever willing to impart their knowledge on the terminals operations which proved vital for this study.

My family, for always believing in me and my ability to complete this dissertation. Mom and Dad, your support goes beyond words.

Lastly, to my Lord and Saviour Jesus Christ, thank you for your wisdom and grace which empowers me to keep going and never give up.

Abstract

Multi-trailer systems (MTS) allow for the transportation of multiple shipping containers in a single movement as opposed to the conventional trailer systems often used within a port terminal environment. The adoption of MTSs creates an opportunity for container terminal operators to reduce the operational costs associated with container movements between the container vessel and stacking areas during the vessel loading and unloading operations while maintaining, and in certain cases improving, the port's quayside productivity. A reduction in operational costs can potentially result in lower tariffs levied to container vessel operators, improving the competitiveness of a port.

While MTSs have been in existence for many years and have been successfully implemented in many international port container terminals, the influence of this type of trailer on the operational costs of the waterside horizontal-transport system and on the quayside productivity within South African ports has not been investigated or demonstrated to date. This study set out to determine the influence which an indigenously designed MTS has on the abovementioned factors at South Africa's largest container port, the Durban Container Terminal.

Discrete event simulations were used to benchmark the current performance of the container movement operations at Pier One of the Durban Container Terminal using the existing tractor-trailer units (TTUs). The performance of the operations was then analysed for the scenario of replacing the TTUs with MTSs that have twice the container carrying capacity. The results showed that nine MTSs can replace the existing fleet of fifteen TTUs without compromising on the quayside performance for the vessel unloading operations, which leads to a 25% reduction in operational costs. A reduction in labour costs accounts for 88% of the saving. Use of MTSs for the vessel loading operations showed minimal benefit and the performance using the existing TTUs for this operation can be considered equivalent. The results imply that an MTS configuration with the ability to uncouple the individual trailers in the set for use as TTUs was required. This led to the selection of a semi-trailer lead MTS configuration incorporating the use of a converter dolly for the indigenous design conducted here.

The indigenous MTS design consisted of two identical semi-trailers connected using a converter dolly, allowing for interchangeability in the MTS set and for use of the semi-trailers as TTUs. The terminal's existing semi-trailers could have been used with the converter dolly designed in this study for the MTS, however an improved semi-trailer design with regards to mass, cost and manoeuvrability has been provided. The new semi-trailer design was shown to have a 21.4% lower tare mass and a 14.1% lower product manufacturing cost over the existing design. For the MTS configuration, up to an 11.6% improvement in manoeuvrability is expected when using the newly designed semi-trailer.

Contents

Preface	i
Declaration - Plagiarism:	ii
Acknowledgements	iii
Abstract	iv
List of Figures:	ix
List of Tables:	xii
List of Acronyms and Abbreviations:	xiii
1 Introduction	1
1.1 Port Container Terminals	1
1.2 Operational Costs of Port Container Terminals	2
1.3 The Waterside Horizontal-Transport System	3
1.3.1 Background	3
1.3.2 Multi-Trailer Systems	4
1.4 The Durban Container Terminal	6
1.5 Research Objectives	8
1.6 Report Layout	9
2 Container Terminal Operation	10
2.1 Introduction	10
2.2 Background	10
2.3 Container Handling Equipment	11
2.3.1 Quay Cranes	11
2.3.2 Trailer Systems	11
2.3.3 Rubber Tyre Gantry Cranes	12
2.4 Durban Container Terminal - Pier One Operation	13
2.4.1 Vessel Unloading Procedure	14
2.4.2 Vessel Loading Procedure	14
2.5 Research Methodology	15
2.6 Chapter Summary	15
3 Container Movement Simulation Model	16
3.1 Introduction	16
3.2 Existing Port Terminal Simulation Studies	16
3.3 The Discrete Event Simulation Model	18
3.3.1 Introduction	18
3.3.2 Model Structure	18
3.3.3 Data Collection	18

3.3.4	Model Input Parameters	19
3.3.5	Vessel Unloading Model.....	21
3.3.6	Vessel Loading Model	22
3.3.7	Model Assumptions	27
3.3.8	Results.....	27
3.3.8.1	Model Verification and Validation	27
3.3.8.2	Vessel Unloading Model Results.....	29
3.3.8.3	Vessel Loading Model Results	30
3.3.8.4	Results Discussion	31
3.4	Preliminary Operational Cost Comparison	32
3.5	Chapter Summary	34
4	Multi-Trailer Design Considerations	35
4.1	Introduction.....	35
4.2	Multi-Trailer System Configuration	35
4.2.1	System Types	35
4.2.2	System Evaluation and Selection.....	37
4.3	Design Requirements	39
4.3.1	Port Terminal Requirements	39
4.3.2	Structural Requirements.....	40
4.3.2.1	Trailer Standards.....	41
4.3.2.2	Design Methods Used by Trailer Manufacturers	42
4.3.2.3	Trailer Design Studies.....	43
4.3.2.4	Load Case Selection.....	46
4.3.3	Manoeuvrability	48
4.4	Material Selection	51
4.4.1	Structural Steel.....	51
4.4.2	High Strength Steel	52
4.4.3	Material Comparison.....	53
4.5	Standard Components	54
4.5.1	Axles	54
4.5.2	Suspension	55
4.5.3	Rims and Tyres	56
4.5.4	Couplings	56
4.6	Chapter Summary	57
5	Multi-Trailer System Design	58
5.1	Introduction.....	58
5.2	Terminal Tractor	58

5.3	System Configuration	60
5.4	Semi-Trailer Design.....	60
5.4.1	General Structural Arrangement	60
5.4.2	Longitudinal Centre Beams	61
5.4.3	Container Supports.....	68
5.4.4	Kingpin Setback.....	71
5.4.5	Auxiliary Structures	72
5.4.5.1	Lower Cross-Bracing	72
5.4.5.2	Towing Hitch Mounting.....	73
5.4.5.3	Landing Gear	73
5.4.5.4	Rear-Underrun Protection Device.....	73
5.4.6	Bogie Assembly Position.....	74
5.4.7	Coupling D-Values	76
5.4.8	Semi-Trailer Structural Analysis	77
5.4.8.1	Finite Element Model.....	77
5.4.8.2	Vertical Load Case.....	79
5.4.8.3	Longitudinal Braking Load Case	84
5.4.8.4	Longitudinal Acceleration Load Case.....	85
5.4.8.5	Lateral Load Case	87
5.4.9	Semi-Trailer Final Design.....	89
5.5	Converter Dolly Design	90
5.5.1	General Structural Arrangement	90
5.5.2	Chassis Structure.....	91
5.5.3	Fifth Wheel Assembly	92
5.5.4	Bogie Assembly	92
5.5.5	Drawbar Arrangement.....	93
5.5.6	Coupling D-Values	94
5.5.7	Converter Dolly Structural Analysis.....	94
5.5.7.1	Finite Element Model.....	94
5.5.7.2	Vertical Load Case.....	95
5.5.7.3	Longitudinal Braking Load Case	97
5.5.7.4	Longitudinal Acceleration Load Case.....	99
5.5.7.5	Lateral Load Case	101
5.5.8	Converter Dolly Final Design	103
5.6	Complete Multi-Trailer System	103
5.7	Chapter Summary	104
6	Turning Analysis.....	105

6.1	Introduction.....	105
6.2	Equivalent Wheelbase for the Tractrix Method.....	105
6.3	BricsTurn® Simulation.....	107
6.3.1	Method Validation.....	107
6.3.2	Input Data.....	110
6.3.3	Turning Manoeuvres.....	111
6.4	Chapter Summary.....	113
7	System Comparison.....	114
7.1	Introduction.....	114
7.2	Comparison.....	114
7.2.1	Mass.....	114
7.2.2	Product Manufacturing Cost.....	115
7.2.3	Turning Performance.....	115
7.3	Operational Cost Comparison.....	118
8	Discussion.....	121
9	Conclusion.....	127
10	References.....	129
	Appendix A - MTS General Assembly.....	137
	Appendix B - Tractive Effort Calculations.....	140
	Appendix C – Critical Weld & D-Value Calculations.....	141
	Appendix D – MTS Coupling Specifications.....	143
	Appendix E - Cost Breakdown.....	145

List of Figures:

Figure 1.1: Schematic illustration of horizontal-transport vehicles. (a) Tractor-trailer unit (TTU).	3
Figure 1.2: Semi-trailer led MTS	4
Figure 1.3: The effect of MTSs on time quality indicator for a ship-to-stack distance of 500 m.	5
Figure 1.4: The effect of MTSs on time quality indicator for a ship-to-stack distance of 1250 m.	5
Figure 1.5: The Durban Container Terminal	6
Figure 1.6: Satellite image of Pier One.....	7
Figure 1.7: Average terminal handling charges (US\$), 2012	7
Figure 2.1: General operation of a container terminal	10
Figure 2.2: QCs positioned to move containers off and onto vessels	11
Figure 2.3: Existing tractor-trailer unit used at the Durban Container Terminal.....	12
Figure 2.4: Three-trailer MTS at the Port of Manila	12
Figure 2.5: RTG stacking containers	13
Figure 2.6: Pier One yard layout at the Durban Container Terminal.....	13
Figure 3.1: Distribution summary for the QC cycle time – vessel unloading.....	20
Figure 3.2: Distribution summary for the QC cycle time – vessel loading.....	20
Figure 3.3: Paths followed by the TTUs and MTSs	22
Figure 3.4: Overview of the unloading model using TTUs	23
Figure 3.5: Model architecture for the vessel unloading procedure using TTUs.....	24
Figure 3.6: Overview of the loading model using TTUs: QC1-Block A2 Pair	25
Figure 3.7: Model architecture for the vessel loading procedure using TTUs.....	26
Figure 3.8: Run controller tool and animation in Arena™	28
Figure 3.9: Average QC productivity – unloading model.....	30
Figure 3.10: Average trailer fleet utilisation	30
Figure 3.11: Average QC productivity – Loading model	31
Figure 4.1: Semi-trailer lead MTS	36
Figure 4.2: Drawbar-trailer lead MTS	36
Figure 4.3: Drawbar connection to the tractor	36
Figure 4.4: Semi-trailer lead MTS with a converter dolly	38
Figure 4.5: Converter dolly	38
Figure 4.6: Converter dolly connecting two trailers	38
Figure 4.7: Off-tracking and swept path	49
Figure 4.8: Maximum low speed off-tracking for a TTU	49
Figure 4.9: Trailer geometric parameters	50
Figure 4.10: Swing clearance	51
Figure 4.11: GO Heavy Duty Axle	54

Figure 4.12: GO Heavy Duty Tandem Suspension - over slung configuration for semi-trailer	55
Figure 4.13: GO Heavy Duty Tandem Suspension - under slung configuration for converter dolly ..	56
Figure 5.1: Kalmar TR626i terminal tractor	59
Figure 5.2: Notional MTS configuration	60
Figure 5.3: Container terminal semi-trailer	61
Figure 5.4: I-section parameters	63
Figure 5.5: Longitudinal centre beam - Web dimensions	63
Figure 5.6: Imposed loads on the longitudinal beam	64
Figure 5.7: Bending moment diagram – longitudinal centre beams	65
Figure 5.8: Shear force diagram – longitudinal centre beams	66
Figure 5.9: Effect of flange and web thicknesses on the overall mass of the longitudinal beam	67
Figure 5.10: Preliminary longitudinal beam design.....	68
Figure 5.11: Orientation of the container-supporting cross members.....	69
Figure 5.12: Guide profiles	70
Figure 5.13: Cross members and guides assembled to the longitudinal beams	70
Figure 5.14: Side view of the kingpin-skid plate assembly	72
Figure 5.15: Aerial view of the kingpin-skid plate assembly	72
Figure 5.16: Mounting of the towing hitch to the semi-trailer chassis	73
Figure 5.17: Load transfer analysis for bogie positioning	75
Figure 5.18: Reaction loads for the MTS	76
Figure 5.19: Meshed semi-trailer geometry	78
Figure 5.20: Full finite element model representation.....	78
Figure 5.21: von-Mises stress plot for the semi-trailer vertical load case – top view.....	79
Figure 5.22: von-Mises stress plot for the semi-trailer vertical load case – bottom view.....	80
Figure 5.23: High stress regions on the skid plate and the longitudinal beams webs	80
Figure 5.24: Scaled deformation of the high stress region.....	81
Figure 5.25: Additional bracing of the skid plate to minimise bending.....	81
Figure 5.26: von-Mises stress plot of the skid plate with the added bracing – top view	82
Figure 5.27: von-Mises stress plot of the skid plate with the added bracing – bottom view	82
Figure 5.28: Finalised von-Mises stress plot for the semi-trailer vertical load case – top view	83
Figure 5.29: Finalised von-Mises stress plot for the semi-trailer vertical load case – bottom view	83
Figure 5.30: von-Mises stress plot for the semi-trailer braking load case – top view	84
Figure 5.31: von-Mises stress plot for the semi-trailer braking load case – bottom view	85
Figure 5.32: Localised high stress region at the web-skid plate bracing interface	85
Figure 5.33: von-Mises stress plot for the semi-trailer accelerating load case – top view	86
Figure 5.34: von-Mises stress plot for the semi-trailer accelerating load case – bottom view	86
Figure 5.35: Localised high stress at the corners of the cross member.....	87

Figure 5.36: von-Mises stress plot for the semi-trailer lateral load case – top view.....	88
Figure 5.37: von-Mises stress plot for the semi-trailer lateral load case – bottom view.....	88
Figure 5.38: Finalised semi-trailer design.....	89
Figure 5.39: Converter dolly – structural arrangement.....	90
Figure 5.40: Converter dolly chassis.....	91
Figure 5.41: Fifth wheel assembly fitted to chassis	92
Figure 5.42: Bogie assembly utilising pedestals for connection to the chassis (tyres hidden)	93
Figure 5.43: Drawbar design.....	93
Figure 5.44: Meshed converter dolly geometry	95
Figure 5.45: Finite element model representation.....	95
Figure 5.46: von-Mises stress plot for the converter dolly vertical load case – top view	96
Figure 5.47: von-Mises stress plot for the converter dolly vertical load case – bottom view.....	96
Figure 5.48: Localised high stress regions for the vertical load case.....	97
Figure 5.49: von-Mises stress plot for the converter dolly braking load case – top view.....	98
Figure 5.50: von-Mises stress plot for the converter dolly braking load case – bottom view	98
Figure 5.51: Localised high stress regions at the corner of the mounting plate support members	99
Figure 5.52: von-Mises stress plot for the converter dolly accelerating load case – top view.....	100
Figure 5.53: von-Mises stress plot for the converter dolly accelerating load case – bottom view	100
Figure 5.54: Localised high stress at the corners of the square sections of the drawbar hinge.....	101
Figure 5.55: von-Mises stress plot for the converter dolly lateral load case – top view.....	102
Figure 5.56: von-Mises stress plot for the converter dolly lateral load case – bottom view.....	102
Figure 5.57: Localised high stress at the drawbar hinge corners	102
Figure 5.58: Finalised converter dolly design.....	103
Figure 5.59: Completed MTS design.....	103
Figure 6.1: Equivalent wheelbase for a three-axle rigid truck	106
Figure 6.2: Turning path for 33D double-trailer combination	108
Figure 6.3: Turning path for 30T triple-trailer combination	108
Figure 6.4: BricsTurn [®] swept path plots for the for 33D double-trailer combination	109
Figure 6.5: BricsTurn [®] swept path plots for the for 30T triple-trailer combination	109
Figure 6.6: BricsTurn [®] input data for the MTS’s turning analyses	110
Figure 6.7: Double 90 ⁰ turn with central exit-entry of storage blocks.....	111
Figure 6.8: Worst case exit-entrance of adjacent storage blocks (underneath RTG).....	112
Figure 6.9: Entering a stacking area (blocks A1 to G1) centrally vs. underneath an RTG.....	112
Figure 6.10: Entering blocks A1, A2 and A3 underneath an RTG during vessel loading	113
Figure 7.1: Double 90 ⁰ turn – central exit and entry showing the swept path difference	116
Figure 7.2: Double 90 ⁰ turn – exit and entry underneath RTG showing the swept path difference ...	117
Figure 7.3: 180 ⁰ turn – Entry into block A underneath RTG showing the swept path difference	117

Figure 8.1: Localised high stress error confirmed using the Structural Error Tool in ANSYS® 124

List of Tables:

Table 3.1: Summary of the simulation model input parameters	19
Table 3.2: A comparison of measured and simulated results.....	29
Table 3.3: Durban Container Terminal’s operational cost parameters	32
Table 3.4: Equipment cost per shift (loading and unloading)	33
Table 3.5: Fuel cost per shift.....	33
Table 3.6: Maintenance cost per shift	33
Table 3.7: Labour cost per shift	34
Table 3.8: Total operating cost per shift	34
Table 4.1: Design load cases & design/safety factors used by trailer manufacturers	43
Table 4.2: Transnet Engineering’s trailer design requirements	43
Table 4.3: Trailer design load cases proposed by Dwarika	46
Table 4.4: Load cases for the present MTS design	47
Table 4.5: Mechanical properties of structural steel grades	52
Table 4.6: Mechanical properties of HSLA steel grades	52
Table 4.7: Material evaluation matrix.....	53
Table 5.1: ISO Container external dimensions and maximum gross mass	62
Table 5.2: Longitudinal beam load parameters.....	65
Table 5.3: Flange and web thickness combinations.....	67
Table 5.4: Rear-underrun protection device dimensions	74
Table 6.1: Comparison of BricsTurn® and AASHTO swept path radii for the 33D and 30T trailers	107
Table 7.1: Mass comparison of the semi-trailer designs.....	114
Table 7.2: Product manufacturing cost comparison for the MTS using each semi-trailer design	115
Table 7.3: Swept path comparison for the MTS using each semi-trailer design	118
Table 7.4: Equipment cost per shift (loading and unloading)	119
Table 7.5: Maintenance cost per shift (loading and unloading).....	119
Table 7.6: Fuel cost per shift (October 2017)	119
Table 7.7: Total operating cost per shift	120

List of Acronyms and Abbreviations:

ADR - Australian Design Rule

AGV - Automatic Guided Vehicle

CCRED - Centre for Competition, Regulation and Economic Development

CTR - Centreline Turn Radius

DES - Discrete Event Simulation

ERLA - Erlang probability function

FE - Finite Element

FEA - Finite Element Analysis

ft. - Foot

g - Gravitational acceleration constant

GCM - Gross Combinational Mass

ISO - International Organisation for Standardisation

LOGN - Lognormal probability function

MTS - Multi-Trailer System

QC - Quay Crane

RTG- Rubber Tyre Gantry

SANS - South African National Standards

SC - Straddle Carrier

TEU - Twenty Foot Equivalent Unit

TQI - Time Quality Indicator

TTU - Tractor-Trailer Unit

WEIB - Weibull probability function

1 Introduction

1.1 Port Container Terminals

Port container terminals are designed for the handling and temporary storage of containerised cargo, where containers are loaded and unloaded from one mode of transport to another for the cargo to reach its intended destination. Intermodal containers, which are uniform steel boxes used for stowing various types of cargo, were introduced into the market for intercontinental transportation of sea freight 50 years ago and have proven to be the most economical method for packing cargo intended for transportation via sea [1]. Port container terminals utilise various handling equipment to facilitate container movement between a vessel (ship) and the container terminal's storage yard, such as quay cranes (QCs), trailer systems, rubber tyre gantry cranes (RTGs) and straddle carriers (SCs).

Studies show that in 1985, 4.9 million TEU (twenty-foot equivalent unit¹) containers were in circulation world-wide and that by 1995 this figure had almost doubled to 9.2 million [2]. Today, there are more than 30 million TEU containers in active circulation being transported by nearly 5000 container vessels [3], with the number of containers expected to increase annually by 8.5% [4].

The growing number of container shipments creates increased competition for business between port container terminals, especially those in close geographic proximity. This in turn places increased demands on the container terminals with respect to container logistics, management of the terminal and the constant innovation in so far as container handling equipment is concerned [2]. The competitiveness of a port container terminal hinges on two main factors which are taken into consideration by ocean carriers, as well as hinterland trucking and railway services when selecting a container terminal [5, 6]:

1. The total time spent at a port by a container vessel (transshipment time).
2. The service rates charged for unloading and loading a vessel.

A container terminal has an advantage over its competitors when it has a low handling turnaround time for the containers, which directly relates to a reduced transshipment time for container vessels, coupled with low service charges for the movement of the containers onto and off a vessel.

¹ A TEU is an approximate unit of cargo capacity based on the volume of a 20-foot-long (6.1 m) intermodal container.

1.2 Operational Costs of Port Container Terminals

The operational costs associated with the daily functioning of port container terminals have a direct impact on the service charges levied to container vessel operators. While fuel prices have fallen in recent times, numerous port terminals have raised container handling charges which results in intermodal costs making up more than 50% of a vessel's voyage operating cost, thus posing a major challenge for container vessel operators [7]. The rise in service charges levied by container terminal operators can be attributed partially to increases in labour and service costs, equipment maintenance costs, energy costs and administrative overheads year-on-year [8].

The United Nations Economic and Social Commission for Asia and the Pacific (ESCAP/UNDP) has developed a model tariff structure consisting of four groups that account for the costs associated with operating a port container terminal i.e. the navigation service, the berthing service, the cargo service, and "other" business services. Each of these groups contain multiple services associated with several port operations [9]. Seedah *et al.* showed that the cost associated with a single vessel calling at a port terminal can be represented by Equation (1.1) [10]:

$$C_T = C_N + C_B + C_C + C_O \quad (1.1)$$

Where: C_T = total cost of the vessel call

C_N = costs associated with navigational services

C_B = costs associated with berth services

C_C = costs associated with cargo operations

C_O = all other costs not captured in any of the variables above

The navigation service includes pilotage and tug services. Berth services, which are regarded as the interface between the marine transport and inland transport at a port, include berth hire and handling using terminal handling equipment such as QCs, trailer systems, SCs and RTGs. Cargo operations include activities and services such as storage and handling of cargo into and out of the port which includes cargo transfer via road trucks and rail. Other costs such as port security, management services, and provision of utilities are necessary for the overall management and operations of the port and fall under "other" business services; they are relatively minor in comparison with the other categories. Determining the exact total cost of a vessel call is complex in nature and varies among ports based on the number of operations associated with a vessel calling, however the generalised model represented by Equation (1.1) provides a relatively good estimate for comparative purposes [10]. Seedah *et al.* [10] showed that berthing service costs can make up almost 40% of the total cost of the vessel call, indicating that a terminal's operational cost surrounding vessel docking duration and the use of terminal handling equipment for container transfer between the vessel and storage area forms a key component in

determining the service tariffs levied to container vessel operators. The efficiency of berthing services thus heavily influences the competitiveness of the container terminal.

1.3 The Waterside Horizontal-Transport System

1.3.1 Background

The waterside horizontal-transport system forms the interface between the ship-to-shore system and the storage system of a port container terminal. The horizontal transport equipment generally utilised by container terminals are SCs, automated guided vehicles (AGVs) and tractor-trailer units (TTUs). When a container vessel calls at a port and is allocated to a berth, QCs (which forms the ship-to-shore system) are used to unload containers from the vessel and transfer them to the waterside horizontal-transport system. The performance objective of waterside horizontal-transport system is efficient, smooth and fast transfer of containers between the QCs and the storage yard of the container terminal [11]. SCs are classified as active vehicles as they are fitted with container lifting devices which allow them to load and unload containers themselves from the terminal's storage area. TTUs and AGVs are classified as passive vehicles as they require the assistance of other terminal equipment for loading and unloading containers [12]. TTUs and AGVs have a safe working load capacity of two TEUs; SCs can carry one 20-foot container, one 40-foot container or two 20-foot containers simultaneously, depending on the lifting device. Figure 1.1 shows an illustration of the horizontal-transport vehicles described.

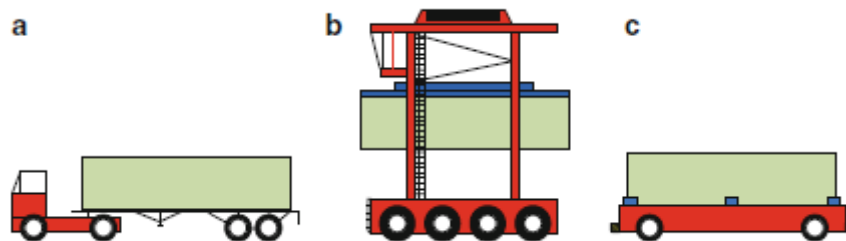


Figure 1.1: Schematic illustration of horizontal-transport vehicles. (a) Tractor-trailer unit (TTU). (b) Straddle carrier (SC). (c) Automated-guided vehicle (AGV). [12]

1.3.2 Multi-Trailer Systems

A multi-trailer system (MTS) allows for the transportation of multiple containers using a single tractor as opposed to the traditional TTU vehicle configuration. An MTS consists of a tractor that pulls several trailers, each trailer having a carrying capacity of two TEUs. Port terminal operators consider the use of MTSs as a potentially attractive option for increasing port terminal efficiency by decreasing operational costs for the waterside-horizontal transport subsystem while maintaining, or even potentially increasing, QC productivity and hence reducing vessel berthing time. In recent times, European container terminal operators have implemented MTSs with two to three trailers in a set for the short distance vessel to stacks operation as a method of increasing container transportation efficiency [13]. Figure 1.2 below depicts a three-trailer MTS at the Port of Manila with a carrying capacity of 6 TEUs.



Figure 1.2: Semi-trailer led MTS [14]

A study conducted by Goussiater [13] on the efficiency of MTSs for vessel to stacks container transportation using discrete event simulation (DES) modelling showed that the use of MTSs can lead to a higher gross QC productivity by reducing the delay between trailer arrivals at the QCs, hence reducing vessel berthing time. Of more significance was his finding that MTSs can achieve the same QC productivity levels as TTUs, but with fewer vehicles in the fleet, leading to a lower operating cost for the waterside horizontal-transport system. The study also showed that a two trailer MTS gives the greatest fleet reduction margin (while maintaining QC productivity) between incrementally longer MTS systems where the length of the trailer set is longer by one trailer. Similar results could be expected for other container terminals using trailer systems. This relationship is depicted in Figure 1.3 and Figure 1.4 for a varying distance between the vessel and storage area. The time quality index (TQI) is a direct measure of QC productivity used in the study, defined by Equation (1.2), where Td is the QC average cycle time and Tw the average time between trailer arrivals at the QC [13]. A 100% TQI is achieved when the delay between trailer arrivals at the QC is reduced to zero, maximising their productivity.

$$TQI = \frac{Td}{Td + Tw} \quad (1.2)$$

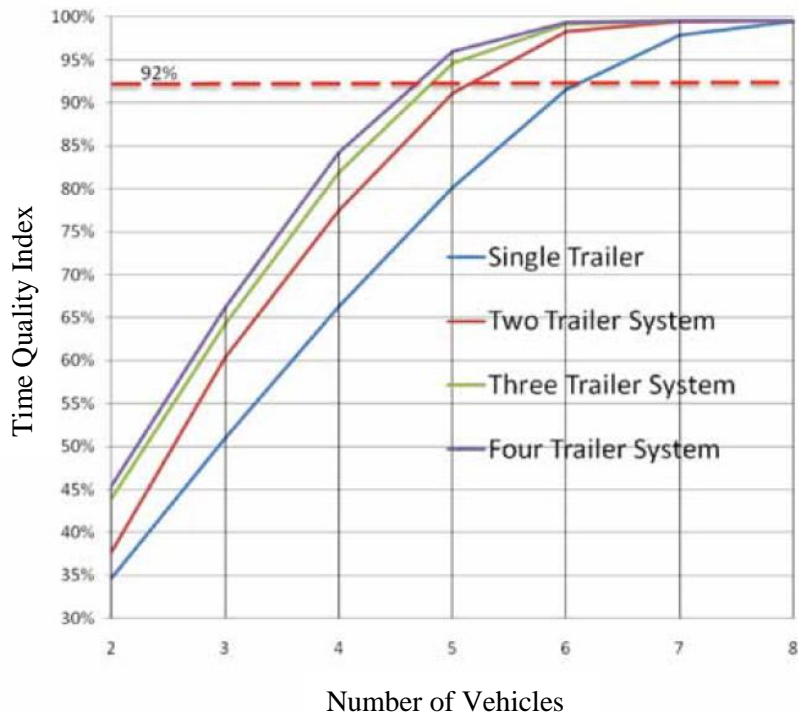


Figure 1.3: The effect of MTSS on time quality indicator for a ship-to-stack distance of 500 m. [13]

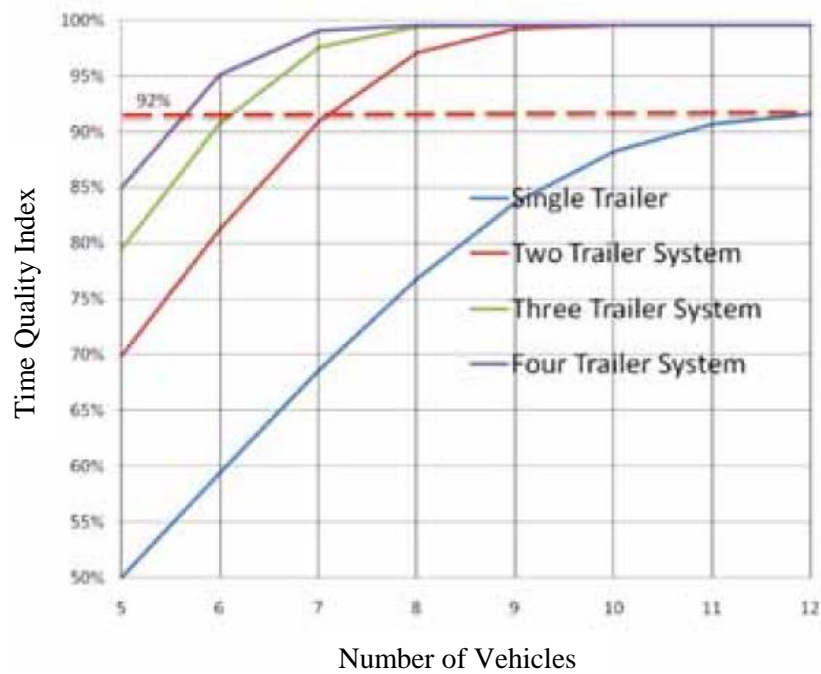


Figure 1.4: The effect of MTSS on time quality indicator for a ship-to-stack distance of 1250 m. [13]

1.4 The Durban Container Terminal

The Port of Durban, which has the largest container terminal in the southern hemisphere, has seen continuous growth from 72000 containers handled per year in 1979, to the current volumes of TEUs exceeding 3.6 million a year [15]. The Durban Container Terminal, which forms part of the Port of Durban and is the largest container terminal in Africa, is divided into two areas which are Pier One and Pier Two. Pier One utilises TTUs to transport the containers between the QCs and the storage yard, where RTGs then transfer the containers between the trailer and the stacking area. The operation at Pier Two differs from Pier One in that straddle carriers are used as the transport vehicle between the QCs and the stacking area. Pier One has a total of three berths where vessels of up to 4,500 TEU can be safely accommodated. The Durban Container Terminal handles 69% of South Africa's national throughput of containerised cargo [16]. Figure 1.5 shows an aerial view of Pier One and Pier Two of the Durban Container Terminal. Figure 1.6 shows a satellite image of Pier one depicting the QCs, stacking areas and a berthed vessel. This study is concerned with the operations at Pier One only, where TTUs are employed.



Figure 1.5: The Durban Container Terminal [17]

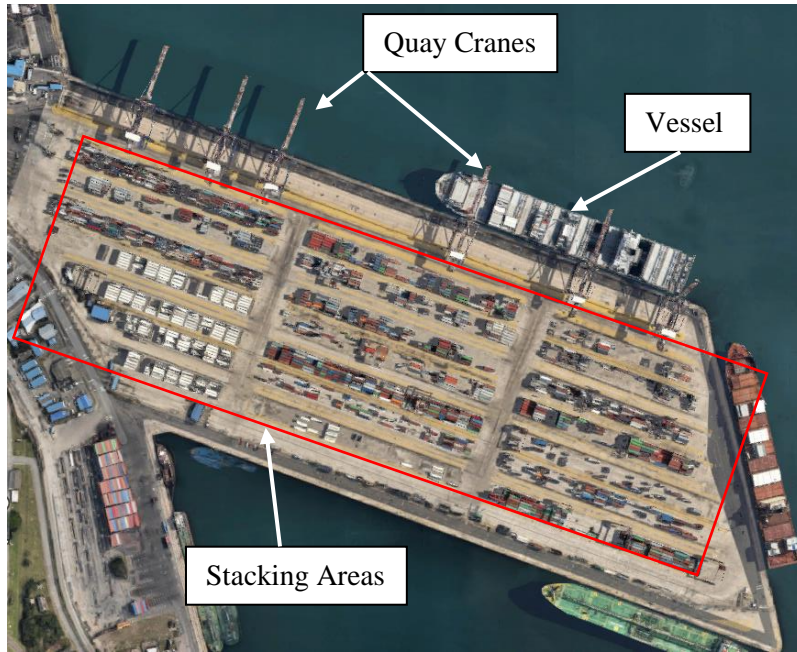


Figure 1.6: Satellite image of Pier One

In a 2012 study by the Centre for Competition, Regulation and Economic Development (CCRED), it was found that the average terminal handling charge per vessel call at the Durban Container Terminal was 84% higher than the global average [18], making it one of the most expensive terminals in the world. As can be seen in Figure 1.7, which shows the average terminal handling charges for 20 ports across the globe, the Durban Container Terminal charges US\$275,000 for an average vessel, significantly more than the global average price of US\$150,000 [18].

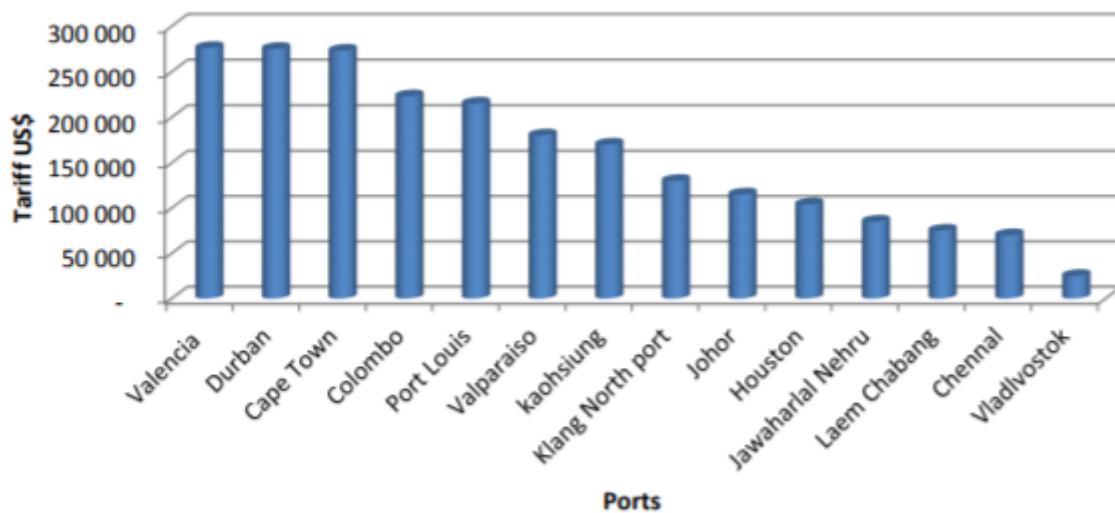


Figure 1.7: Average terminal handling charges (US\$), 2012 [19]

While the study acknowledges the difficulty of accurately comparing port charges because port pricing structures differ worldwide, it also states that “*South Africa’s port charges have been said to be among the most expensive in the world, and if correct this would undermine the government’s strategy to promote growth of the manufacturing sector and the export of manufactured goods*” and “*A concerted effort is required to reduce South African tariffs in order to stimulate economic development*” [18]. Research conducted by Simpson [20] shows that there is mixed evidence on the operational efficiency at the Port of Durban and that a reduction in operational costs coupled with an increase in the efficiency of the operations should be a key focus for the terminal. Inherently, reductions in operational costs as well as an increase in operational efficiency can potentially lead to reductions in the charges levied to container vessel operators while maintaining the profitability of a port terminal.

1.5 Research Objectives

This study set out to determine whether an indigenously designed two-trailer MTS can reduce operational costs of the waterside-horizontal system and increase productivity at Pier One of the Durban Container Terminal. Specifically, the study addresses the following objectives:

1. Characterise the existing container terminal operation at Pier One with respect to container movement.
2. Model the container operations to establish the effects of using an MTS fleet instead of the existing TTUs.
3. Propose a design of an indigenous MTS based on the results from (2) above.
4. Carry out a full analysis of the design and optimise with respect to mass, cost and manoeuvrability.

Numerous international port terminal operators use MTSs for the movement of containers between the vessel and stacking area, but to date, the use of MTSs within South African ports has not been demonstrated and the potential effects have not been investigated. Using vehicles that are capable of transporting a larger number of containers in a single movement may enable South African terminal operators to reduce labour and equipment costs without negatively affecting the terminal’s performance, but no study has been done in this regard and the Port of Durban has not considered the use of trailer systems capable of carrying more than two TEUs in the container terminal environment. Chapters 2 and 3 address this shortcoming.

While there are various internationally designed and manufactured MTSs available in the market, there is no locally developed product able to meet the technical and functional requirements for trailer equipment allowed to be operated in the Durban Container Terminal, therefore there exists an opportunity to implement an indigenous MTS design. A system which is designed and manufactured using predominantly locally available components not only adds to the capabilities and skills

development of the country, but is also in line with the South African Government's policies on localisation for economic growth [21]. The results from Chapters 2 and 3 serve as motivation for the proposed design of the MTS described in Chapters 4 to 7.

1.6 Report Layout

The layout of this dissertation is as follows:

- a) Chapter 2 presents relevant information about container terminal operation, container handling equipment and the vessel unload and loading procedures at the Durban Container Terminal. The research methodology and approach for carrying out this project are also described.
- b) Chapter 3 details a comparative study of the vessel loading and unloading procedure at the Durban Container Terminal for the conventional TTUs used versus a two-trailer MTS using discrete event simulation (DES) modelling.
- c) Chapter 4 discusses relevant trailer design methods and equipment which will be used in the design of a suitable MTS.
- d) Chapter 5 presents a detailed and indigenous MTS design suitable for the Durban Container Terminal.
- e) Chapter 6 presents a turning analysis for the designed MTS.
- f) Chapter 7 details a system comparison between the MTS designed and the TTUs used at the Port of Durban.
- g) Chapters 8 and 9 provide a discussion of the results and a conclusion of the study, respectively.

2 Container Terminal Operation

2.1 Introduction

In this chapter, the background on container terminal operation, container handling equipment and the container movement operations at Pier One are presented. It is drawn from the first part of the journal article published in the South African Journal of Industrial Engineering (SAJIE) by the author and supervisors (Govender *et al.*, 2017) [22]. The methodological approach followed for this study is also provided.

2.2 Background

Steenken *et al.* [2] defines a container terminal as “open systems of material flow with two external interfaces”. These two interfaces are the quayside where vessels are either loaded or unloaded with containers and the landside system where containers are loaded or unloaded from external trucks or trains. When a container vessel arrives at a port, it is assigned to a berth which is equipped with QCs. The QCs are used to load and unload containers to and from the vessel. Unloaded containers are transported to the storage yard using equipment such as TTUs. These containers are then picked up by external trucks or placed onto trains for transportation to their final destination. Containers to be exported are transported to the terminal by external trucks or trains where they are then placed into the storage yard. The containers are subsequently transported from the yard to the QCs where they are loaded onto the vessel. Figure 2.1 shows the general operation of a container terminal.

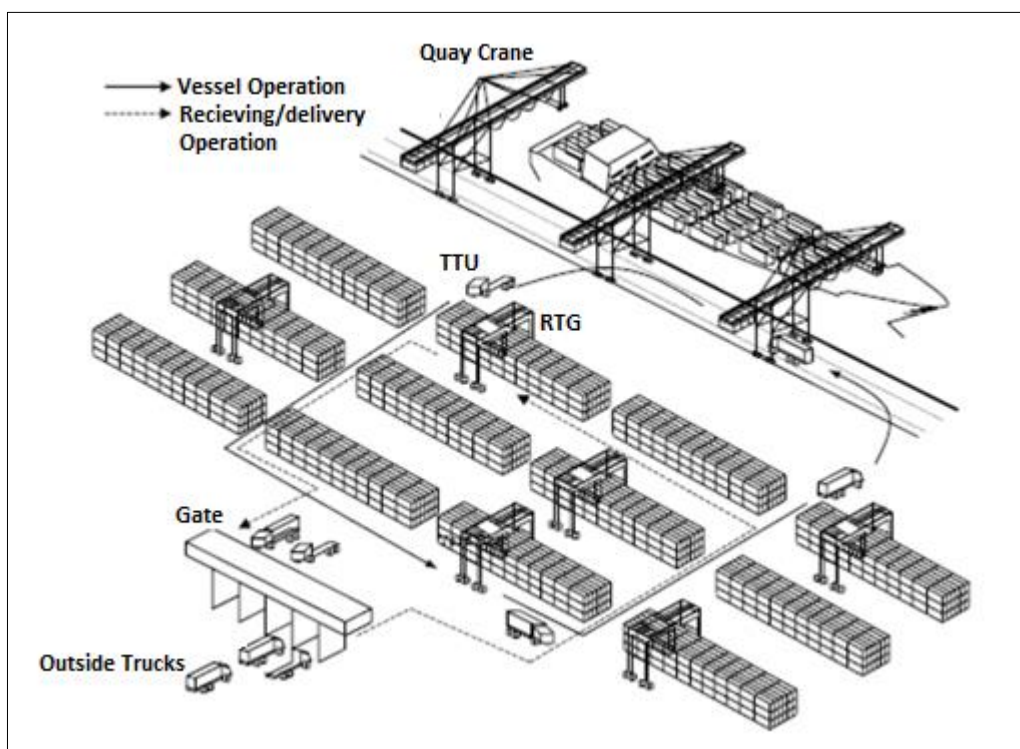


Figure 2.1: General operation of a container terminal [23]

2.3 Container Handling Equipment

2.3.1 Quay Cranes

A QC is a type of crane used at container terminals for the loading and unloading of containerised cargo from vessels. Unlike conventional cranes which utilise hooks, QCs are equipped with a handling device called a spreader that is lowered onto the top of a container and then locks into its four corner castings. QCs usually transport a single container during movements, however most modern QCs have the ability to move four TEUs at once (four 20 ft. containers or two 40 ft. containers). Figure 2.2 depicts multiple QCs in position, ready to move containers onto/off a vessel.

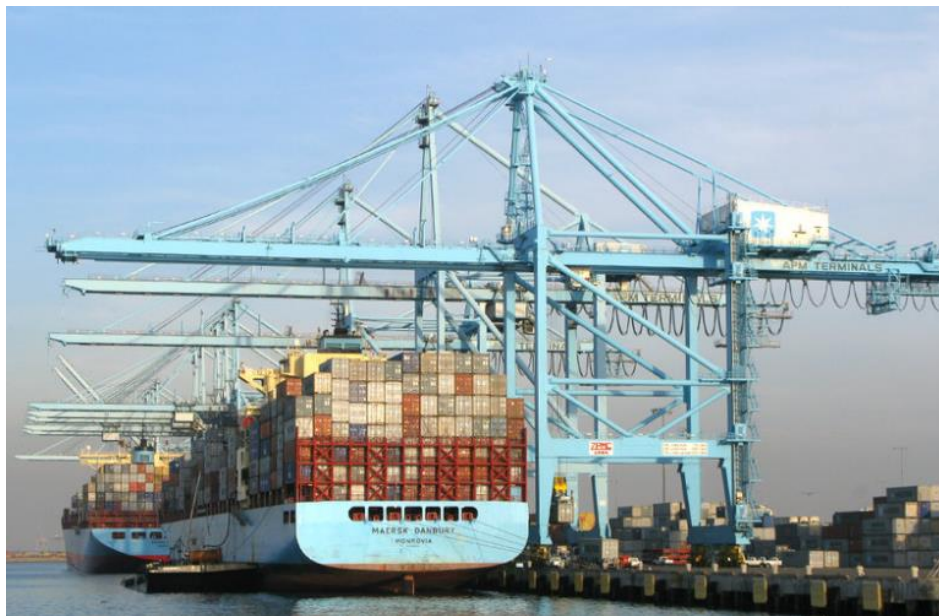


Figure 2.2: QCs positioned to move containers off and onto vessels [24]

2.3.2 Trailer Systems

Movement of containers between the QCs and the storage yard is achieved using equipment such as TTUs or MTSs. The trailers, which are generally of a skeletal type, are connected to terminal tractors. The tractors are designed for optimal speed-to-tractive-effort performance to move the heavy loads between the QCs and storage yard. As mentioned previously, trailer systems fall into the category of ‘passive’ vehicles since they are unable to lift containers by themselves. Figure 2.3 depicts a TTU used at the Durban Container Terminal, while Figure 2.4 shows a three-trailer MTS with a 6 TEU carrying capacity at the Port of Manila.



Figure 2.3: Existing tractor-trailer unit used at the Durban Container Terminal



Figure 2.4: Three-trailer MTS at the Port of Manila [14]

2.3.3 Rubber Tyre Gantry Cranes

For terminals using TTUs or MTSs as the horizontal transport medium, RTGs are used to lift and place containers from the stacking areas onto the trailers and vice versa. The stacking area of a container terminal is a temporary storage area for containers waiting to be loaded onto a vessel for export or imported containers waiting to be transported to their final destination by external trucks or train. Containers are stacked on top of each other to a maximum of five or six containers high depending on the height and span of the RTG used. Figure 2.5 depicts an RTG stacking containers.



Figure 2.5: RTG stacking containers [25]

2.4 Durban Container Terminal - Pier One Operation

Pier One of the Durban Container Terminal is an RTG terminal which utilises TTUs as the horizontal transport medium between the vessel and stacking area. Pier One has a total of three berths - 105 to 107. A vessel is said to be at berth 106 when it is positioned midway between berths 105 and 107. A total of six QCs service the three berths. The QCs and the RTGs at Pier one are fitted with single lifting devices which can only lift one container at a time. The storage yard for Pier One has 21 storage blocks (block A1 to G3) where containers are stacked five-high and six-wide. Figure 2.6 shows the yard layout of Pier One.

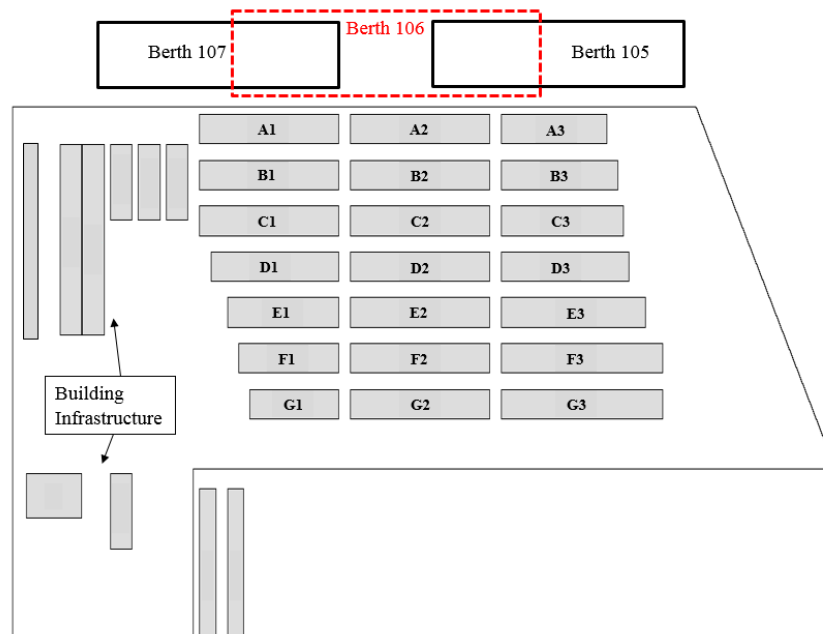


Figure 2.6: Pier One yard layout at the Durban Container Terminal

2.4.1 Vessel Unloading Procedure

Three QCs are used per vessel for the unloading procedure at Pier One for vessels in excess of 250 meters in length with over 2000 containers on board [26]. For smaller vessels (less than 250 meters), one or two QCs are used. The terminal uses a rule of five TTUs per QC when determining the number of TTUs required for a vessel unloading operation, however the TTUs are not bound to a specific QC but can service any QC being used to unload the vessel concerned [26]. Storage blocks D1 to G3 (Figure 2.6) are allocated for containers unloaded from a vessel (imported containers) [26]. The terminal has a rule of two RTGs per QC when determining the number of RTGs required for a vessel unloading operation [26]. These RTGs are positioned at the respective storage blocks which the containers to be unloaded are assigned to. The TTUs circulate between the QCs and the RTGs until all the containers which are to be unloaded from the vessel are stacked in the correct storage blocks. Unloaded containers are allocated a predefined position to be placed in a stacking block; the position at which a container is placed in the yard is recorded after it has been placed [26].

2.4.2 Vessel Loading Procedure

Similar to the vessel unloading procedure, three QCs are used per vessel for the loading procedure at Pier One for vessels in excess of 250 meters in length with over 2000 containers on board [26]. One or two QCs are used for smaller vessels. The Durban Container Terminal's rule for determining the number of TTUs and RTGs required for the loading procedure is the same as that for the unloading procedure, that is, five TTUs and two RTGs per QC. Storage blocks A1 to C3 are designated for containers to be loaded onto a vessel (export containers). Unlike the vessel unloading procedure, the containers to be loaded onto a vessel have predefined blocks and stacking positions in which they are stored in the yard [26]. Five TTUs are designated to service one particular QC and these TTUs will circulate between their assigned QC and the storage block which holds the containers to be loaded onto the vessel by the assigned QC [26]. It is common practice for the terminal to keep most of the containers that are designated to be loaded onto the vessel by a particular QC in a single storage block. Export containers are generally stacked in the yard according to the position they are to be loaded onto the vessel, that is, containers to be loaded towards the bottom of the vessel are usually stacked towards the top end of the storage blocks [26]. This is done to minimise container shuffling in the yard, which can become a common occurrence.

2.5 Research Methodology

One of the objectives of this project was to determine if a reduced fleet of MTSs can replace the current fleet of TTU's at Pier One of the Durban Container Terminal to reduce operational costs of the waterside-horizontal system and potentially reduce vessel berthing time by improving QC productivity. The analysis was carried out by means of discrete event simulation using ArenaTM software. Based on the results of the simulation, the required MTS configuration was determined and a suitable vehicle was then designed based on the terminal's functional requirements for trailer equipment. The designed MTS was structurally verified using finite element analysis (FEA) software package ANSYS[®] and its turning performance assessed using the software package BricsTurn[®].

The progression phases for the study were as follows:

1. Simulate the unloading and loading procedure for a container vessel at Pier One using TTU's as the transport medium between the vessel and stacking area by means of a DES model to replicate the present operation of the terminal.
2. Simulate the same procedure from (1) above but increase the carrying capacity of the trailers to 4 TEUs to simulate that of a two-trailer MTS. Determine the effect on the QC productivity and perform a preliminary operational cost comparison of the waterside-horizontal transport system to understand the benefits of using an MTS fleet.
3. Based on the simulation results from 2, determine the MTS configuration required.
4. Design a suitable MTS using locally available components and verify the integrity of the structure using FEA. Ensure that the vehicle designed can be manoeuvred within the terminal yard based on the current layout of the stacking area.
5. Compare the performance of the designed MTS to the current vehicles used at the terminal with regards to mass, manufacturing cost, turning performance and the operational costs associated with each vehicle type.

2.6 Chapter Summary

This chapter has presented the background information on container terminal operation as well as a detailed description of the vessel loading and unloading procedures used at Pier One of the Durban Container Terminal. Information on the types of container handling equipment and vehicles used in this environment was also presented. Lastly, the methodological approach followed for this research was described.

3 Container Movement Simulation Model

3.1 Introduction

This chapter concentrates on the DES models that were developed using ArenaTM to simulate the vessel loading and unloading procedure at Pier One of the Durban Container Terminal. The model parameters were estimated using physical data obtained from time and measurement studies at the terminal. The aim of the simulation was to determine the effect on QC productivity and operational costs for the waterside-horizontal transport system when using two-trailer MTSs instead of the current fleet of TTUs. This chapter is drawn from the second part of the journal article by Govender *et al.* [22] published in the South African Journal of Industrial Engineering.

3.2 Existing Port Terminal Simulation Studies

Several analyses of port terminals and their cargo transportation activities using simulation techniques can be found in literature [2, 27, 28, 29, 30, 31]. While queuing theory and mathematical algorithms are used by some authors to model the complex activities of a port terminal, simulation modelling has been adopted by numerous researchers as an alternative method for analysing port terminal systems at the macroscopic level of operations. The use of queuing theory and other analytical methods for modelling provides acceptable results for non-complex systems, however for systems where the probability distributions used to represent the service time of the various activities involved differ from the Erlang family, analytical methods have been found to lead to unsatisfactory results [27]. Additionally, the complex and dynamic nature of a container terminal's operations can lead to difficulty in obtaining theoretical solutions using analytical methods [28].

Robinson [29] describes a discrete event simulation as “*a simulation which models the operation of a system as a discrete sequence of events in time*”. Each event occurs at a particular instant in time and marks a change of state of the system. The ability to model complex systems accurately has led to various simulation studies using DES for port terminal operations. A few authors have conducted studies on the operation of container terminals using DES. Adam [30] used DES to identify and investigate the logistic bottlenecks which exist at the Male' Commercial Harbour. The model was used to analyse vessel berthing time, berth capacity, yard capacity and utilisation of the various container handling equipment at the port. The results showed that the berth capacity was the main contributor to the long queues and vessel delays experienced at the harbour. Kotachiav *et al.* [31] proposed a generic DES which modelled container terminal port operations with various resource types which included the different container handling equipment. The analysis considered the effect of varying model inputs to measure the impact on the outputs which included equipment utilisation, waiting times and throughput. Park [23] presented a DES model for analysing the performance of four Korean container terminals. Their model focused on obtaining the optimal container throughput for each terminal and the associated financial implication for the Korean Busan Container terminal for the optimum throughput. Data was

collected at each of the terminals and used as inputs into the model. The results showed that for an optimal throughput of 550 000 TEUs for the Korean Busan Container terminal, the associated social costs (the terminal's cost of operation plus the external costs borne by third parties) rise sharply while there is a minimal increase in corporate profit. Kulaka *et al.* [32] developed an ArenaTM-based simulation model to analyse the operations of the Haydarpasa Container Terminal. This was aimed at identifying potential bottlenecks at the quay cranes, storage yard and the transportation system by examining the terminal's equipment productivity, utilization and average waiting times. Gori *et al.* [33] developed a micro-simulation model using discrete events to analyse the operations at the Port of Civitavecchia. The entire process from vessel arrival to departure is modelled, which includes vessel navigation to the berth, handling operations at the berth and external truck arrivals. The model allows for specific calibration for each kind of vessel and the type of freight transported.

The research presented by the above authors generally focused on port performance from a macroscopic level and little work has been published regarding dedicated analysis of the waterside horizontal-transport system. Recently, Kulatunga *et al.* [34] investigated the effect of changing a container terminals' equipment fleet size on the performance of the terminal during the vessel unloading procedure only. The research methodology was twofold; the performance and operational efficiency for a generalised container terminal layout was determined analytically, thereafter an optimised layout was determined using DES. The optimum TTU fleet size was then determined using DES for the previously determined optimal yard layout and for a minimised QC idle time. One of the few available reports on the use of MTSs in container terminals was a dedicated investigation into the efficiency of multi-trailer systems used for transporting containers from the QC to the stacking area, conducted by Goussiater [13] using DES. The focus of the investigation was on the influence of the travel distance between the quayside and the stacking area has on the optimum trailer fleet size and container carrying capacity per MTS for maximised crane productivity. The study, which analysed the vessel unloading operation only, showed that for a ship-to-stacks distance exceeding 500 meters a fleet of single TTUs can be replaced by a smaller fleet of two-trailer MTSs while maintaining the same crane productivity at a lower operating cost per shift.

This work builds on the study done by Goussiater [13], who considered only a single QC and RTG for the unloading operation with assumed statistical distributions to represent the container handling and transporting equipment's cycle times. As an extension to that study, the present work considers both the vessel loading and unloading operations with a larger fleet of QCs, TTUs and RTGs, each represented by statistical distributions obtained from physically measured data sets. The model described in this chapter takes into consideration each of the individual activities of the various handling equipment and vehicles during the loading and unloading process and represents the cycle times of these activities as separate statistical distributions, whereas Goussiater adopted the use of single

statistical distributions to represent the holistic cycle time for each type of transporter. Similarly, this simulation study looks at reducing operational costs of a container terminal by using MTSs instead of TTUs.

3.3 The Discrete Event Simulation Model

3.3.1 Introduction

Discrete event simulation is the method of using computer software to imitate the behaviour of a complex system as an ordered sequence of well-defined events over period of time [35]. The simulations involve objects known as “entities” which move around, change status and affect each other and the state of the system [36]. These entities compete for service from resources that represent equipment, people or space in a storage area. An entity seizes a resource when available and releases it when finished [30]. In the model created in this study, the entities are the 20 ft. and 40 ft. containers and the resources are the QCs, TTUs, MTSs and the RTGs which are modelled as transporters. The QC and RTG container processing times are represented using probability distributions, as well as the time delays representing the transfer of containers from the QCs/RTGs to the trailer systems and vice versa. The sequence of events associated with container movements during the loading and unloading operations are modelled using process logic to replicate the actual operations observed at the terminal.

3.3.2 Model Structure

The loading and unloading models created in Arena™ were set up for a single vessel with a length of 300 meters and a carrying capacity of 2000 containers with a 45% 20 ft. : 55% 40 ft container ratio [37]. The vessel length and quantity of containers selected was based on the average vessel calling at Pier One of the Durban Container Terminal [26]. The vessel was positioned at berth 106 for each scenario, analogous to the berth used when only a single vessel has called at the terminal. Three QCs, fifteen TTUs and six RTGs were used in the simulations to conform to the general equipment assignment rule used by the terminal. The models were set up to represent the procedure observed at the terminal for both the loading and unloading operations. The models were then modified by replacing the TTU fleet with a fleet of two-trailer MTSs capable of transporting four TEUs and the results compared.

3.3.3 Data Collection

Qualitative and quantitative data was collected by conducting interviews, on-site observations and time measurements at Pier One. Qualitative data was obtained from interviews with the operational staff at the terminal to understand the logistics, operational processes and performance of the terminal with the current TTU setup for the vessel loading and unloading procedures. The data collected during the interviews and on-site observations was used to replicate the actual container movement processes between the vessel and the stacking area using the DES models created for the current layout of the terminal yard. Quantitative data was obtained by conducting physical time studies at the terminal for

the individual core processes which make up the complete operations. Data sets for the QC cycle time, RTG cycle times and the various transfer delays observed in the processes were collected to map the movement of the containers for the simulation. Distance measurements were conducted for the TTU routing from the quayside to the stacking areas and incorporated into the model.

3.3.4 Model Input Parameters

The data sets collected for the QC cycle times, RTG cycle times and the various observed transfer delays were used to generate suitable probability distributions for use as input parameters in the DES model. This was achieved using the Arena™'s Input Analyser which is designed specifically to fit probability distributions to measured data sets, provide approximations of the parameters and assess the accuracy of the probability distributions assigned to a set of data [36]. Arena™ requires the data sets to be recorded using text files (.txt) for processing and distribution estimation, therefore all the individual data sets were organised as such. Arena™'s Input Analyser automatically provides numerical measures for the quality of a fit for an assigned distribution, which is the mean square error, Chi-square and Kolmogorov-Smirnov goodness-of-fit tests. These tests were evaluated for all data sets to ensure accurate distributions were obtained. Table 3.1 shows a summary of the simulation model input parameters. Figure 3.1 and Figure 3.2 shows the distribution summary of the QC cycle times.

Table 3.1: Summary of the simulation model input parameters

Designation	Unloading Model Inputs	Loading Model Inputs	Units
QC Cycle time	0.63 + ERLA(0.23, 5)	0.73 + ERLA(0.174, 6)	Minutes
RTG Cycle Time to Stacks - Tier 1	1.21 + WEIB(1.19, 2.37)	3 + ERLA(0.0786,5)	Minutes
RTG Cycle Time to Stacks - Tier 2	0.26 + LOGN(1.07, 0.581)		Minutes
RTG Cycle Time to Stacks - Tier 3	0.16 + 2.84 * BETA(2.44, 2.82)		Minutes
RTG Cycle Time to Stacks - Tier 4	0.03 + 2.97 * BETA(1.82, 2.42)		Minutes
RTG Cycle Time to Stacks - Tier 5	0.18 + LOGN(1.15, 0.611)		Minutes
Trailer Lowered / Lifted	5	5	Seconds
Trailer lifted plus twist locks removed	8	-	Seconds
Trailer to QC transfer delay	16.5 + WEIB(2.99, 1.73)	20 + WEIB(2.31, 1.69)	Seconds
Trailer to RTG transfer delay	20.5 + WEIB(2.99, 1.73)	23 + WEIB(2.15, 1.46)	Seconds
TTU/MTS average velocity	20	20	km/hr

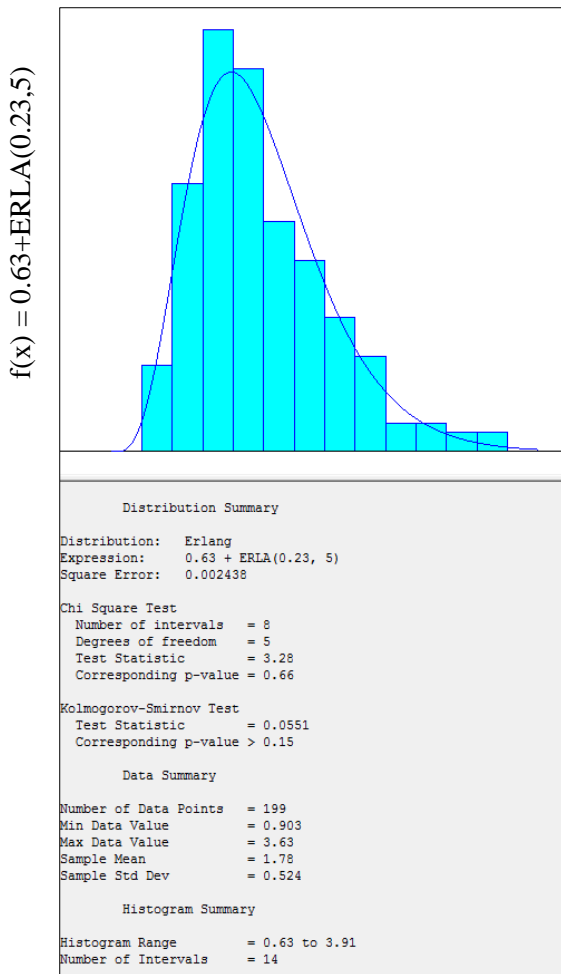


Figure 3.1: Distribution summary for the QC cycle time – vessel unloading

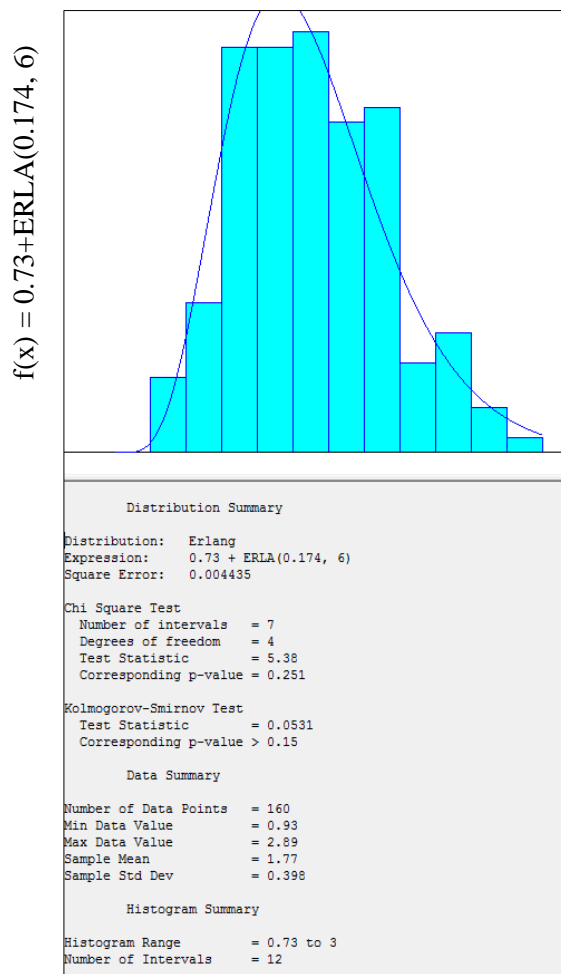


Figure 3.2: Distribution summary for the QC cycle time – vessel loading

As can be seen in Table 3.1, a single statistical distribution is used to represent the RTG cycle time in the loading model, as opposed to the RTG tier-based cycle time distributions used in the unloading model to represent stacking of the containers in the five-high storage blocks. This is due to shuffling of containers in the yard during the loading process whereby containers in the stack are sometimes moved around to get to the required container to be loaded onto the vessel in the correct sequence. For the vessel unloading model, 20% of each container type (20 ft. or 40 ft.) is assigned to a single tier since different container types are not stacked on top of each other in the yard. An average velocity of 20 km/hr. was used to model the TTU/MTS movement (loaded and unloaded), analogous to the velocities used in the studies conducted by Goussiatiner [13] and Yun *et al.* [37]. This velocity is approximately consistent with the average TTU velocity at the Durban Container terminal, which has a maximum speed limit of 30 km/hr for these vehicles. The time involved in aligning the RTG or QC spreader when lifting a container from a trailer, as well as aligning the trailer to accept a container by a RTG or QC, was based on observation and modeled as a transfer delay using Weibull (WEIB) distributions. The time delay for lowering and lifting a trailer by the tractor, as well as the time delay for removing the

twist locks in the unloading model, was modelled as a constant value rather than a probability distribution as the time to perform these processes were observed to be approximately constant. The Erlang (ERLA) probability function was assigned to the QC data set for both models, while the use of the Beta (BETA) and Lognormal (LOGN) probability functions were utilised for the Tier 2 to Tier 5 RTG cycle time to stacks for the unloading model,

3.3.5 Vessel Unloading Model

The storage blocks selected for the offloading simulation model were F1 to F3 and G1 to G3 as these are the areas allocated for containers unloaded from the same vessel (Figure 3.3). Each of these storage blocks operates with a single RTG, as per the terminal's stacking operation. The three QCs were spaced equally along the length of the vessel while the RTGs were positioned at the middle of the respective storage blocks. The QCs have an equal number of each type of container to unload from the vessel. When a QC offloads a container from the vessel, a TTU is requested by the QC for the container to be loaded onto. If a 20 ft. container is loaded, the trailer will wait underneath the QC for another 20 ft. container to be loaded before it leaves for the stacking area. This is consistent with the operations at the terminal to ensure that a TTU is loaded to its maximum carrying capacity of two TEUs during container movements. When the TTU leaves for the stacking area it will travel along the side between blocks A1 to F1 and enter the stacking area between blocks F and G. Figure 3.3 shows the path followed by the TTUs/MTSs. Depending on RTG availability, a TTU will either drive up to a non-busy RTG or join a queue with the least number of TTUs at an RTG waiting to be served. The RTGs stack containers five high by six wide in the storage blocks. Once the TTU has been completely unloaded by the RTG it will return to the quayside and be loaded by a QC requesting its service, restarting the cycle. The TTUs are not bound to a specific QC or RTG, as per operational practice. Figure 3.4 shows the unloading model using ArenaTM with the QC, TTU and RTG operation cycles highlighted. To compare the performance of the unloading procedure when using a fleet of MTSs instead of TTUs, a modified model was created with vehicle capacities of four TEUs to simulate an MTS with two trailers in its set. Figure 3.5 shows the model architecture for this operation with the logic processes referenced to Figure 3.4. The setup of the MTS model is similar to that shown in Figure 3.4, with modifications made to the model logic to accommodate the increased carrying capacity of the trailers.

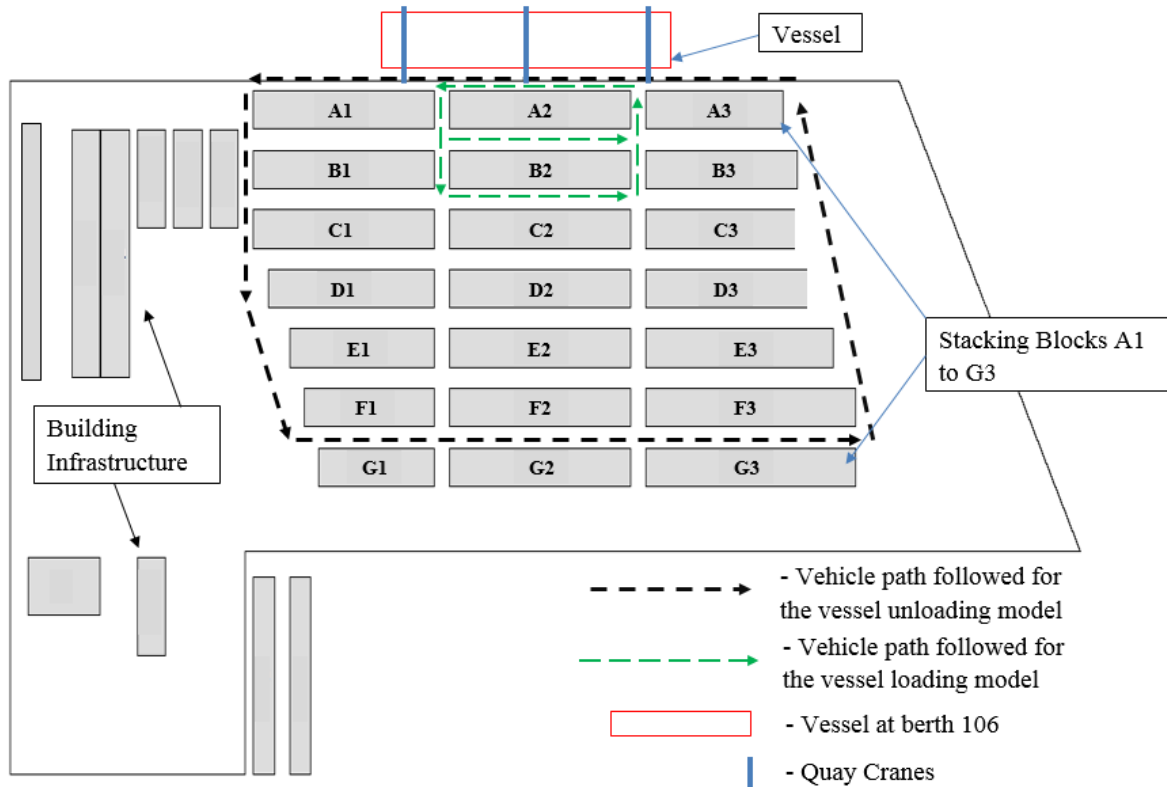


Figure 3.3: Paths followed by the TTUs and MTSs

3.3.6 Vessel Loading Model

The storage blocks selected for the loading operation were blocks A2, B2 and C2 (See Figure 3.3), analogous to the stacking blocks used at the Durban Container Terminal for the loading of vessels that are at berth 106. Two RTGs were assigned to each block, with each RTG having an equal number and type of container to be offloaded from the stacking area. All the containers from an individual block were assigned to a specific QC; containers from block A2 were assigned to QC 1 which was positioned towards the left end of the vessel, containers from block B2 were assigned to QC 2 which was positioned at the middle of the vessel and containers from block C2 were assigned to QC 3 which was positioned towards the right end of the vessel. Unlike the multi-serving TTUs from the vessel unloading operation, the five TTUs per QC for the vessel loading operation circulate between a single QC and its corresponding storage block. The TTUs are loaded with either two 20 ft. containers or one 40 ft. container by the RTGs and then travel to the respective QC to be unloaded. Once unloaded, the TTUs travel back to the stacking area to be loaded with containers again, repeating the cycle until the storage blocks are void of all containers. Figure 3.6 shows the Arena™ model logic for the QC 1 – block A2 pair. To compare the performance of the loading procedure when using a fleet of MTSs, a modified model was created with vehicle capacities of four TEUs to simulate a short MTS with two trailers in the set. Figure 3.7 shows the model architecture for this operation with the logic processes referenced to Figure 3.6. The setup of the MTS model is similar to that shown in Figure 3.6, with modifications made to the model logic to accommodate the increased carrying capacity of the trailers.

Container transfer- QC unloads container from vessel and places it onto the TTU (Process A)

Container transfer - RTG to stacks, TTU returns to quayside. (Process C)

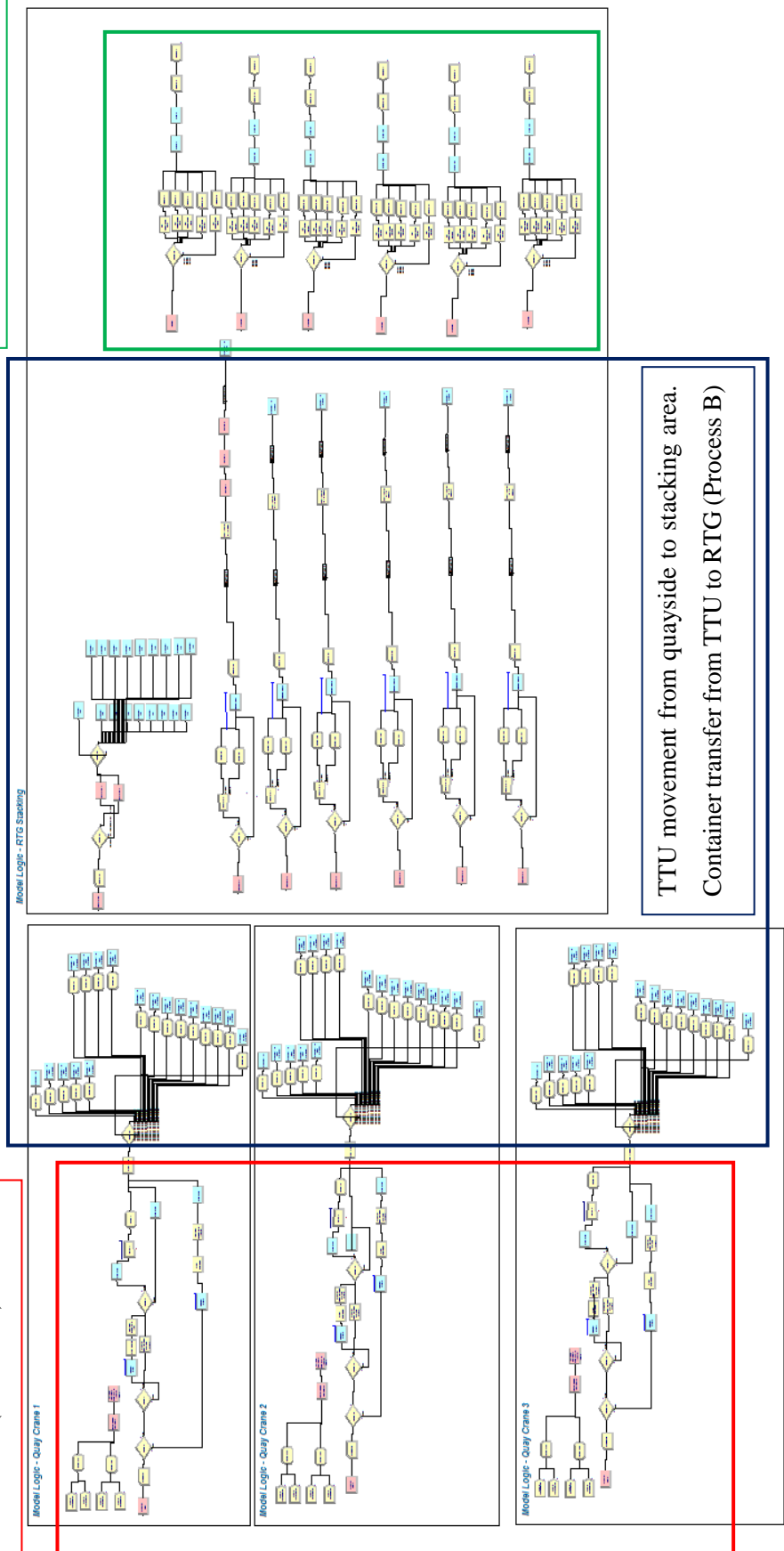


Figure 3.4: Overview of the unloading model using TTUs

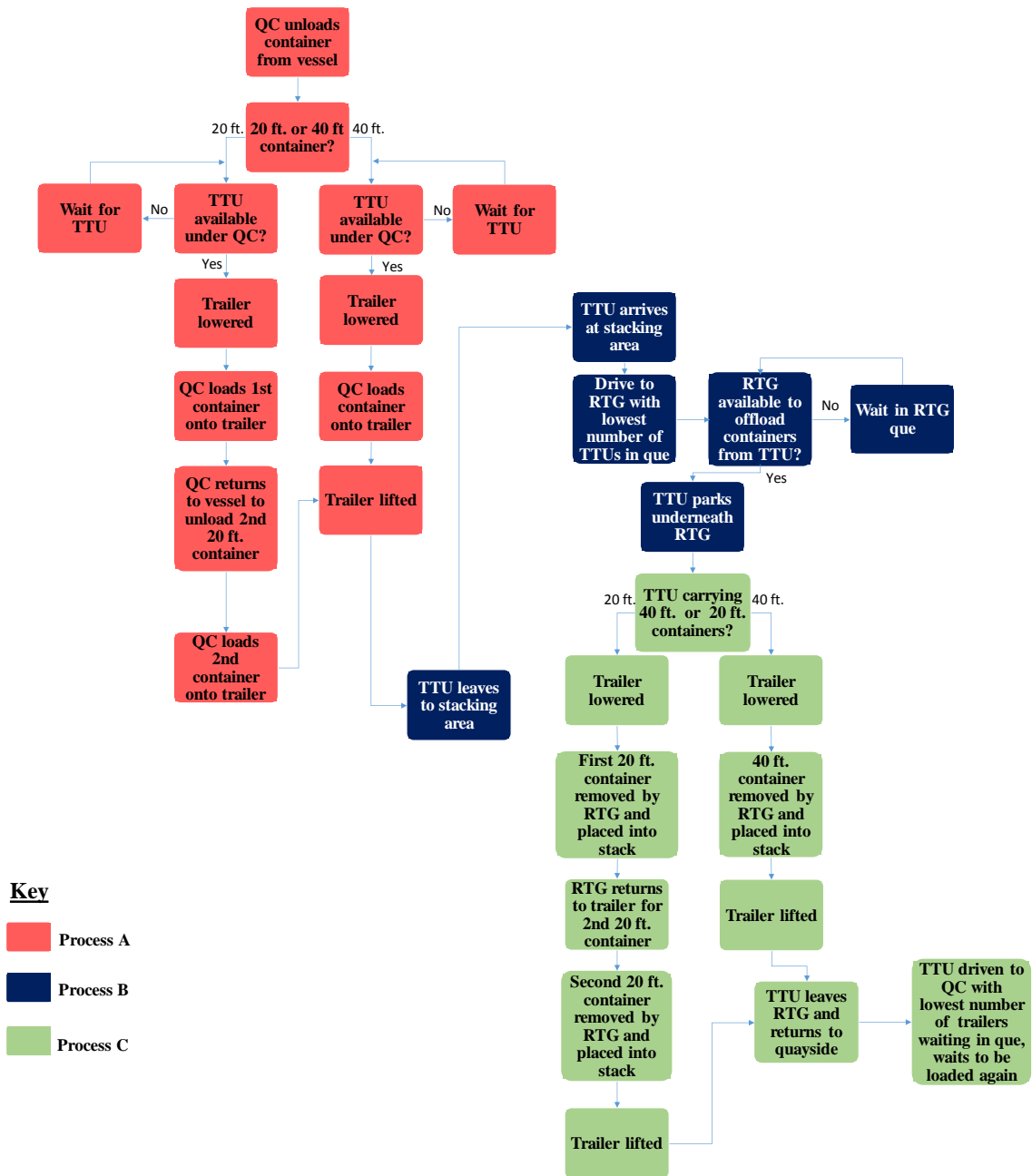


Figure 3.5: Model architecture for the vessel unloading procedure using TTUs

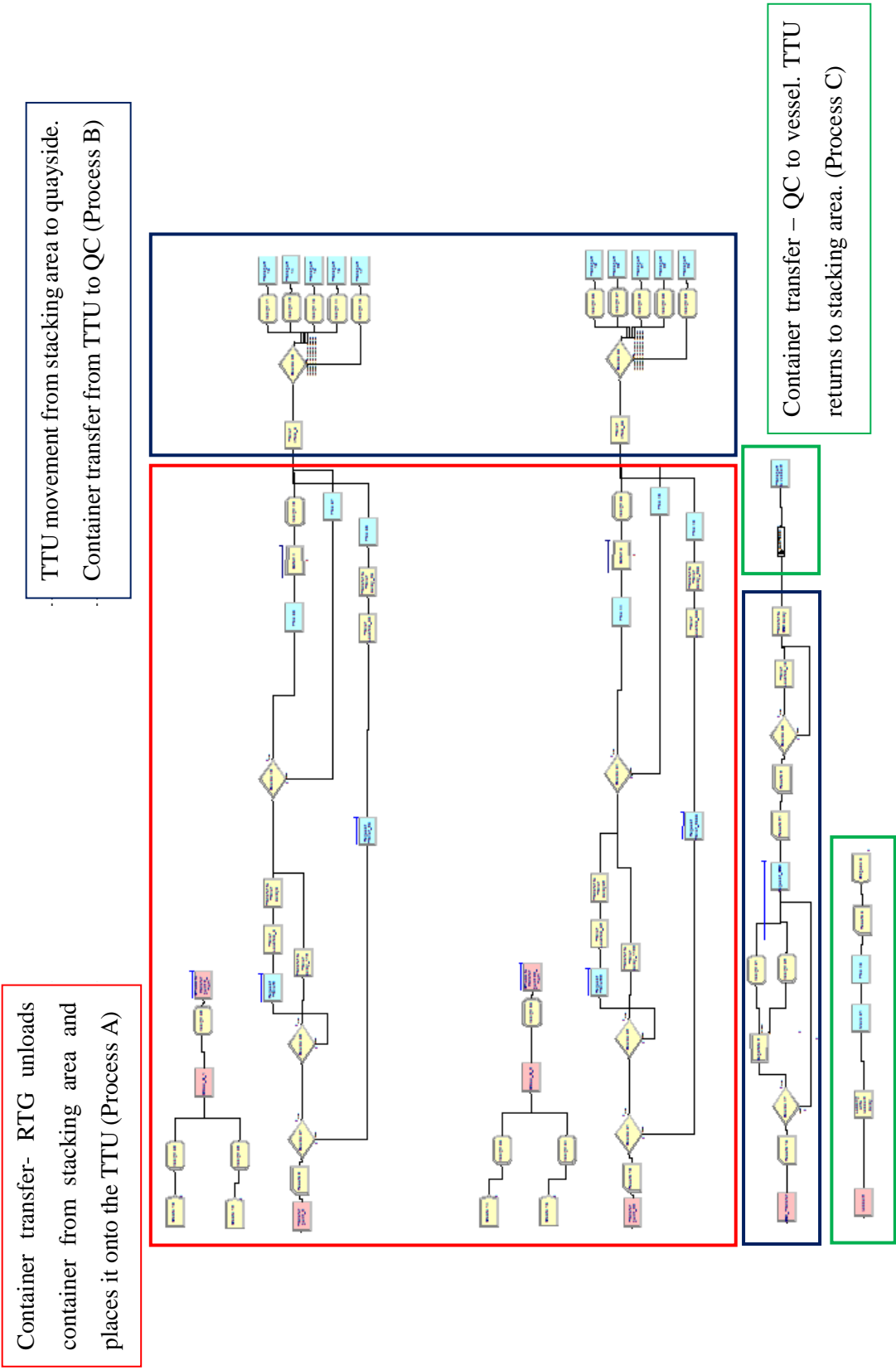


Figure 3.6: Overview of the loading model using TTUs: QC1-Block A2 Pair

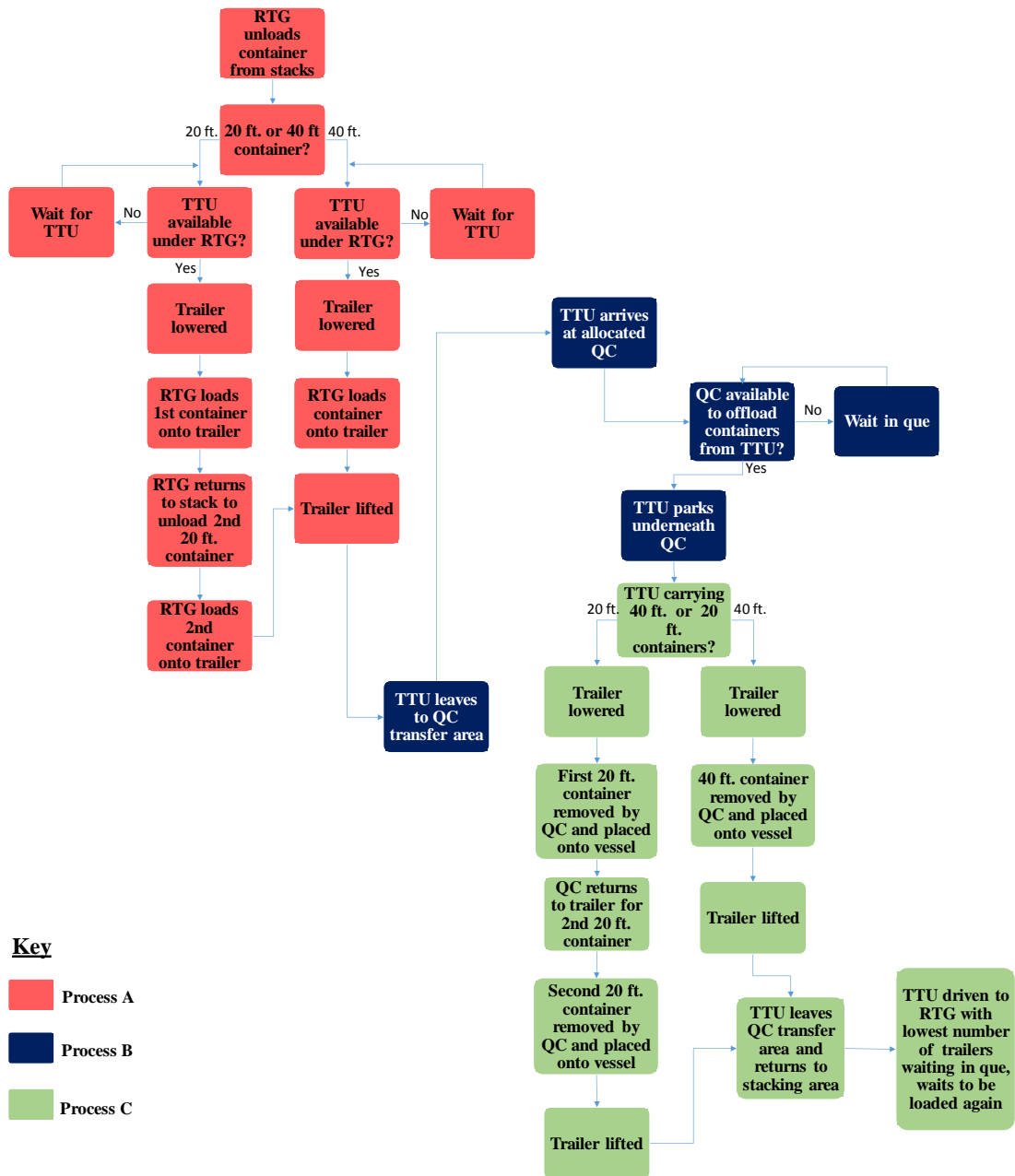


Figure 3.7: Model architecture for the vessel loading procedure using TTUs

3.3.7 Model Assumptions

Due to the extremely complex nature of modelling the operations at container terminals [38], assumptions were made while developing the models for the loading and unloading operations at Pier One for the currently used TTUs and the proposed MTSSs. These assumptions are as follows:

- The trailers are always loaded to their maximum carrying capacities i.e. 2 TEUs for the TTUs and 4 TEUs for the MTSSs.
- The 3 QCs are equally spaced apart at berth 106.
- The QCs and RTGs are fixed in space i.e. the transfer points with the trailers are always the same.
- The QCs and RTGs each have the same quantity and type of containers to load onto the trailers for the unloading and loading models respectively.

The assumptions made are consistent with the studies conducted by Goussiater [13], Yun *et al.* [37] and Kulatunga *et al.* [34].

3.3.8 Results

3.3.8.1 Model Verification and Validation

Kelton *et al.* [36] describes model verification as “the task of ensuring that the model behaves as intended”, alternatively known as debugging the model. Model validation is ensuring that the model behaves in the same manner as the real system being simulated [36].

The models were verified using ArenaTM's run controller tool to monitor the simulation programme in stages as the entities (containers) moved from one resource to the next to ensure that the correct transfers and process time delays occurred as required. An animation was also created in ArenaTM so that the activities and movements which were occurring in the system could be viewed. This was done to confirm that logic implemented created the system intended. Figure 3.8 shows the run controller tool and the animation created for the models. The simulation models were each run for 20 statistically independent replications to obtain a better estimate of the mean performance by using multiple samples [39].

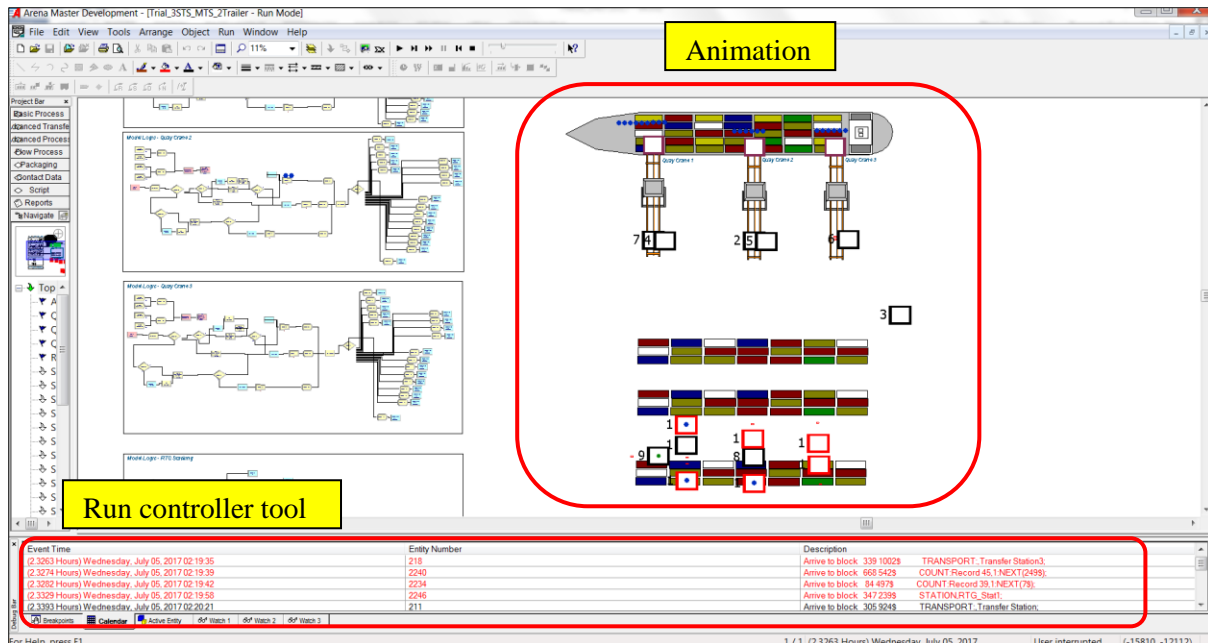


Figure 3.8: Run controller tool and animation in Arena™

Quay crane productivity, which is measured as the average number of containers moved per hour by the QCs, is the parameter used by the terminal to measure its vessel loading and unloading performance as this productivity determines the total time required to load/unload a vessel. The total number of containers which are loaded/unloaded from a vessel is divided by the sum of the individual operation times for the QCs utilised, yielding the average QC productivity for the vessel concerned. The general terminal performance for the unloading procedure is approximately 28 moves/hour, whereas for the loading procedure 26 moves/hour is most commonly achieved [26]. The simulation results for the average QC productivity of each operation were validated against the actual terminal performance. The average TTU cycle time, measured from arrival underneath the QC until returning to the quayside, was recorded for both operations for the scenarios of carrying a single 40 ft. container or two 20 ft. containers and compared to the average simulation results. Table 3.2 shows the comparison between the simulated and measured results for each procedure. The average results for the QC productivity and TTU cycle time from the simulation versus the actual average measured data shows marginal difference and provides acceptable accuracy of the model.

Table 3.2: A comparison of measured and simulated results

Parameters	Units	Vessel Unloading			Vessel Loading		
		Measured Average	Simulation Average	% Difference	Measured Average	Simulation Average	% Difference
QC Productivity	Moves/hour	28	27.21	2.90%	26	26.15	0.57%
TTU Cycle Time - 2 x 20 ft. Containers	Minutes	9.62	10.31	6.67%	8.56	8.69	1.51%
TTU Cycle Time - 1 x 40 ft. Container	Minutes	6.03	6.35	5.06%	2.67	2.78	3.96%

3.3.8.2 Vessel Unloading Model Results

The average QC productivity results for a varying fleet size of TTUs and MTSs were obtained from the respective unloading simulations and graphed, shown in Figure 3.9. The number of QCs and RTGs in the system was kept constant to analyse the effect that the trailer type and fleet size has on the terminal performance for the unloading procedure. For an equivalent fleet size of fifteen vehicles each, the MTS allows the QCs to operate at a productivity of 28.48 moves per hour, marginally higher than the QC productivity achieved with the current TTU setup. This is attributed to the average QC ‘waiting for a trailer’ delay being lower when using a fleet of MTSs. Waiting for trailers is constantly experienced in a terminal due to the fact that trailers arrive at irregular intervals at the QCs. For equivalent fleet sizes, the average QC ‘waiting for a trailer’ delay will be lower for a fleet of MTSs since this delay will only be experienced after every four 20 ft. containers or two 40 ft. containers offloaded from the vessel, in comparison to the QCs having to wait for a trailer after every two 20 ft. containers or one 40 ft. container for a fleet of TTUs. Waiting for a trailer delay can be eliminated by using a large number of trailers in the fleet however this will lead to low equipment utilisation levels and congestion at the terminal [13] (Figure 3.10). Of greater significance is the smaller fleet size of MTSs required to maintain the same QC productivity as that of the TTU fleet; the fifteen TTUs can be replaced by nine MTSs without negatively affecting QC productivity. Figure 3.9 shows that the TTU fleet requires additional vehicles to maximise the QC productivity whereas the QCs are able to operate at maximum productivity with only ten MTSs in the system.

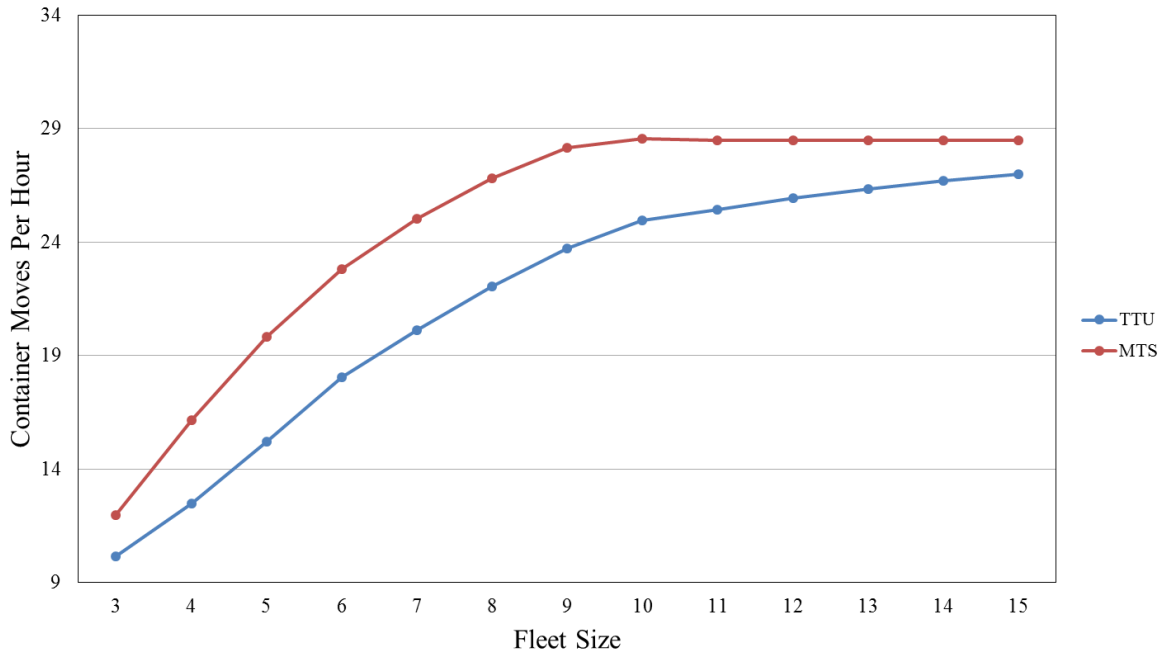


Figure 3.9: Average QC productivity – unloading model

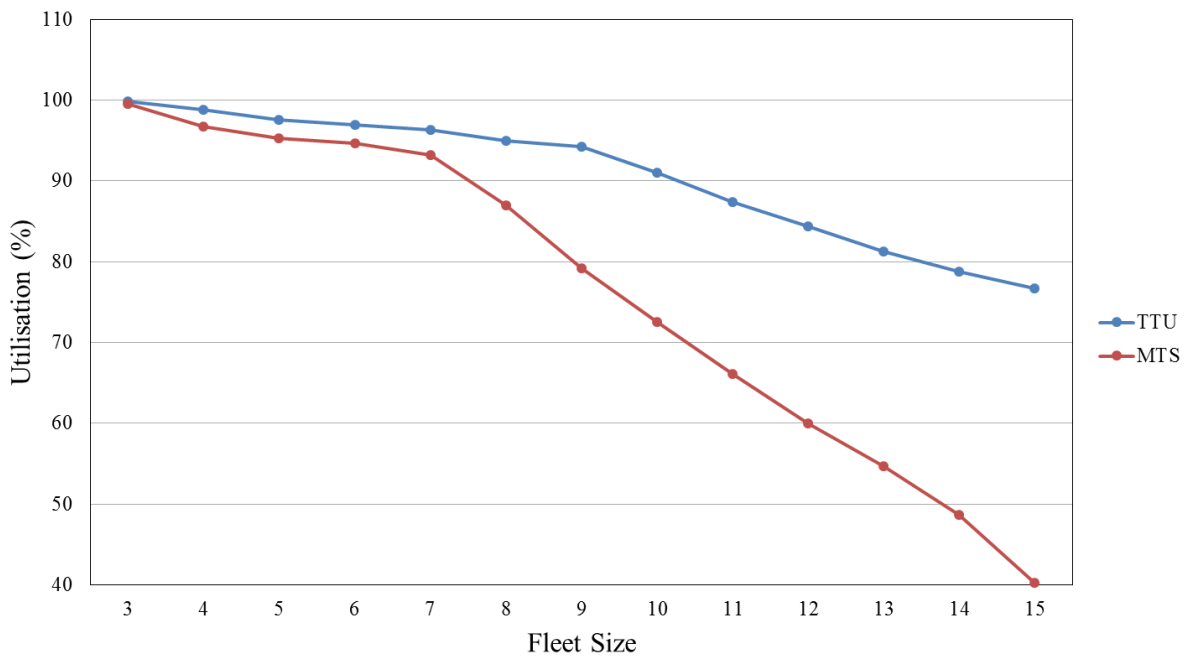


Figure 3.10: Average trailer fleet utilisation

3.3.8.3 Vessel Loading Model Results

The average QC productivity results for a varying fleet size of TTUs and MTSs were also obtained from the respective loading simulations, graphed in Figure 3.11. These results were obtained for a varying fleet size per QC since the vehicles are dedicated to a particular crane, unlike the unloading procedure where the entire fleet services all three QCs. The results were recorded for a maximum fleet size of five vehicles per QC. Figure 3.11 shows that there is a small increase in the QC productivity for

the vessel loading procedure when using an equivalent fleet of TTUs and MTSs above three vehicles. QC productivity is maximised when using three TTUs per QC which shows that there are more TTUs in the current system (15) than is required.

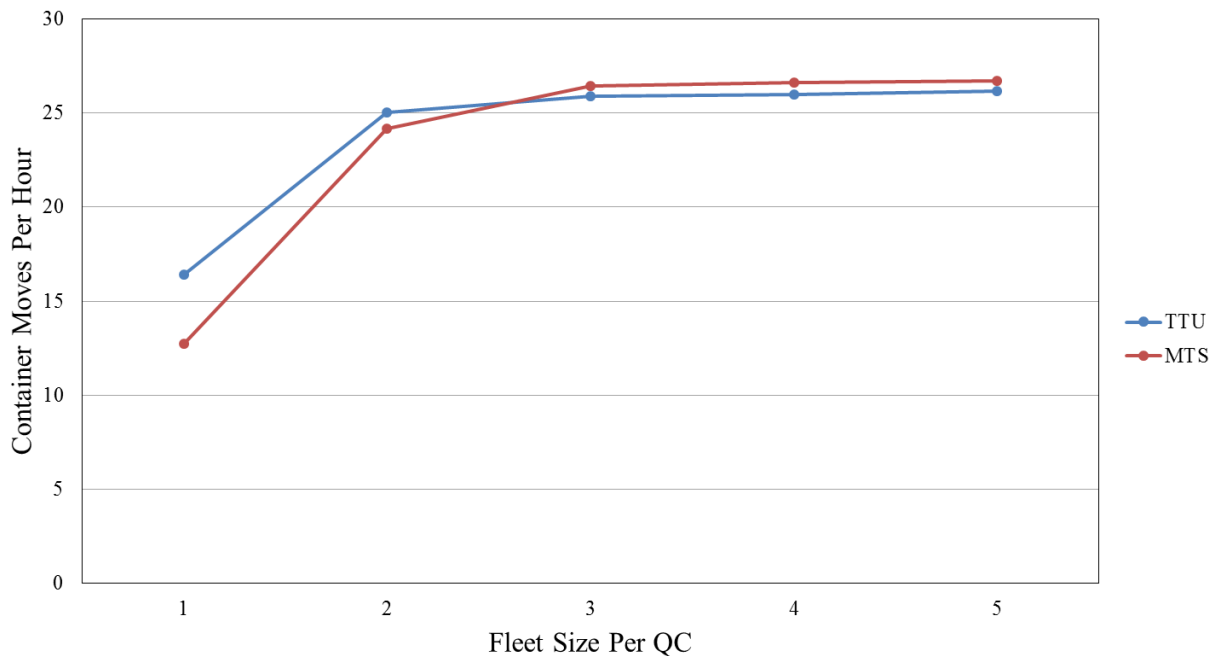


Figure 3.11: Average QC productivity – Loading model

The DES results show that using MTSs for the loading procedure is not very beneficial; three TTUs per QC creates almost the same crane productivity as three MTSs per QC and the performance of both vehicles can be considered equivalent. As can be seen by the flattening of the curve from Figure 3.11, when scheduling a minimum of nine TTUs in total for three QCs for the loading procedure the QC ‘waiting for a trailer delay’ is reduced almost to zero.

3.3.8.4 Results Discussion

The simulation results show that a significantly reduced fleet of MTSs can be used at Pier One for the vessel unloading procedure without negatively affecting the crane productivity and hence the terminal performance, however for the loading procedure the use of MTSs shows minimal to no benefit. For the unloading procedure using TTUs, the system can be viewed as having three producers (QCs) and six consumers (RTGs) of containers. The average RTG cycle time is marginally less than the average QC cycle time, meaning that the delay between trailer arrivals at the QC is largely dependent on the travel time of the trailers. Due to an MTS having to wait longer underneath a QC, the delay between trailer arrivals is experienced less frequently and a smaller fleet of MTSs can replace the TTU fleet for equivalent crane productivity.

For the loading procedure using TTUs, the system can be viewed as having three dedicated sets of two producers (RTGs) and one consumer (QC) of containers. In this setup, even though the producers have

a cycle time approximately double that of the consumer, the supply of containers by the two RTGs collectively creates an abundance at the QC. This creates a queue of trailers waiting at the QC to be unloaded. Figure 3.11 shows that a delay between trailer arrivals at the QC is only experienced for less than three TTUs or MTSs per QC in the system. Figure 3.11 also shows that for equivalent fleet sizes less than three, using MTSs creates a marginally lower QC productivity than its TTU counterpart due to the MTS having to wait much longer than a TTU underneath the RTG. This leads to long delays between trailer arrivals at the QC as there isn't a sufficient number of empty trailers able to be continuously loaded by the RTGs and sent to the QCs.

The results positively show that a fleet of two-trailer MTSs can be implemented at the terminal. To maintain the current productivity of the terminal, nine two-trailer MTSs can be used per three QCs during a vessel unloading process. For the loading process, the same fleet size of MTSs can be used with either one or two trailers in the set. The results also show that using a fleet of nine or more MTSs can improve QC productivity and hence reduce the total time of the vessel unloading procedure, however the benefit is marginal. The more significant benefit would be from a potential reduction in operating costs for the waterside-horizontal system due to a smaller fleet of vehicles required.

3.4 Preliminary Operational Cost Comparison

The data shown in Table 3.3 was used to conduct a preliminary operational cost comparison per shift to run each vehicle type. Even though fifteen TTUs are used in practice for both the unloading and loading process, nine vehicles were used for the cost analysis for the loading operation since this is the number of vehicles required to achieve maximum crane productivity, based on the results of the DES.

Table 3.3: Durban Container Terminal's operational cost parameters [26, 40]

Equipment Life Cycle	5 Years
Working Hours/Day	21.83 Hours
Shift Duration	8 Hours
Fuel Cost	R10.64 Per Litre
Annual Maintenance Cost (% of the equipment value)	10%
Labour Rate	R 200 Per Hour

Table 3.4 shows the equipment cost per shift for the trailer systems. This cost is calculated using the life cycle of the trailers and the total number of shifts per year which the trailers are operated. The terminal recapitalises its trailer equipment every 5 years, hence the 5 year life cycle. While the equipment unit cost is higher for an MTS, the total equipment cost is lower when compared to the fleet

of TTUs since the required fleet size for equal crane productivity is smaller. This leads to a lower equipment and maintenance cost per shift for the MTS. This MTS equipment cost is based on the average unit price of MTSs designed and manufactured by European original equipment manufacturers [13] as there is currently no locally manufactured product available.

Table 3.4: Equipment cost per shift (loading and unloading)

Type	Unit Cost	Required Fleet Size	Total Equipment Cost	Cost Per Shift
TTU	R 2 300 000	15	R 34 500 000	R 6 947
MTS	R 3 700 000	9	R 33 300 000	R 6 705

Due to the MTS prime mover (terminal tractor) pulling a greater load than its TTU counterpart the fuel consumption over a distance is larger for the MTS, however due to the MTS being able to move twice the number of containers in a single movement than a TTU the overall distance travelled to move all containers to the stacking area is half that of the TTUs. This leads to the fuel usage per shift being lower for the MTS system. Table 3.5 shows this preliminary comparison. The fuel consumption is based on the use of a CVS Ferrari FR270 terminal tractor which is part of the Durban Container Terminal's fleet of vehicles.

Table 3.5: Fuel cost per shift

Type	Total Distance Covered in 1 Shift (km)		Prime Mover Fuel Consumption (km/litre)	Fuel Cost per Litre	Cost Per Shift	
	Loading	Unloading			Loading	Unloading
TTU	266.2	885	1.079	R 10.64	R 2 625	R 8 727
MTS	133	442	0.557		R 2 541	R 8 443

The annual maintenance cost for each trailer type was approximated as 10% of the total cost of the equipment. This is an acceptable approximation and has been adopted by Goussiater [13] and Isalgue *et al.* [41] in determining the annual maintenance costs of terminal trailers. Table 3.6 shows that the maintenance cost per shift for a fleet of MTSs is 3.5% lower than that of the TTU fleet.

Table 3.6: Maintenance cost per shift

Type	Total Equipment Cost	%	Annual Maintenance Cost	Cost Per Shift
TTU	R 34 500 000.00	10.00	R 3 450 000	R 694.68
MTS	R 33 300 000.00		R 3 330 000	R 670.52

Use of an MTS fleet also results in a lower labour cost per shift for the waterside-horizontal transport system due to a fewer number of tractor drivers required. A labour cost of R 200 per hour was used as the remuneration rate for the vehicle drivers, which is consistent with the earnings of these drivers at the terminal. Table 3.7 shows the labour cost comparison.

Table 3.7: Labour cost per shift

Type	Drivers Required		Labour Rate (Per hour)	Cost Per Shift	
	Unloading	Loading		Unloading	Loading
TTU	15	9	R 200	R 24 000	R 14 400
MTS	9	9		R 14 400	R 14 400

As can be seen from Table 3.4 to Table 3.7, the main saving contributor when using a fleet of MTSs is from a reduction in labour costs in the unloading procedure. Table 3.8 below shows the comparison of the total operating cost per shift for the vehicle types and process. The labour cost saving when using the required fleet size of MTSs for vessel unloading makes up 95% of the overall 25% saving in operating costs. The savings when using MTSs for the loading procedure are marginal; an approximate saving of 1% in operating costs can be expected when compared to the TTU fleet.

Table 3.8: Total operating cost per shift

Type	Vehicles Required		Total Operating Cost Per Shift	
	Unloading	Loading	Unloading	Loading
TTU	15	9	R 40 368	R 24 666
MTS	9	9	R 30 219	R 24 316

3.5 Chapter Summary

A discrete event simulation was described to evaluate the effect of using MTSs instead of TTUs to transport containers between the vessel and the stacking area at Pier One. A review of existing port terminal simulation studies was also presented. The results of the simulation showed that a fleet of two-trailer MTSs, each with a capacity of four TEUs, can be implemented at Pier One to reduce operating costs of the waterside-horizontal transport system while maintaining the performance of the terminal. Use of a fleet of MTSs for the unloading procedure has shown significantly greater benefits than for the loading procedure, however the system can be used for both operations without negatively affecting terminal performance or operating costs of either. The results of the study show that operational costs for the vessel unloading procedure can be reduced by approximately 25% when using nine MTSs instead of the currently used fifteen TTUs.

4 Multi-Trailer Design Considerations

4.1 Introduction

Having established the value of implementing an MTS solution for Pier One at the Durban Container Terminal, this chapter considers the different types of MTSs currently available, methodologies employed in trailer design and whether an indigenously designed vehicle is feasible. The design aspects affecting the manoeuvrability of the MTS are also investigated.

A review of the different types of MTSs available was conducted with the intention of finding a suitable configuration for the design approach, taking into account the results from Chapter 3. An investigation into the standards and guidelines for trailers was conducted to determine appropriate load cases and safety factors needed to be taken into account during the design. This was done by analysing standards, information from trailer manufacturers and research into vehicle design and testing. Manoeuvrability of the MTS, in particular the swept path during turning and how the trailer's geometrical parameters influence this factor, is examined. Suitable locally available trailer components such as axles, suspension, rims and tyres, as well as a variety of materials were investigated and compared to select that most appropriate for the MTS design.

4.2 Multi-Trailer System Configuration

4.2.1 System Types

MTS manufacturers group the system configuration into three main types [13], namely a semi-trailer lead MTS, a drawbar-trailer lead MTS and a bidirectional MTS.

Semi-Trailer Lead MTS

A semi-trailer lead MTS is a short MTS made up of a tractor, a lead semi-trailer and typically one to two drawbar trailers. The tractor is connected to the lead semi-trailer using a fifth-wheel. During the operation, the trailer set can change its size from one to three trailers, but the tractor remains connected to the same semi-trailer. A semi-trailer lead MTS with two trailers in the set is shown in Figure 4.1.

Drawbar-Trailer lead MTS

A drawbar-trailer lead MTS is a long MTS made up of multiple drawbar trailers, pulled by a heavy-duty terminal tractor fitted with a ballast to reduce wheel slip. The lead trailer is connected to the tractor using a towing hitch. During operation, the trailer set remains intact. Figure 4.2 shows an example of this system type, with Figure 4.3 showing the drawbar connection to the tractor.

Bidirectional MTS

A bidirectional MTS is similar to a drawbar-trailer lead system, except that drawbars are present on both sides for connection to the tractor. This allows the MTS to change its moving direction without having to turn around. The feature is beneficial for congested and narrow areas, for instance narrow quays where turning around is not possible. This type of system is still in its experimental stages and is yet to be implemented in a terminal environment.



Figure 4.1: Semi-trailer lead MTS



Figure 4.2: Drawbar-trailer lead MTS



Figure 4.3: Drawbar connection to the tractor

4.2.2 System Evaluation and Selection

The analysis presented in Chapter 3 focused on the effect of using two-trailer MTSs for the unloading and loading procedure at Pier One of the Durban Container Terminal. Results showed that using a fleet of these MTSs is beneficial for the vessel unloading procedure, while for the loading procedure a single trailer system shows equivalent performance to the MTS. The results imply that the system configuration implemented at the terminal should allow for changes in the size of the trailer set such that a two-trailer MTS can be used for the unloading procedure, while for the loading procedure the individual trailers from the MTS should be able to be uncoupled and used separately as TTUs, should the terminal decide to do so. The Durban Container Terminal favours the use of fifth wheel couplings over the use of drawbars for the connection of the tractors to the trailer systems (see Figure 2.3) since specialised tractors are required for drawbar connections, as shown in Figure 4.3. Tractors with drawbar connections are generally used for high gross combinational mass (GCM) applications (excess of 250 tons) where ballasts are fitted to the tractors. This is due to the vertical load transfer from the trailer through a fifth wheel connection not being large enough to provide sufficient friction at the tyre-road surface interface to prevent wheel slip, hence the area on the tractor where a fifth wheel coupling is present is replaced with a heavy ballast and a drawbar connection is utilised. Currently, the terminal only uses tractors with fifth wheel couplings for trailer movements.

Based on the above considerations, a semi-trailer lead MTS configuration is the most suitable system for implementation at Pier One when compared to a drawbar-trailer lead and bidirectional MTS since only two trailers will be in the set and the terminal has sufficient space for turning this vehicle. A drawback of the conventional semi-trailer lead MTS configuration shown in Figure 4.1 is that it has a permanent drawbar connection on the second trailer, therefore the trailer positions cannot be interchanged in the set. Furthermore, when the second trailer is removed it can only couple to another tractor using the drawbar connection. For the MTS designed for Pier One it is desirable to have identical semi-trailers in the set, connected to each other via a removable drawbar. This will allow for interchangeability in the set and allow for each semi-trailer to be connected to a tractor via a fifth wheel coupling, creating a uniform vehicle fleet. To achieve this, a converter dolly fitted with a fifth wheel coupling must be used as the removable drawbar connection between 2 identical semi-trailers to form the semi-trailer lead MTS design. An example of this configuration is shown in Figure 4.4, with a converter dolly shown in Figure 4.5. Figure 4.6 depicts how a converter dolly connects the two semi-trailers together.



Figure 4.4: Semi-trailer lead MTS with a converter dolly [42]



Figure 4.5: Converter dolly [43]

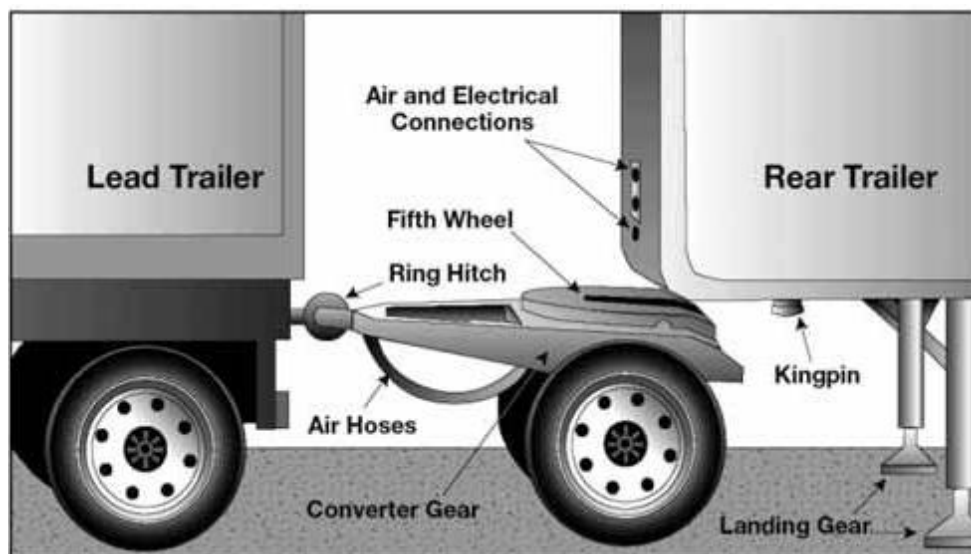


Figure 4.6: Converter dolly connecting two trailers [44]

For the proposed MTS design consisting of two identical trailers coupled together via a converter dolly, the existing semi-trailers at the terminal could be modified by adding towing hitches at the rear of each trailer and used with a converter dolly to form the MTS configuration, however, an opportunity exists for a better designed semi-trailer with regards to mass, cost and manoeuvrability since the Port of Durban recapitalises its trailer fleet every 5 years. A better designed semi-trailer will allow for a greater reduction in operational costs if a lower tare mass results in a saving in manufacturing costs. Chapter 7 presents a comparison of the existing semi-trailers versus the more optimised semi-trailer design when used in the MTS configuration.

4.3 Design Requirements

4.3.1 Port Terminal Requirements

The Durban Container Terminal has specific requirements for the trailer equipment supplied and operated at Pier One [45]. While MTSs have never been designed for Pier One previously, TTUs have been utilised at the terminal since its inception and general design requirements for these trailers have been developed. The key functional and technical requirements for these trailers are shown below, which will be applicable to an MTS designed specifically for Pier One.

A) Equipment Functional Requirements

- The trailers will be utilised to transport one 40 ft., one or two 20 ft. ISO containers or one 20 ft. tank container (each semi-trailer in the MTS must comply with this). These containers can be empty or fully laden up to its maximum design loads.
- The trailers will be subjected to shock impact loads of fully loaded containers being loaded by container handling equipment.
- The trailers must be designed for short hauls with an average distance of 2 km per trip at a maximum speed of 30 km/hr with a full load. They will be subject to frequent intermittent stops and will have to negotiate corners in and out of the container stacks.
- The trailers must be of the cornerless type, designed to allow the fitting and removal of twist lock connectors on containers loaded on the trailer without having to climb onto or crawl under the trailer.

B) Technical Specific Requirements

- The trailer structure must be constructed from a readily available carbon steel grade of a recognised specification that is fit for the application.
- The trailer structure must be braced adequately to withstand all stresses at the fifth wheel king-pin.

- The side and end guides of the trailer must facilitate the accurate self-positioning of containers when placed onto the trailer.
- Heavy duty tandem axles capable of hauling the rated payload at 30 km/hr and capable of withstanding shock impacts by containers when loaded, are required.
- The axles brake system must enable the trailer to comply with SANS 1447 – Part 2.
- Tyres manufactured in the Republic of South Africa or standard tyres which are readily available in South Africa must be used.

Container terminal trailers are generally of a skeletal chassis type and consists of two core centre beams with cross members to form the structure. The cross members perform two functions; to support the payload as well as to form a connection between the centre beams to create the chassis. The design of the chassis takes into account the position and spacing of the suspension, position of the coupling equipment and auxiliary equipment such as the braking system and lubrication system. The chassis must be able to withstand shock impact loads which can occur when the containers are not gradually lowered onto the trailers. The length and width of the trailer chassis must accommodate the type and quantity of containers required. As mentioned in the equipment functional requirements, the design of the individual semi-trailers in the MTS must allow for the fitting and removal of twist lock connectors on containers. This implies that the containers need to be supported on the outer edges of the bottom of the container frame to ensure that its corner castings are accessible at all times. This is the case on the existing trailers used at Pier One, shown in Figure 2.3.

An important requirement is the use of tandem axles for trailer equipment intended for use at the terminal. These must be fitted with an adequate braking system to ensure compliance to SANS 1447-2 (Braking of low speed trailers). A low speed trailer is defined as a trailer, which according to its design, is intended to be coupled to a towing vehicle with a maximum operating speed of 40 km/hr. [46]. The Durban Container Terminal has a speed limit of 30 km/hr for these trailers, therefore the application of this standard for the braking performance of the axles is relevant. Tandem axles are used for reduced axle loads at the terminal to minimise wear and damage to the road surface. They are attached to the chassis of the trailers via a leaf spring suspension rather than an air suspension system due to the road surface of the terminal yard being extremely flat and uniform, without any gradient. An air suspension system is generally used on trailers intended for use on irregular, uneven road surfaces where impact absorption is required for sensitive cargo.

4.3.2 Structural Requirements

A review of the literature surrounding the structural requirements for trailer designs, in particular that of the loading requirements and stress safety factors, was conducted. A review of the available standards, trailer design methods employed by trailer manufacturers and relevant literature on

theoretical trailer design and data collection from field testing is presented in this section to determine appropriate load cases and safety factors to be used in the design of the MTS.

4.3.2.1 Trailer Standards

South African National Standards (SANS), were investigated to determine if there was any formal guideline for the design of trailer equipment. Many standards surrounding the compliance of sub-systems such as the lighting equipment, warning signs, underrun protection devices and braking equipment for low speed applications can be found [47, 48, 49, 46], however no standard is available which details the structural requirements and load capacity for the design of a trailer or converter dolly chassis. The South African Road Traffic Act (Act 93 of 1996) stipulates the general requirements for road going vehicles to be declared roadworthy, such as the dimensions of the vehicle, braking performance and axle loads however no recommendations are made with regards to the strength requirements of the vehicles chassis. While the MTS does not have to comply with the South African Road Traffic Act due to it being operated on private property, the compliance standards were investigated to determine if there are any structural requirements and load capacity guidelines available which could be adopted for the design of the MTS.

The Australian Design Rules (ADRs) are national standards for vehicle safety, anti-theft and emissions for passenger vehicles, goods vehicles, trailers and two and three wheeled vehicles. The ADRs are performance based and cover matters such as occupant protection, lighting, structures, engine exhaust emissions, noise, braking and a range of other items [50]. A review of the ADRs applicability summary for trailers has shown that rules have been created for the design and use of trailer equipment such as braking systems, fuel systems, axles and wheels, external noise reducers and mechanical connection between vehicles, however no structural and load capacity guidelines for a chassis design is mentioned.

The *European Agreement Concerning the International Carriage of Dangerous Goods by Road* is a United Nations treaty that governs the transport of hazardous materials using public roads [51]. The agreement has defined dangerous goods using nine classes which range from explosive substances to radioactive and corrosive substances. The agreement stipulates that trailer designs intended for the carriage of dangerous goods must be able to withstand minimum accelerations of two times gravity in the direction of travel (longitudinal acceleration) and in the vertical direction in which the payload exerts its mass. Trailers must also withstand a minimum of one times gravity at right angles to the direction of travel (lateral acceleration). Each of these accelerations must be applied together with the maximum payload which the vehicle chassis is designed to carry, however the standard makes no mention of the required material strength safety factors to be used in the design. The trailers designed according to the agreement are intended for road use up to a maximum speed of 120 km/hr.

A review of the published ISO standards applicable to trailer design has shown many standards applicable to the compliance of components used in the design of a trailer. Examples of this include ISO 611:2003 [52] and ISO 4148:2004 [53] which address the braking of vehicles and their trailers, and the dimensions of warning lights respectively. Similar to SANS, no standard guidelines are available with regard to the strength requirements of a chassis design.

The above-mentioned standards relate to trailers intended for road use. While the MTS is intended for use solely within the confinement of Pier One of the Durban Container Terminal which is private property and thus not requiring the MTS to comply to the South African Road Traffic Act (Act 93 of 1996), these standards were examined for the purpose of finding proven trailer structural design codes and guidelines which could be implemented in the design of the MTS.

4.3.2.2 Design Methods Used by Trailer Manufacturers

Research into the load cases and safety factors used by trailer manufacturers was undertaken to gain an insight into the industry norms for trailer design with regard to the structural design methods employed. Due to a lack of conclusive design data highlighted in the previous section on trailer standards, in particular safety factors; load cases and safety factors used in industry were examined. By knowing the load cases and safety factors used, similarities were observed and similarly applied to the MTS design. Most of the information with regards to this was adopted from Cowling [54] as obtaining information directly from manufacturers proved difficult owing to their reluctance to disclose design methods.

Table 4.1 summarises the information obtained by Cowling on the load cases and the safety factors used by various trailer manufacturers.

Afrit and Transpec CC, which are South African manufacturers, use safety factors which range from 1.4 to 2.8 and from 2 to 2.5 respectively against material yield strength, depending on whether the trailer is intended for light or heavy industrial use. The load cases used for the design were not disclosed.

John Pilcher Designs produce designs of trailer for agricultural use for the South African market. A safety factor of 3 against material yield strength is used for the static load case of the payload mass with a 1g vertical acceleration during the design process.

Wabash International and East MFG, which are American manufacturers, use design factors of 2.5 and 2 to 3 respectively. The static design loads are multiplied by the design factor to form the load cases. Wabash International applies the factor to a loading scenario dependent on the use of the trailer, while East MFG applies the factor to worst case legal loads, however the exact load cases used by both manufacturers were not made available. The design factors are used to accommodate for dynamic loading conditions in a static analysis.

Haulmark, an Australian manufacturer, use design factors ranging from 2.5 to 3.0 depending on the usage and the expected life of the trailer. Similar to the other manufacturers listed, the load cases to which this factor is applied was not disclosed.

Table 4.1: Design load cases & design/safety factors used by trailer manufacturers [54]

Trailer Manufacturers	Load Cases (LC)	Design Factors incorporated into LC	Safety Factors
Afrit	Not Disclosed	Not Disclosed	1.4 – 2.8
Transpec CC	Not Disclosed	Not Disclosed	2 - 2.5
John Pilcher Designs	Payload + 1g vertical acceleration	1	3
Wabash International	Not Disclosed	2.5	Not Disclosed
East MFG	Not Disclosed	2 - 3	Not Disclosed
Haulmark	Not Disclosed	2.5 - 3	Not Disclosed

Transnet Engineering is the current manufacturer and supplier of semi-trailers to the Port of Durban, which range from skeletal trailers used in TTUs, to heavy duty multipurpose trailers. Direct discussions with their design team revealed the load cases and safety factors used in their designs [55]. The skeletal semi-trailers manufactured for container movement at Pier One are designed using the load cases shown in Table 4.2. For each of these load cases, the design requirement is that the maximum stress must fall below the yield stress of the materials used (minimum safety factor of 1). Design factors have been incorporated into the load cases, however the exact factors used were not disclosed. For each load case, the mass of the payload is applied together with the acceleration magnitude in the respective directions. S355 steel, which has a yield stress of 355 MPa [56], is used in the design of their trailers. These trailers have been successfully operated at the terminal for several years without structural failure.

Table 4.2: Transnet Engineering’s trailer design requirements

Load Cases	Maximum Stress Criteria
Vertical: Payload + 2g	Yield Stress
Longitudinal: Payload + 0.8g	
Lateral: Payload + 0.3g	

4.3.2.3 Trailer Design Studies

A review on the literature applicable to the theoretical design and field testing of trailers is presented in this section. The review was done to gain an insight into the static and dynamic forces acting on the chassis of a trailer, and which have been incorporated into theoretical designs, as well as any potential

correlation between these theoretically assumed loads and physically measured results. The information presented is not intended to be an in depth review of the literature, but rather an analysis of the available information and data with potential applicability to this study.

Koszalka *et al.* [57] presented the design process of a frame for a semi low-loader for the transportation of oversize loads, in particular wheel and tracked machines. The design of the trailer revolved around an initial central beam design, with the rest of the frame developed around to the shape of the central beam and the load support requirements. The initial model of the frame was analysed using finite element analysis (FEA) and thereafter modified based on the initial von Mises stress results. The assumptions were that the trailer should be designed with a load capacity of 58 tons, with the quad-axle group carrying 69% of this load. The remaining load should be transferred to the fifth wheel of the prime mover. The initial bending moments in the box-type central beam were determined and the cross-sectional thicknesses was calculated taking into account the strength requirements using steel with a yield strength of 360 MPa. The FEA model was setup using shell elements and a combination of rigid beam and spring elements to represent the suspension structure. The structural analysis took into account the possibilities of payloads with different sizes placed at varying positions on the deck of the trailer. The anticipated payloads were increased by 20% to take into account dynamic load effects. This was used as a basis for the forces applied to the trailer in the static FEA model which took into account only vertical loading. The trailer geometry was continuously modified until the stresses in the structure were found to be below the yield stress of the material used for the design.

An analytical optimisation of a chassis for a dual axle flatbed trailer was conducted by Iqbal *et al.* [58]. The objective of their study was to reduce the tare mass of the trailer by 10% for a 36 ton payload. Analytical calculations were done to determine the optimum dimensions for the main beams and cross members of an existing trailer for the intended payload. Bending and shear stress calculations were undertaken using a safety factor of 1 against the material yield strength, which resulted in a mass saving of approximately 15%. Only static load effects were taken into account in this study.

Martins *et al.* presented a method to optimize the mass and material costs for a semi-trailer in [59]. FEA was used as the tool for reducing the mass of a fifteen meter long semi-trailer designed by a Portuguese manufacturer. Using ANSYS®, the material and thickness for each structural member were independently defined. Using genetic algorithm implementation from MATLAB® and linking this to the FEA software, the material thicknesses were varied according to an optimisation function to reduce the trailer mass and manufacturing costs by using standard structural sections available for the specific material thicknesses obtained from the mass optimisation. The boundary conditions and the load cases for the structural analysis were defined to simulate real life situations. Displacement constraints were applied to the kingpin and where the chassis linked to the suspension. The suspension was simulated using spring elements with an elastic constant equal to the stiffness of the actual suspension. A vertical

load equivalent to 150% of the maximum payload anticipated was used in the static analysis. Torsional effects on the chassis as a result of lateral loads was also accounted for. The initial stresses in the trailer structure, before mass optimisation, were all below 130 MPa. On completion of the optimisation study, the stresses in the structure were found to approach the yield strength of the materials used, resulting in a 6% reduction in mass and a 10% reduction in material costs.

An analysis on the effect that road roughness has on the stress distribution of a heavy duty trailer chassis was conducted by Rahman and Kurdi [60]. The study involved static analyses of the trailer chassis carrying the maximum payload for which it was designed, as well as cyclic loading using measured acceleration profiles from field tests. The results of the experiment showed that fatigue life can be improved by using suitable design factors for the loads in the static analysis. It was mentioned that further research into the effect of cyclic loading on the lifespan of the trailer is required to accurately predict fatigue failure.

Ebrahimi *et al.* [61] designed, fabricated and tested a trailer used for the transportation of hay bales. The trailer consists of a drag-chain deck fitted with hydraulic rams to incline the trailer for ease with unloading the bales. The forces on the trailer were calculated using the average mass of the hay bales and this was used as the loading conditions for the structural analysis conducted in ANSYS®. The trailer was subjected to zero load, medium load and maximum load (fully laden). Safety factors in the range of 1.6 to 3.4 against yielding were obtained from the analysis.

A design optimisation of a cane haulage vehicle was carried out by Cowling in [54]. The aim of the study was to improve the efficiency of raw sugarcane transportation using a mass optimised trailer. Cowling initially conducted an optimisation of the geometrical parameters of the trailer's main chassis beams for a reduced maximum bending moment, which resulted in a lower section modulus requirement and hence a lower mass of the main beams. This was conducted using the SCILAB® software package. FEA was then used to verify the structural integrity of the main beams for the load cases selected. Cowling chose five load cases for the analysis:

- Vertical static payload
- Braking (longitudinal load)
- Accelerating (longitudinal load)
- Cornering (lateral load)
- Torsion (due to road unevenness)

The vertical load case incorporated a design factor of 2.75 (the static load was increased by a factor of 2.75) to take into account dynamic loading in the vertical direction. Cowling chose the upper limit of the recommended range from American trailer manufactures, Wabash International and East MFG, due

to the severe operating conditions often experienced by cane haulage vehicles. For this load case, the stress results corresponded to a safety factor of 2 against yielding. The load case for braking was determined from the required braking performance of the vehicle, multiplied by a design factor of 2 to account for emergency stops and the uncertainties in braking forces. The acceleration load case was determined in a similar manner. Both the acceleration and braking load cases included the static load of the payload. The cornering load case, which accounts for the cornering forces experienced by the trailer, was taken as 0.3g in combination with the static payload.

A significant study describing the forces experienced by trailer equipment operating in a port terminal environment was conducted by Dwarika [62]. Field testing of trailers used at the Port of Durban and Port of Richards Bay was carried out using accelerometers to determine the range of accelerations the trailers are exposed to in their daily operations. This data was then used as a basis for determining appropriate load cases to be used in the design of trailers for a port terminal environment. From the data collected, Dwarika proposed the following load cases shown in Table 4.3.

Table 4.3: Trailer design load cases proposed by Dwarika [62]

Load Cases
Vertical: Payload + 1.5g
Longitudinal: Payload + 0.5g
Lateral: Payload + 0.25g

The vertical load case proposed by Dwarika incorporated a design factor of 1.5, hence the 1.5g acceleration. The longitudinal and lateral load cases were determined by applying a design factor of 2.31 and 1.25 respectively to the maximum measured accelerations from the field tests such that values of 0.5g and 0.25g could be used as the loading accelerations, in line with the recommendations of Winkler *et al.* [63]. These load cases were used to better design the existing trailers with regards to mass. Similar to the various studies described previously, static analyses were conducted by Dwarika in his finite element analysis of the trailers. The yield stress of the material was used as the criteria for determining the safety factors for the trailer designs, where factors in the range of 1.2 to 2.5 were used as per the recommendations of Ugural [64].

4.3.2.4 Load Case Selection

The investigation into the strength requirements for trailer designs has shown that there is no single comprehensive design guideline in this regard. A review of local and international standards has shown minimal structural and load capacity guidelines for the design of a semi-trailer or converter dolly chassis, while the information from manufacturers and a review of trailer design studies has shown varying design requirements. The information obtained from trailer manufacturers has shown that these

designs have developed through experience, based on the requirements for each type of trailer and its operating environment. This can be seen by the absence of a specific design standard detailing the structural requirements for a trailer. A common method of analysis found in the literature, as well as from manufacturers, is the use of static load cases incorporating a design factor [54, 62, 61, 60, 57]. This allows for a static analysis to be conducted while taking into account the effects of fatigue without a dedicated dynamic analysis [54, 62]. The same approach has been adopted in this study. Table 4.4 shows the load cases selected for the MTS design, adopted from information presented in [54] and [62].

Table 4.4: Load cases for the present MTS design

Load Case	Safety Factor
Vertical: Payload + 2g vertical acceleration	1.2 – 2.5 (Against yielding)
Longitudinal (Braking): Payload + 0.52g longitudinal acceleration	
Lateral (Cornering): Payload + 0.25g lateral acceleration	
Longitudinal (Accelerating): Payload + Coupling forces during take-off	

From [54], a design factor of 2 is used for the MTS for the vertical and braking load cases. The factor is selected from the lower region of the range recommended in [54] due to the predominantly uniform operating conditions expected for the MTS. Dynamic loading effects are expected to be minimal due to the flat terminal yard, careful loading of containers onto the trailer equipment and gradual braking of the trailers which was noticed from observations at Pier One. An acceleration of 2g for the vertical load case has been determined by applying the design factor of 2 to the static load (1g), while an acceleration of 0.52g has been obtained by applying the design factor to the required braking performance of the proposed MTS (0.26g) as set out in SANS 1447-2 [46], which is a design requirement for trailers operated in the Durban Container Terminal. This is consistent with the method implemented by Cowling [54]. The lateral load case has been adopted from [62], where an acceleration of 0.25g is suggested. This value incorporates a design factor of 1.25 to the maximum measured lateral acceleration of the trailers at the Durban Container Terminal.

To account for the effect of the forces on the trailer chassis and converter dolly during take-off, the forces at the coupling points, arising from the tractive effort of the terminal tractor, are used for the accelerating load case. These horizontal forces are applied directly onto the semi-trailer kingpin and the towing eye of the converter dolly, replicating the typical loading scenario expected during take-off.

For the braking, cornering and accelerating load cases the payload, together with a vertical acceleration equivalent to gravity, is applied. The recommended range of safety factors (1.2-2.5) from [64] is adopted for the MTS design for the abovementioned load cases.

4.3.3 Manoeuvrability

The turning ability of the MTS within the confinement of Pier One is an important feature in the design of the vehicle. With any type of trailer system, more space is required for the execution of a turn as the vehicle combination becomes longer. The increase in the required space is due to a phenomenon known as off-tracking, where the centreline of the steering axle of the tractor does not coincide with the centreline of the axle set of the towed trailer as it traverses a curve or turn. The swept path of the vehicle during the turn is defined as the distance between the path of the front outside wheel of the tractor and the path of the rear inside wheel of the last trailer in the combination [65]. This is used to determine the area required to manoeuvre the vehicle. Figure 4.7 depicts the off-tracking phenomenon and the resulting swept path of a TTU. Research conducted by Sayers [66] has shown that for reduced off-tracking and hence a reduced swept path, the wheel base of a trailer should be kept to a minimum. This can be seen from Equation (4.1) [66] which describes the maximum off-tracking (OT) of a TTU as a function of the tractor and trailer wheel bases (L_1 & L_2), the kingpin offset (KO) and radius of the turn (R_1) (referenced to Figure 4.8). This relationship holds true for multiple trailer combinations at low speeds (below 40 km/hr) [66].

$$OT = R_1 - R_3 = R_1 - \sqrt{R_1^2 + KO^2 - L_1^2 - L_2^2} \quad (4.1)$$

Figure 4.8 shows the maximum off-tracking that occurs for a vehicle combination once a turn has reached “steady state” i.e. the turn is large enough for the transient off-tracking to have reached a steady value where the off-tracking becomes constant. In practice, most turns do not reach a steady state since the curve path being followed by the leading axle is not long enough to achieve this.

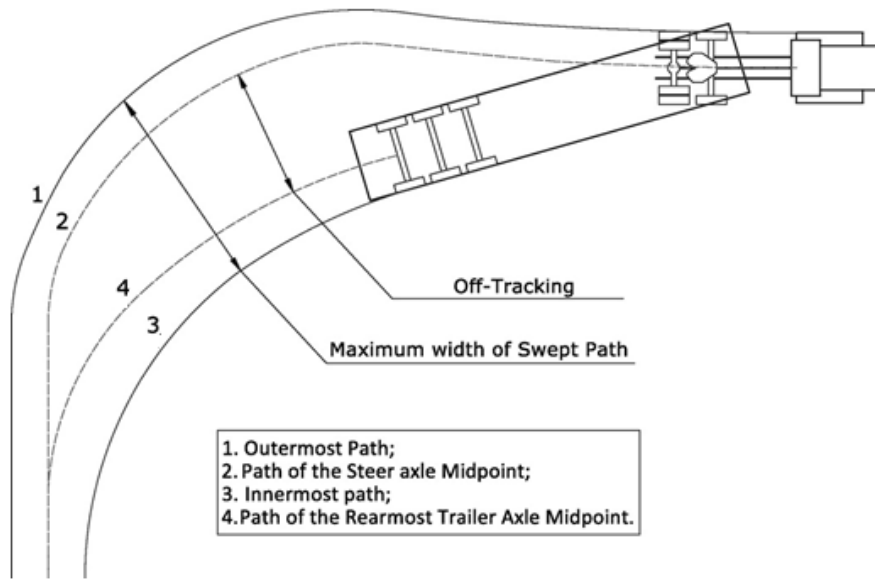


Figure 4.7: Off-tracking and swept path [67]

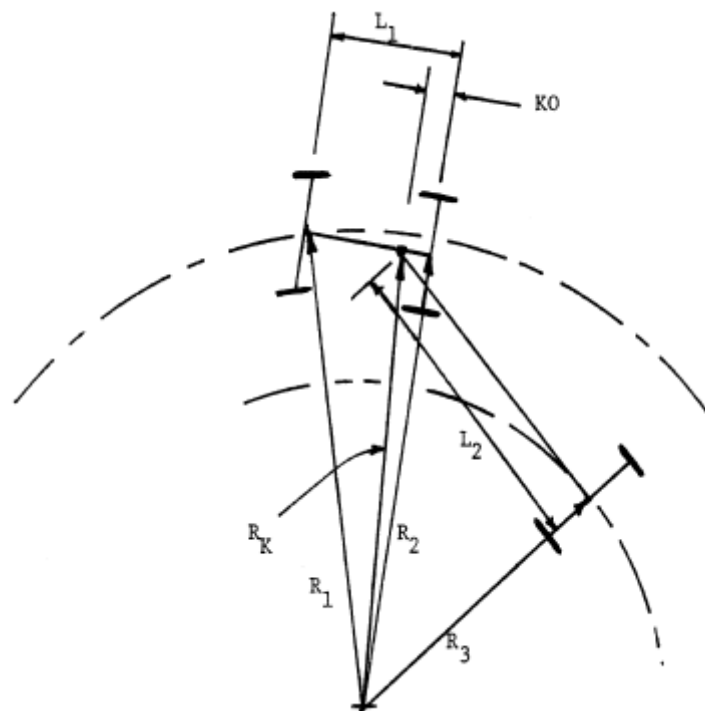


Figure 4.8: Maximum low speed off-tracking for a TTU [66]

Sayers [66] showed that the steady state off-tracking performance is directly related to the off-tracking experienced during the transient phase of a turn. The analysis of the transient off-tracking phenomenon is considerably more complex than the maximum steady state off-tracking prediction represented by Equation (4.1) and is generally predicted using turning manoeuvre software packages. The software package BricsTurn[®] is used in this study to verify the manoeuvrability of the designed MTS.

While the observations in [66] hold true, minimising the wheelbase of a trailer depends largely on the load carrying capacity of the axles and the allowable distance between the trailer's kingpin and the rear of the driver's cabin of the tractor. The kingpin setback, a feature of the geometrical vehicle parameters shown in Figure 4.9, is limited by the swing clearance between the first trailer and the tractor to ensure that no interference occurs between the two during turning manoeuvres. The swing clearance between the trailer and tractor is depicted in Figure 4.10. Once the kingpin setback is determined, the position of the axle group can be calculated using the maximum load capacity of the axle group for a minimum wheelbase. These parameters are taken into account during the current MTS design.

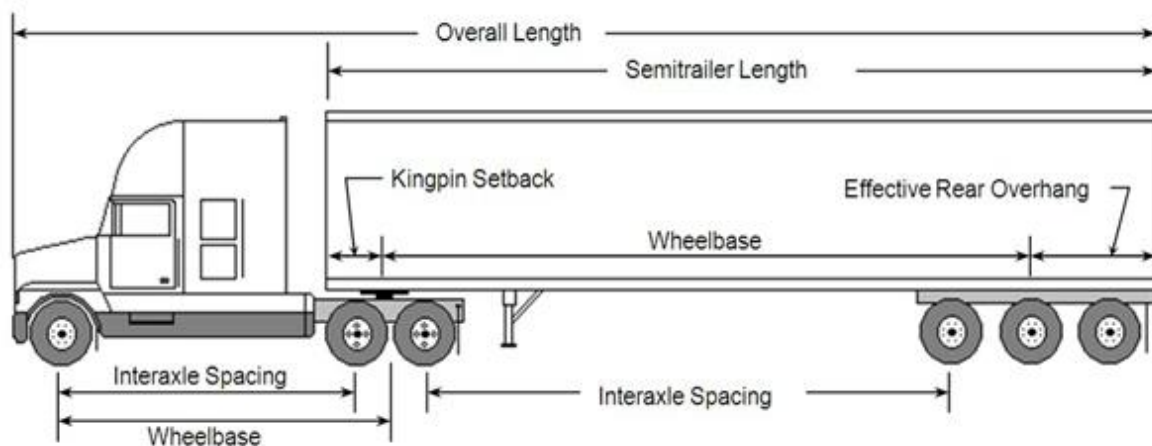


Figure 4.9: Trailer geometric parameters [68]

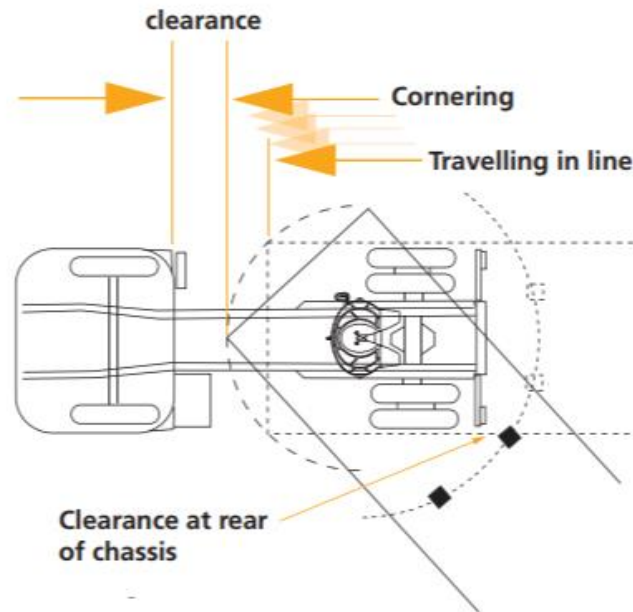


Figure 4.10: Swing clearance [69]

4.4 Material Selection

Material selection plays a vital role in the mass, strength and cost of a trailer design. Together with design optimisation methods, manufacturers have considered various alternatives with regards to material types in an effort to reduce the tare mass of trailers and the associated manufacturing costs, without compromising on the load carrying capability of these vehicles. The mechanical and physical properties of a material such as its yield strength, density, elasticity and resistance to fatigue plays an important role in making an appropriate selection. A common method of comparing materials is by using their modulus of elasticity/density and yield strength/density ratios as a method of determining potential mass savings [54]. These factors, together with the cost and availability of each material, are compared in this study to determine a suitable material for the indigenous MTS design.

While many material types have been used in the design of trailers such as aluminium and composite materials, steel is by far the most commonly used material for trailers intended for heavy payload applications due to its availability, ease of manufacturing (weldability) and resistance to fatigue. For these reasons, this investigation is limited to the steel grades, ranging from mild steels to high strength steels, most commonly used for trailer designs.

4.4.1 Structural Steel

Structural steel is an iron alloy which contains a 0.05% – 0.25% carbon content by weight. Other alloying elements can also be found in these steels such as manganese, silicon, phosphorous and sulphur which are used to augment the metal to produce the desired mechanical properties [70]. Structural steel is the most common form of steel used in the design of trailers due to it being cheaper

than high strength steels coupled with easy manufacturing techniques [54, 62, 58]. Structural steels have yield strengths in the range of 235-450 MPa. Table 4.5 shows the different grades of structural steel and its mechanical properties, locally produced and available in South Africa, used in the design of trailer equipment [62, 60].

Table 4.5: Mechanical properties of structural steel grades [56]

Grade	Yield Strength (MPa)	Tensile Strength (MPa)	Density (kg/m ³)	Elastic Modulus (GPa)	Yield Strength/Density (10 ⁻³)	Elastic Modulus/Density (10 ⁻³)
S235	235	360	7850	200	29.9	25.4
S275	275	430	7850	200	35.0	25.4
S355	355	510	7850	200	45.2	25.4
S450	450	550	7850	200	57.3	25.4

4.4.2 High Strength Steel

High strength steels, commonly known as HSLA steels (high-strength low-alloy), are steel alloys containing elements such as cobalt, molybdenum, titanium and vanadium that are added to achieve enhanced mechanical properties. The high strength is obtained from precipitation hardening by micro alloying elements and then carefully controlling the processing parameters during hot rolling [71]. The high strength steels available in South Africa are Domex and Supraform, manufactured by SSAB and Arcelor Mittal respectively, which have yield strengths in the range of 460-600 MPa. Domex has been extensively used by South African trailer manufacturers for reduced tare mass designs in low payload applications [54]. Table 4.6 shows the mechanical properties of the various grades of Domex and Supraform.

Table 4.6: Mechanical properties of HSLA steel grades [71, 72]

Grade	Yield Strength σ_y (MPa)	Tensile Strength σ_{UTS} (MPa)	Density ρ (kg/m ³)	E (GPa)	$\frac{\sigma_y}{\rho}$ (10 ⁻³)	$\frac{E}{\rho}$ (10 ⁻³)
Domex 460 MC	460	520	7870	210	58.4	26.6
Domex 500 MC	500	550	7870	210	63.5	26.6
Domex 550 MC	550	600	7870	210	69.9	26.6
Supraform TM 460	460	530	7850	205	58.5	26.1
Supraform TM 600	600	650	7850	205	76.4	26.1

4.4.3 Material Comparison

An evaluation matrix is used to compare the materials presented in 4.4.1 and 4.4.2 by rating them based on their material properties such as the elasticity/density and yield strength/density ratios, resistance to fatigue, as well as cost and availability. The materials are rated relative to each other using a linear 5 point scale (-2 to 2) based on the minimisation of cost and mass of the design, with -2 being very bad, 0 being neutral and 2 being very good. The final scores are obtained by adding the individual ratings of each property for the material.

As can be seen in Table 4.7, the HSLA steels scored better for the yield strength/density ratio; the higher yield strength dominated the result due to all the steels compared having very similar densities. The stiffness/density ratio showed very similar results for the high and low strength steels due to their closely related elastic modulus, with the high strength steels scoring marginally higher than the low strength steels. Ratings for fatigue resistance also favoured the higher strength steels due to an increased tensile strength which directly improves its resistance to fatigue [73]. The cost and availability factors influenced the final scores considerably, mainly due to the significantly greater cost and lower availability of the HSLA steels. Even though these steels are available locally, they are not produced as frequently as structural steels due to a much lower demand and are thus not readily available at all times. The HSLA steels, which can cost up to three times more than structural steels, are limited in size variations and thickness while structural steels are produced in multiple thicknesses and sizes. Standard sections such as I-beams and C-channels are produced using structural steel grades in numerous sizes, while the range of size variations for these sections in the high strength steel grades are limited.

Table 4.7: Material evaluation matrix

Material	$\frac{\sigma_y}{\rho}$	$\frac{E}{\rho}$	Fatigue Resistance	Cost	Availability	Final Score
S235	-1	0	-1	2	2	2
S275	-1	0	0	2	2	3
S355	1	0	1	2	2	6
S450	1	0	1	1	2	5
Domex 460 MC	1	1	1	0	0	3
Domex 500 MC	2	1	2	-1	-1	3
Domex 550 MC	2	1	2	-2	-1	2
Supraform TM 460	1	1	2	-1	0	3
Supraform TM 600	2	1	2	-2	-1	2

As mentioned in chapter 4.4.2, the existing semi-trailers at Pier One could be used as the individual semi-trailers in a short MTS coupled together via a converter dolly, however an opportunity exists for a better optimised semi-trailer design with regards to a lower tare mass which could lead to a lower overall product cost in order to maximise the operational cost reduction for the terminal created by the use of MTSs. Using a higher strength material will result in a lower tare mass, however the cost benefits may be minimal when compared to the existing semi-trailers due to the lower mass/higher cost trade-off. As can be seen from Table 4.7, grade S355 has scored the highest of all the materials evaluated mainly due to its low cost and its availability in the required shapes, it has been selected as the material to be used in the design of the MTS.

4.5 Standard Components

4.5.1 Axles

The axles selected for a trailer design depends on several factors, including the nature of the trailer's physical geometry, its operating speed and the magnitude of the payload being transported. Part of the technical specific requirements for trailers operated at Pier One is the use of tandem axles fitted with a braking system to ensure compliance to SANS 1447-2 [45]. For the MTS design, GO Heavy Duty Axles which are rated at maximum load of 22 700 kg [74] are utilised due to their high load capacity when compared to other axles available in the market. These axles, which are designed and manufactured within South Africa, have a track length of 1 930 mm and main beam centre mountings of 1 000 mm [74]. S-cam drum brakes are present which enables the axles to be compliant with the required braking performance as set out in SANS 1447-2 [75]. The axles are manufactured using solid 130 mm diameter round cross-sections of EN 19 steel. Figure 4.11 depicts the GO Heavy Duty Axle.

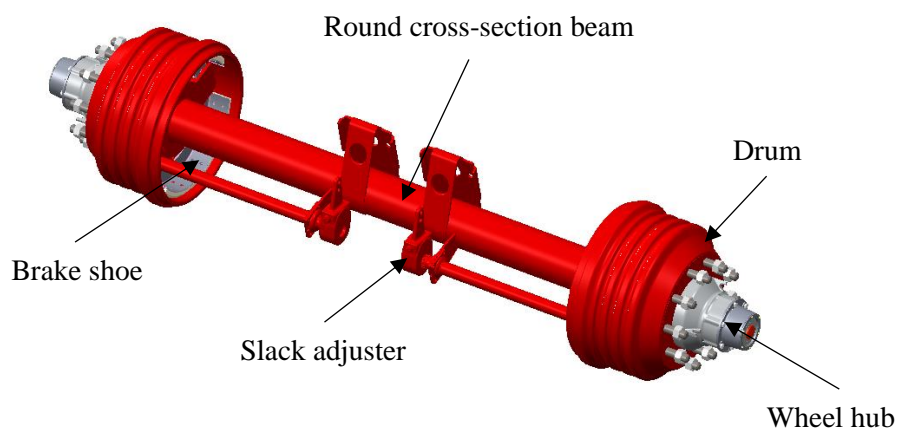


Figure 4.11: GO Heavy Duty Axle [76]

4.5.2 Suspension

The function of a suspension is to connect the chassis of the vehicle (trailer or converter dolly) to the axles by means of a mechanical device which reduces vibrations occurring during motion due to the dynamic effects created by load movement and road unevenness. Different types of suspensions exist for trailer equipment such as air, hydraulic and leaf spring suspensions [54]. Leaf spring suspensions are most commonly used for container carrying trailers due to their low cost and ease of application when compared to the other systems mentioned. While their performance in off-road usage is lower than that of air and hydraulic suspensions [54], its performance in a terminal yard environment will be adequate due to the flat, uniform road surface. They are thus chosen for use in the present MTS design. The leaf spring suspension system selected is the GO Heavy Duty Tandem Suspension with a load capacity of 46 000 kg. The over slung suspension configuration (where the axles are fastened to the bottom of the leaf spring sets) is used for the semi-trailers, while the underslung configuration (where the axles are fastened to top of the leaf spring sets) is used for the converter dolly, purely for geometric reasons. The axles and suspension assembly is commonly referred to as a bogie. These configurations are shown in Figure 4.12 and Figure 4.13.

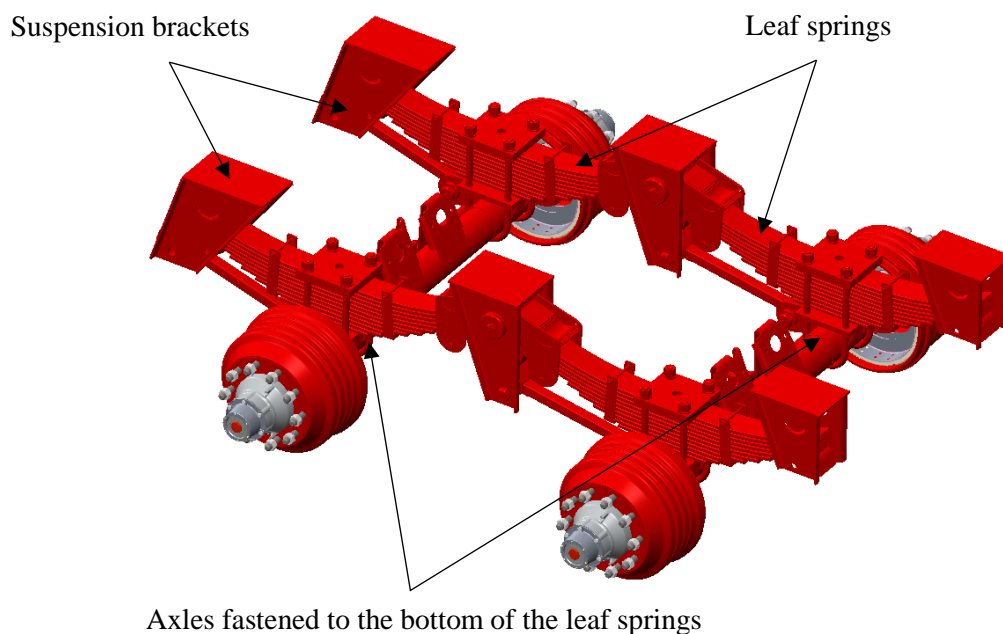


Figure 4.12: GO Heavy Duty Tandem Suspension - over slung configuration for semi-trailer [76]

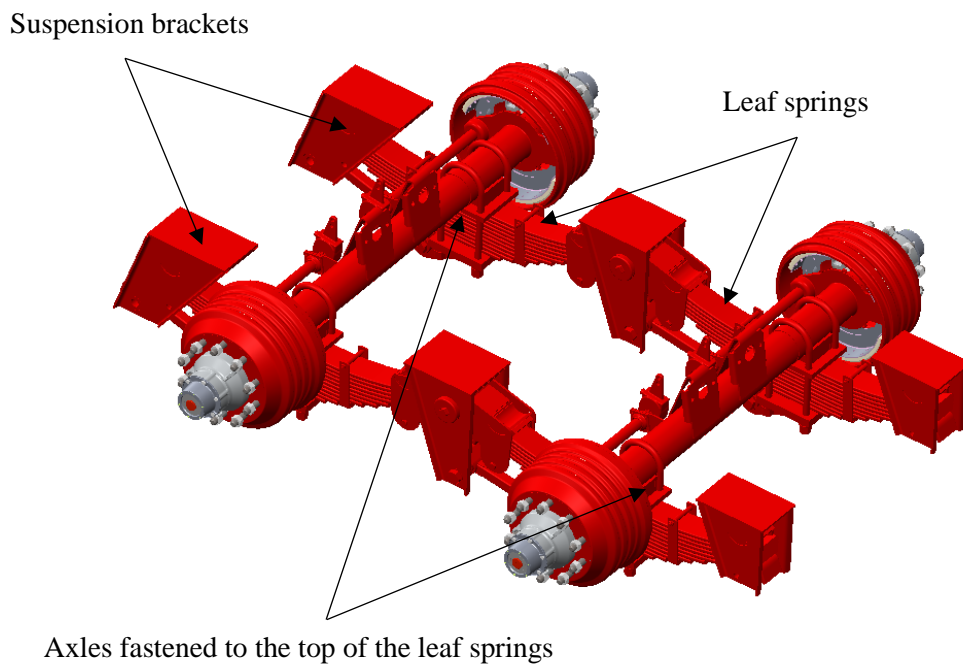


Figure 4.13: GO Heavy Duty Tandem Suspension - under slung configuration for converter dolly [76]

4.5.3 Rims and Tyres

The selection of suitable rims and tyres for an MTS depends on the maximum axle load which the wheels must safely handle as well as the intended operating environment. The rim selected for use in the MTS design is the Metaforge heavy duty rim (Part Number: MF900225HD), while the tyre selected is the Continental Terminal Tyre (Part Number: 0730044). This rim and tyre combination has a maximum load capacity of 6 300 kg, thus four of these will be used on each axle to satisfy the load carrying capacity of the axles. The Continental Terminal Tyre, apart from its load capacity, has been selected due to its greater resistance to wear when compared to standard trailer tyres [77]. Both these items are available in South Africa.

4.5.4 Couplings

The mechanical coupling equipment used for interconnectivity of the trailers in the MTS set and connection to the terminal tractor is selected from the range available from Jost South Africa, a local manufacturer and supplier of commercial vehicle components. Kingpins and towing hitches will be fitted to the semi-trailers, while a fifth wheel and a towing eye will be incorporated into the design of the converter dolly. The strength requirement for the mechanical coupling equipment selected is based on the D-value calculation which is used in trailer design [69] and is dependent on the mass of the vehicles before and after each coupling point. These calculations which are used to select the appropriate mechanical couplings are presented in Chapter 5.

4.6 Chapter Summary

This chapter presented the design considerations surrounding the MTS for this study. Different MTS configurations were investigated, with the semi-trailer led MTS being selected as the most appropriate configuration to be used for the design. The functional and technical requirements for trailer systems designed to operate at Pier One were discussed for implementation onto the MTS. A survey of the literature on the structural strength requirements for trailers was presented, yielding the load cases and safety factors to be incorporated into the design. The locally available materials and standard trailer components which will be used in the design were also assessed and presented. One of the guiding principles in the design of the MTS is the use of locally available components so as to reduce manufacturing costs and to raise the likelihood of the design being implemented at the Durban Container Terminal. Literature surrounding the manoeuvrability of trailers and the influence of the wheelbase dimension on the turning performance of a vehicle was discussed.

5 Multi-Trailer System Design

5.1 Introduction

This chapter details the design of the MTS proposed for use at Pier One of the Durban Container Terminal with the aim of reducing the operational cost of the waterside horizontal transport system. The geometric design of the semi-trailers and converter dolly for the MTS using the material and standard components discussed in Chapter 4.4 and 4.5 is presented, including the structural analysis conducted in ANSYS® using the load cases discussed in Chapter 4.3.2.4. The MTS design incorporated the port terminals functional and technical requirements, as well as the geometric factors affecting manoeuvrability.

Due to the port not having any existing terminal tractors with a load capacity and tractive effort capable of moving the gross mass of the proposed MTS, a suitable tractor was first selected for this application. This was to ensure that the MTS is designed with the appropriate geometrical features and clearances to allow it to function without any structural interference with a prime mover that is capable of hauling the required load. The Kalmar TR626i terminal tractor, discussed in Chapter 5.2, is selected for use as the prime mover for the MTS due to its load haulage capacity and fifth wheel coupling connection, which is a requirement for the semi-trailer led MTS design configuration chosen.

5.2 Terminal Tractor

The Durban Container Terminal currently owns four different models of terminal tractors, each having a maximum gross combinational mass (GCM) within the range of 75 000 - 90 000 kg. These models are the MAFI MT25YT and MT30YT, the Terberg YT222 and the CVS Ferari FR270. A tractor's GCM rating is an indication of the maximum trailer mass (combined tare mass and payload) that the tractor can move at a rated speed determined by the vehicle manufacturer. The GCM rating includes the mass of the tractor itself, thus the mathematical difference between the GCM rating and the tractor mass gives the maximum trailer mass that the tractor can safely move. Since the MTS in question has a container carrying capacity of four TEUs which results in a maximum payload of 121 920 kg (30 480 kg per TEU), the existing tractors cannot be considered for use as the prime mover in the MTS due to the maximum mass of the MTSs payload exceeding the GCM rating of these tractors. For this reason, a tractor capable of hauling the required load of the MTS was selected for which the MTS could be designed. The tractor selected for this application was the Kalmar TR626i terminal tractor, shown in Figure 5.1 with its general assembly dimensions.

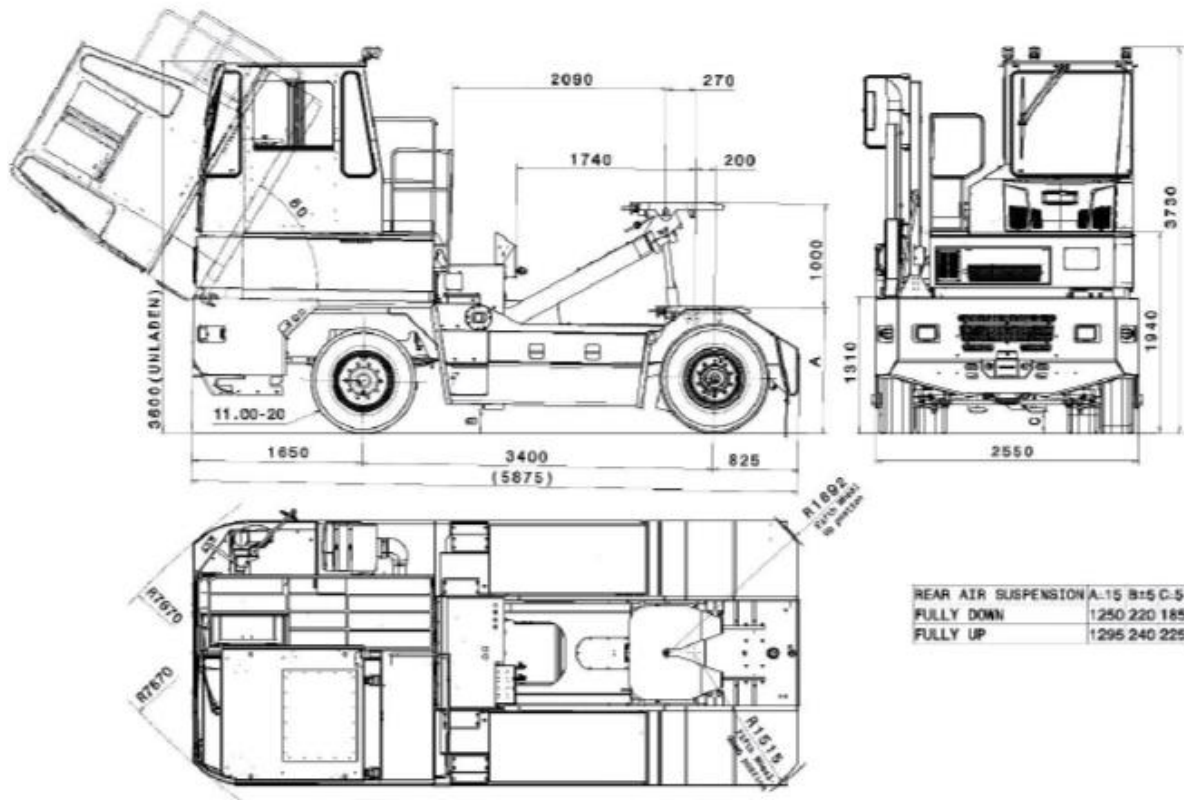


Figure 5.1: Kalmar TR626i terminal tractor [78]

The TR626i terminal tractor has a maximum GCM of 240 000 kg with a tare mass of 14 000 kg, allowing for the use of an MTS with a total mass of up to 226 000 kg. While the proposed MTS will have a total mass considerably lower than the maximum mass which the tractor can safely handle, use of this tractor will result in better acceleration and speed capabilities when compared to a tractor with a lower GCM rating. As mentioned in Chapter 4.2.2, a semi-trailer led MTS has been selected as the configuration for the proposed design, therefore a tractor with a fifth wheel coupling is required for connection to the leading trailer in the MTS set. This vehicle contains a hydraulically lifted fifth wheel coupling mechanism, capable of withstanding a maximum vertical load of 32 000 kg imposed by the trailer it is connected to. This tractor model is designed specifically for use in heavy payload applications in a port terminal environment, in particular for the use as the prime mover in an MTS [79].

5.3 System Configuration

The system configuration of the proposed MTS is a semi-trailer led system with two trailers in the set. The arrangement selected was that of two identical semi-trailers coupled together via a converter dolly which allows for the interchangeability of trailers within the set and connection to the tractor via a fifth wheel coupling, as well as allowing for the use of each semi-trailer separately to form a TTU for use during the vessel loading operation. This configuration was determined based on the results of the DES presented in Chapter 3 which showed that it is beneficial to use a two-trailer MTS for the vessel unloading operation, while the use of either a two-trailer MTS or a TTU showed similar results for the loading operation. Figure 5.2 shows the notional configuration for the MTS design consisting of the tractor, identical semi-trailers and a converter dolly.

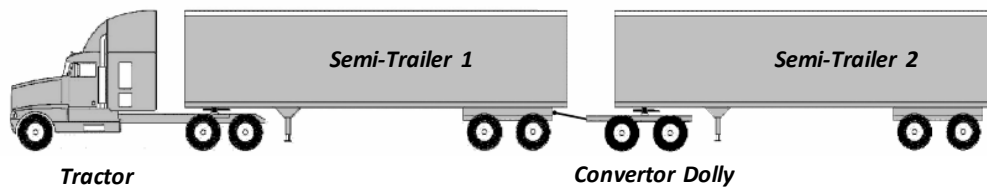


Figure 5.2: Notional MTS configuration

The design of the MTS consists of two main assemblies; the design of the semi-trailers and the design of the converter dolly. For this study, the semi-trailer used in the MTS is designed first based on the geometry and magnitude of the payload to be transported, taking into account the geometry of the terminal tractor selected. The converter dolly was designed thereafter based on the geometry of the semi-trailers and its imposed loads.

5.4 Semi-Trailer Design

5.4.1 General Structural Arrangement

The semi-trailers used for container movement within a port terminal environment are generally of a skeletal type and are constructed from two longitudinal centre beams joined together using cross members to create the trailer chassis. The lengths of the beams are determined from the length of the ISO containers which the semi-trailer is intended to transport, while the distance between the beams are governed by the centre mounting distance of the axles. Unlike trailers intended for road use which have twist locks fitted to the chassis for securing the containers at its corner castings to prevent movement, container terminal trailers are designed with guides for positioning and securing the containers, which allow for the corner castings of the containers to be accessible at all times. This is to allow for containers to be loaded onto the trailers without removing the twist locks which are used to secure the containers that are stacked on a vessel [45]. The guides are fitted at the front, back and sides of the trailer to

accommodate the width and length of the ISO containers. The suspension for the semi-trailer is fitted to the bottom of the longitudinal beams towards the rear end of the beam, while the kingpin is fitted to a plate which is welded onto the bottom of the front end of the beam. Figure 5.3 depicts a container terminal semi-trailer showing the structural features described. This general structural arrangement is used as a guideline for the geometrical setup of the structural members which forms the chassis of the semi-trailer designed for the MTS.

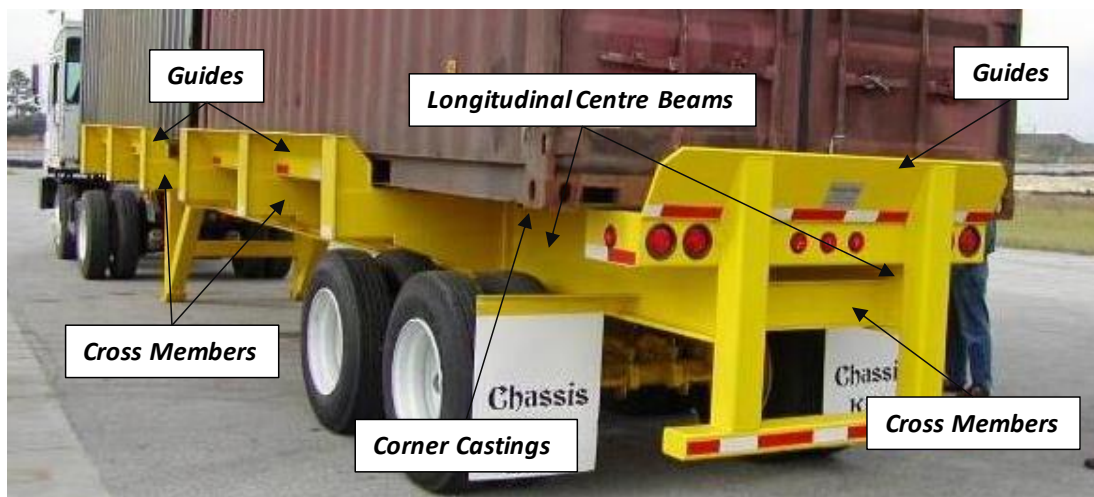


Figure 5.3: Container terminal semi-trailer [24]

5.4.2 Longitudinal Centre Beams

The longitudinal centre beams can be viewed as the most critical structural members of a trailer due to them being the foundation upon which the rest of the chassis is designed [62]. Each beam consists of a single I-section with a varying web height along its length based on the clearances required for connection to the tractor, the height of the axle and suspension assembly for levelled coupling purposes, as well as the strength required due to the design loads and safety factors. The length of the beam is dependent on the number and type of ISO containers required to be transported. Each semi-trailer in the MTS must be able to transport a maximum of 2 TEUs at any given instance, which is one 40 ft. container or two 20 ft. containers. Table 5.1 shows the external dimensions and gross mass of these container types.

Table 5.1: ISO Container external dimensions and maximum gross mass

		20 ft. Container	40 ft. Container
External Dimensions	Length (m)	6.058	12.192
	Width (m)	2.370	2.370
	Height (m)	2.591	2.591
Maximum Gross Mass (kg)		30 450	30 450

As shown in Table 5.1, a single 40 ft. container has a length of 12.192 m, while two 20 ft. containers have a combined length of 12.116 m. Based on these dimensions, the longitudinal beams for an MTS semi-trailer must have a minimum length of 12.192 m for it to be able to transport the required container combinations. In practice, these beams are manufactured to be slightly longer than the maximum container length to allow for a clearance between the front and rear container guides which are mounted onto the ends of the beam, as well as for a clearance between the two 20 ft. containers when loaded onto the semi-trailer. Transnet Engineering’s trailer design team requires that a clearance allowance of 5% is used in the design of the longitudinal beams for their container terminal trailers and this has proven adequate for container loading [80]. The same approach is adopted for this design, resulting in a length of 12.8 m for the semi-trailer longitudinal beams.

The cross-sectional shape selected for the longitudinal beams is that of an I-section due to its efficacy with supporting loads which cause bending of the structure and its resistance to flexure [62, 81]. I-sections have been successfully used as the shape for longitudinal beam designs in the trailer industry for many years due to their structural effectiveness and ease of manufacturing. Figure 5.4 shows the orientation of the flanges and web which form an I-section, together with key parameters.

The longitudinal beam consists of three steel plates welded together to form the I-section. The two flanges (top and bottom) are connected to a single web via fillet welds. The web height, also known as the flange depth, is a variable feature of the longitudinal beam while the web thickness together with the width and thickness of the flanges are constant along its length.

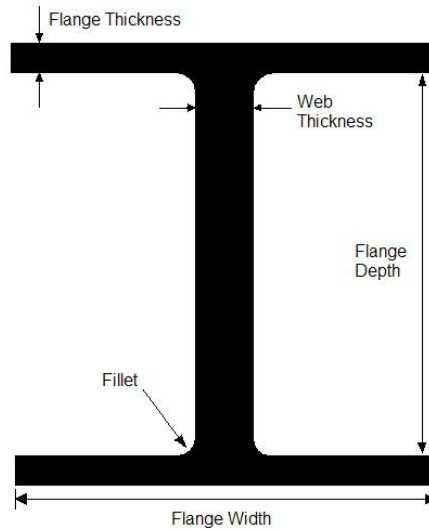


Figure 5.4: I-section parameters [82]

The flange width was selected based on the size required for mounting the suspension onto the beam, while the web height varies along the length of the beam based on the clearances required for connection to the tractor and the height of the bogie assembly for levelled coupling purposes, as well as based on the strength requirements for the design. For these reasons, a flange width of 130 mm and a web height varying between 240 mm and 530 mm was preselected for the longitudinal beam design, which is in accordance with the recommendations from [62] for the general beam dimensions of a container terminal trailer. Figure 5.5 shows the web dimensions of the longitudinal centre beam determined from the above-mentioned considerations.

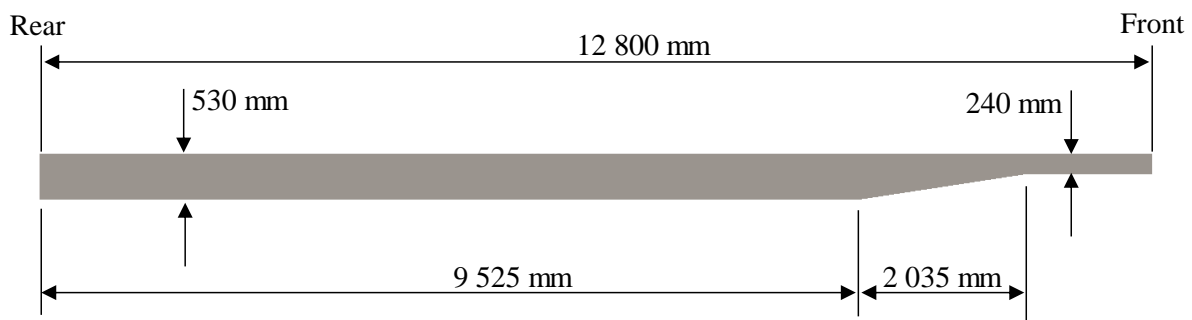


Figure 5.5: Longitudinal centre beam - Web dimensions

The thickness of the web and flanges for the required design safety factors are dependent on the load transferred to the longitudinal beam from the container-supporting cross members, as well as from the portion of the container base which rests directly on the top flange of the beam. By allowing a portion of the base to rest on the top flange, the load on the container-supporting cross members is reduced, resulting in lower material stresses in those members. These cross members are positioned transversely to the web of the longitudinal beam, taking into consideration the loading of 20 ft. and 40 ft. containers

to ensure that access to the corner castings and fork lift pockets are not obstructed, as well as taking into account space requirements for mounting of the kingpin. The function of the cross members in a trailer chassis is twofold; to support the vertical load of the containers and to maintain the shape of the structure during torsional loading. A review of trailer chassis design, in particular that of the effect of cross bracing a ladder frame structure, revealed that between six and twelve cross members are typically recommended to support the payload. This recommendation ensures adequate stiffness of the structure without a substantial increase in mass [54, 83, 84, 85]. While the amount of cross bracing required is highly dependent on the magnitude of the payload and the induced dynamic loads due to the operating environment of a trailer, the above findings were applied to the design of the MTS semi-trailers and verified using FEA methods in Chapter 5.4.8. As shown in Figure 5.6, eight container-supporting cross members are used for the semi-trailer design, with their position and transferred loads (F_1) depicted relative to the longitudinal beam. The load where the container rests directly on the top flange is depicted by the uniformly distributed load (W). The highest vertical loads occur when transporting two 20 ft. containers, with the cross-member load being split equally. The preliminary thickness of the web and flanges of the longitudinal beam are calculated using the loads shown in Figure 5.6 with Table 5.2 to achieve the strength required based on a design factor of 2 for the vertical load case. The suitability of the calculated thicknesses for all other load cases is assessed in Chapter 5.4.8 using FEA methods on completion of the geometrical design of the chassis. Each beam carries half the maximum 20 ft. container payload of 60 900 kg. Table 5.2 provides the magnitude of the parameters from Figure 5.6.

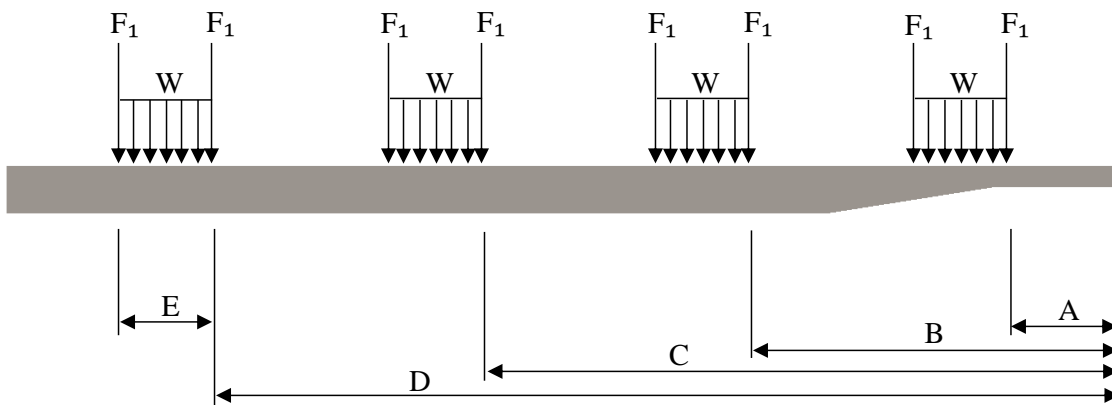


Figure 5.6: Imposed loads on the longitudinal beam

Table 5.2: Longitudinal beam load parameters

Parameter	Unit	Magnitude
F₁	kg (kN)	566 (5.56)
W	kg/m (kN/m)	7364 (72.24)
A	m	1.18
B	m	4.62
C	m	7.08
D	m	10.52
E	m	0.88

The longitudinal beam is supported by the bogie towards the back end of the beam (left section in Figure 5.5) and the fifth wheel of the tractor towards the front end of the beam. The position of these supports, detailed in Chapter 5.4.4 and 5.4.6, results in bending and shear stresses experienced along the beams length (see Figure 5.17 for the support layout). Figure 5.7 shows the bending moment diagram while Figure 5.8 shows the shear force diagram for the beam as a result of the imposed loads, taking into consideration a design factor of 2 in the vertical direction. Note that the zero position on the horizontal axis for both the graphs refers to the front end of the beam.

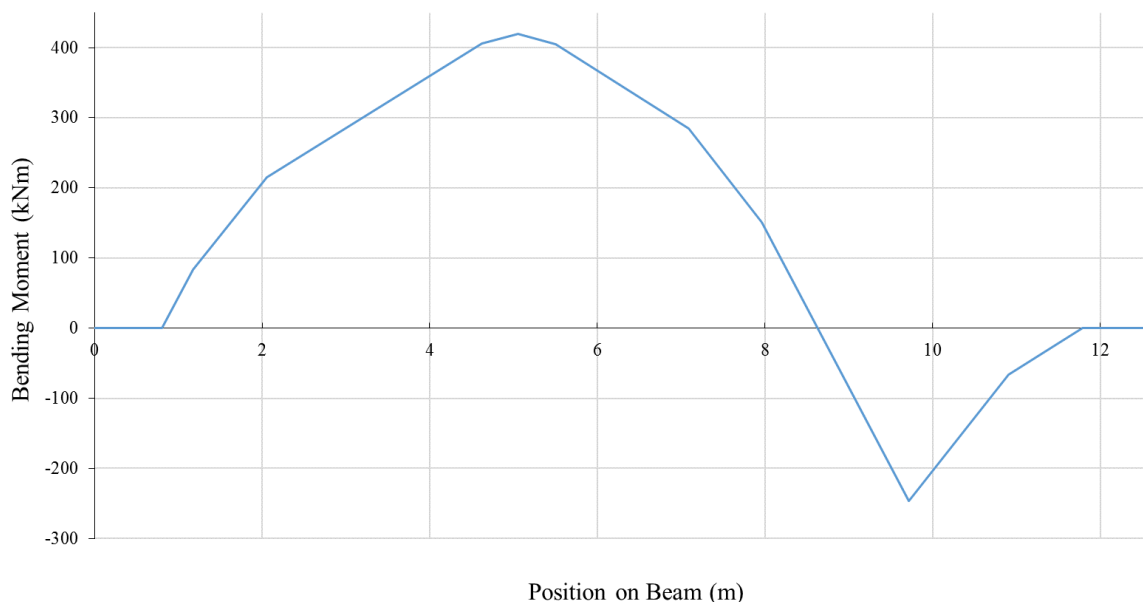


Figure 5.7: Bending moment diagram – longitudinal centre beams

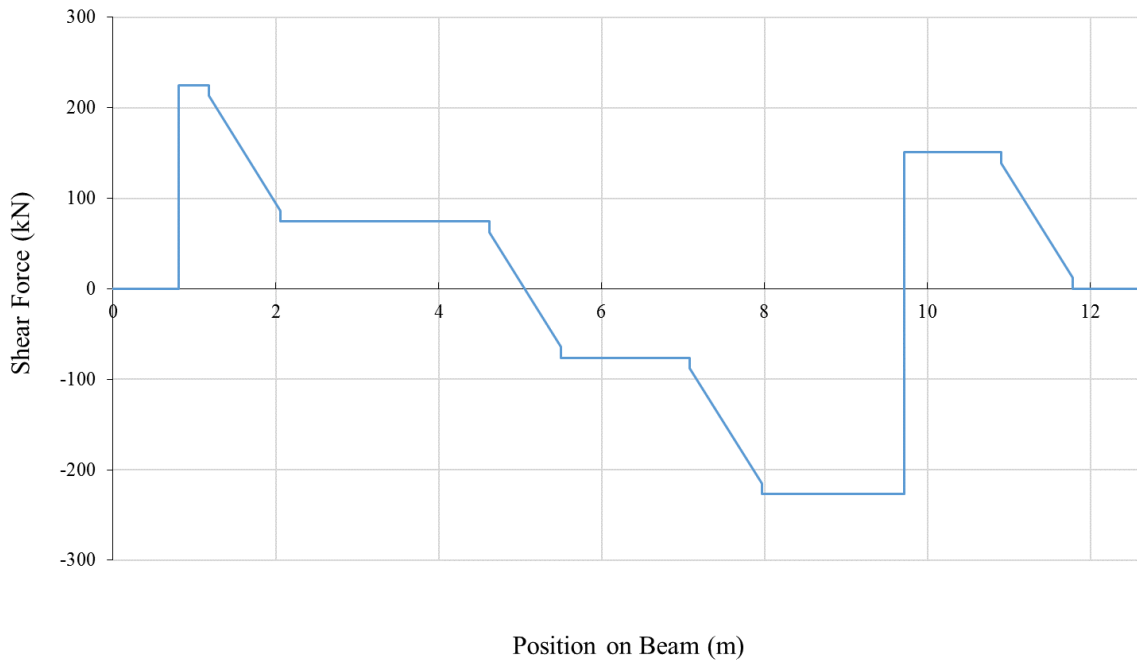


Figure 5.8: Shear force diagram – longitudinal centre beams

Bending moment capacity is generally the limiting factor for the static load case, thus the bending stresses as a result of the bending moment experienced by the beam are used to determine the material thicknesses for the required design strength [54]. The maximum bending moment experienced by the longitudinal beam as a result of the imposed loads is 419.54 kN.m at a distance of 5.05 m from the front end of the beam (see Figure 5.7). Using this maximum bending moment and a safety factor of 1.2 [64] against the yield strength of S355 steel (as per the deductions reached in Chapters 4.3.2.4), the thickness combinations for the flanges and web to achieve the required strength were obtained using Equation (5.1), where $\sigma_{Bending}$ is the bending stress, M is the bending moment and c is the distance from the neutral axis to the flange surface.

$$\sigma_{Bending} = \frac{M \cdot c}{I} \quad (5.1)$$

The lower limit of the safety factor range was chosen with a view to obtain a reduced mass while maintaining the required strength of the beam. The thickness combinations of the flange and web was determined for a maximum bending stress of 296 MPa (safety factor of 1.2 against a yield stress of 355 MPa). The effect of the flange and web thicknesses on the overall mass of the longitudinal beam is shown in Figure 5.9 for a range of 5-20 mm. This range was chosen since it spans the commonly used material thicknesses for the design of longitudinal beams in trailers [54, 62, 85, 58].

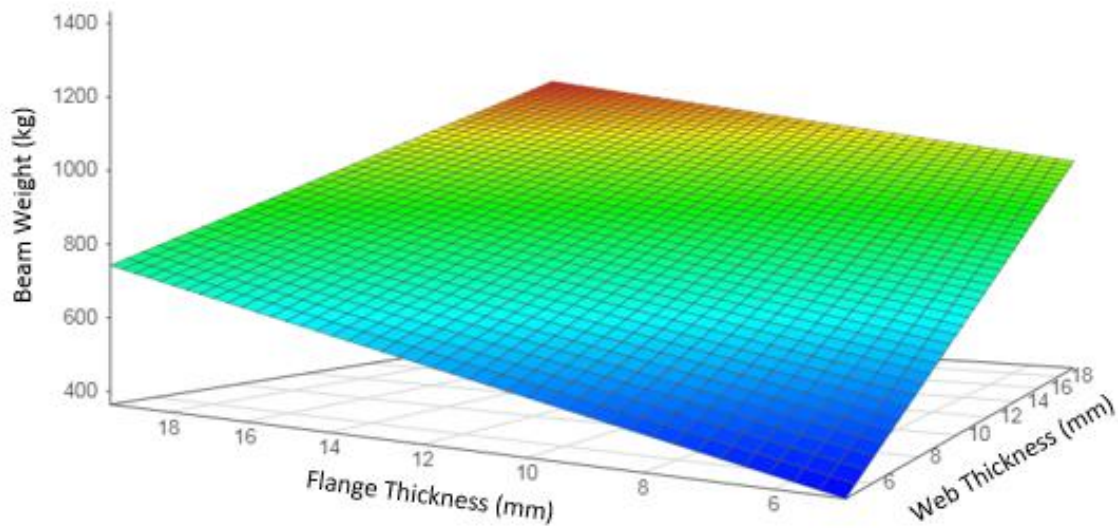


Figure 5.9: Effect of flange and web thicknesses on the overall mass of the longitudinal beam

Table 5.3 shows the thickness combinations of the web and flanges for the safety factor and design loads used, as well as the resulting mass of the beam for each thickness combination. These material thicknesses were limited to that which is readily available in the Republic of South Africa for the selected S355 steel grade for manufacturing purposes, thus the thickness values yielded by Equation (5.1) were rounded off to the nearest available sizes.

Table 5.3: Flange and web thickness combinations

Flange Thickness (mm)	Web Thickness (mm)	Mass (kg)	Safety Factor
12	20	1251	1.22
16	16	1166	1.29
16	20	1355	1.41
20	8	893	1.23
20	10	987	1.29

As can be seen in Table 5.3, the combination of 20 mm flanges with an 8 mm web thickness yields the lowest mass (893 kg) with a resulting safety factor of 1.23 which falls within the recommended range from [64]. These material thicknesses are used as the initial parameters for the beam and refined during the structural analysis of the trailer to ensure safety factors within the recommended range of 1.2 -2.5 are achieved [64] based on the FEA results. Figure 5.10 depicts the preliminary longitudinal beam design for the semi-trailers with manufacturing considerations accounted for.

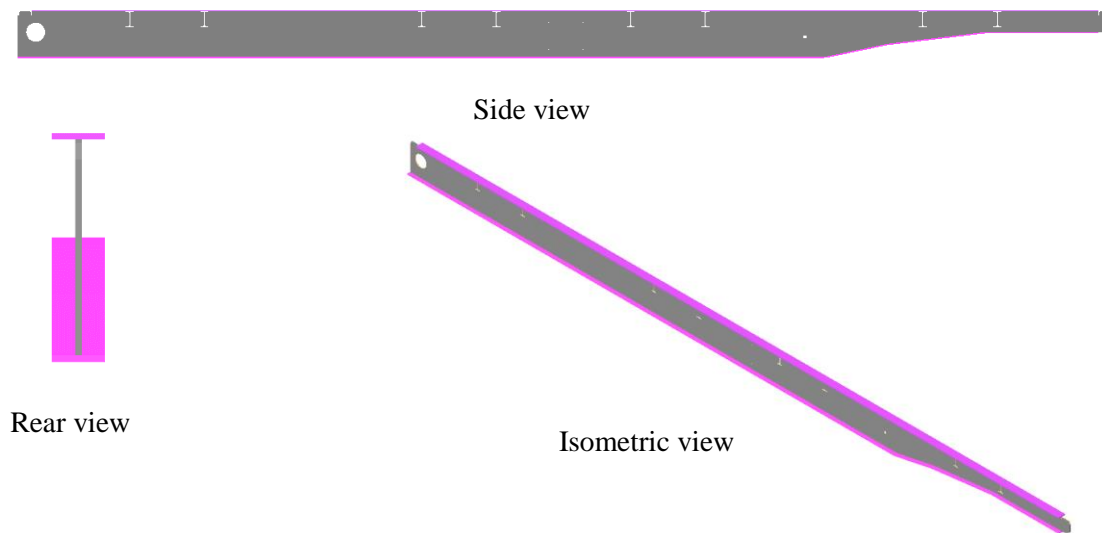


Figure 5.10: Preliminary longitudinal beam design

5.4.3 Container Supports

Cross members that pass through the webs of the pair of longitudinal beams are utilised with guides on each end to support each ISO container across its width (see Figure 5.3). These are used to secure the containers from moving laterally during transportation, as well as to aid the loading of containers onto the deck of the chassis by QCs and RTGs. Similar to the method used to determine the required length of the longitudinal beam based on the length of the containers carried, the length of the container-supporting cross members was determined using the width of the containers carried by the semi-trailer and increased by 5% [80] for clearance between the containers and the guides. Using the width of the ISO containers presented in Table 5.1, together with the added clearance, the required length of the container-supporting cross members was found to be 2 489 mm. Eight cross members strategically positioned along the length of the longitudinal beams are used to support the containers. The orientation of the cross members, that pass through the webs of the longitudinal beams that are spaced 1 000 mm apart to satisfy the axle centre requirements, results in bending of the members owing to the mass portion of the containers that the cross member carries. This is depicted in Figure 5.11. The mass of the containers resting on the cross members is represented as a point load due to the outer edges of ISO containers being lower than the under surface of the floor, concentrating the load towards the ends of

the cross members. This orientation is used to determine the geometry of the cross members based on the structural requirements for the chassis.

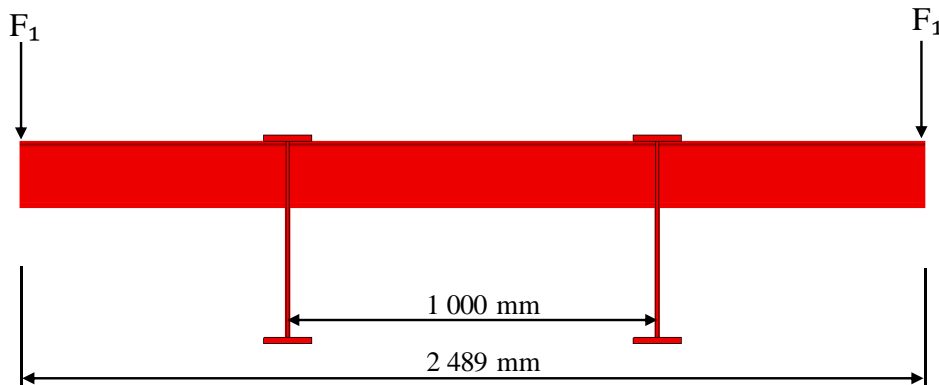


Figure 5.11: Orientation of the container-supporting cross members

Standard structural sections are extensively used as cross members in trailer designs due to their availability and reduced cost when compared to equivalent fabricated sections formed by welding steel plates together, thus a standard structural section is desirable for the container-supporting cross members of the MTS semi-trailers. Similar to the longitudinal beams, standard I-sections are predominantly used due to their efficacy with supporting bending loads, these were selected for use as the container-supporting cross members in the present design.

An appropriate structural section was determined from the minimum elastic section modulus required to prevent bending stresses beyond a predefined limit. This relationship is defined by Equation (5.2), where $\sigma_{Bending}$ is the maximum allowable bending stress, M is the maximum bending moment and Z_e is the elastic section modulus of the cross section.

$$\sigma_{Bending} = \frac{M}{Z_e} \quad (5.2)$$

Using a design factor of 2 for the vertical load, as per the deductions from Chapter 4.3.2.4, the maximum bending moment experienced by the cross members was determined using Figure 5.11 and applied to Equation (5.2) with an allowable bending stress of 296 MPa (safety factor of 1.2 [64] against a yield stress of 355 MPa) to determine the minimum required elastic section modulus of the cross members. For geometric reasons, the IPE 180 parallel flange I-section which has a section modulus greater than the minimum required value obtained using Equation (5.2) ($27\,930\text{ mm}^3$) was selected as the container-supporting cross members.

The guides, which are assembled onto either end of the container-supporting cross members as well as to the front and back end of the longitudinal beams to facilitate accurate self-positioning of containers when lowered onto the trailer, have profiles that are dictated by the technical requirements for trailers operating at Pier one [45]. This profile requirement, shown in Figure 5.12, is adhered to for the geometry of the guides designed for the semi-trailers.

Figure 5.13 shows the arrangement of the container-supporting cross members, as well as the container guides, assembled with the pair of longitudinal beams. Support plates have been added to allow the sides as well as the container base to rest on the chassis due to the height difference between the base of the container and its outer edges.

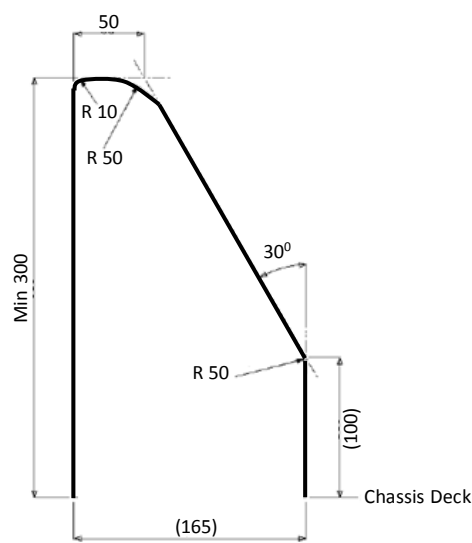


Figure 5.12: Guide profiles [45]

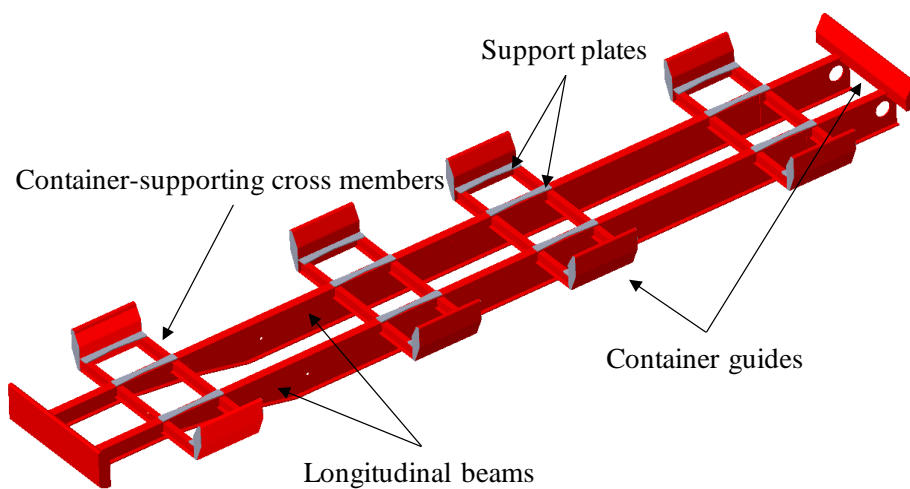


Figure 5.13: Cross members and guides assembled to the longitudinal beams

5.4.4 Kingpin Setback

The kingpin setback on a trailer is limited by the required swing clearance between the chassis and the terminal tractor to ensure that no interference occurs between the two vehicles during turning manoeuvres. It is desirable to have as short a wheel base as possible for the semi-trailers of the MTS in order to reduce the swept path of the vehicle during turning manoeuvres, hence improving manoeuvrability. To achieve this, the kingpin setback should be at its maximum allowable distance in order to have a minimum wheel base. Since the Durban Container Terminal does not stipulate the minimum required swing clearance or maximum kingpin setback for trailers designed for use at Pier One, the recommendations from [54] on the minimum swing clearance between a semi-trailer and a prime mover are used to determine the kingpin setback for the MTSs semi-trailers. A minimum swing clearance of 300 mm is recommended, resulting in a maximum kingpin setback of 931 mm for the semi-trailers based on half the width of the chassis (1 414.5 mm) and the distance between the Kalmar TR626i tractors fifth wheel centre and the rear of its cabin (1 470 mm). This relationship is described by Equation (5.3) [54], where SC is the swing clearance, L_1 is the kingpin setback, L_2 is the distance between the centre of the fifth wheel and rear of the cabin and W is the half width of the semi-trailer chassis.

$$SC = L_2 - \sqrt{L_1^2 + \frac{W^2}{4}} \quad (5.3)$$

To mount the kingpin to the chassis of the semi-trailer, a structure known as a skid plate is used. This plate has a circular cut-out for fitment of the kingpin and is welded onto the underneath surface of the longitudinal beams, spanning the distance between them. The leading edge of the skid plate has a 30° bend to allow for a “skid” type operation when coupling the semi-trailer to the tractor. This was determined from measurements of the bend angle on the existing trailer’s skid plates to guide the chosen design. Figure 5.14 and Figure 5.15 shows the orientation of the kingpin and the skid plate on the chassis. The method used to select the appropriate kingpin is presented in Chapter 5.4.7

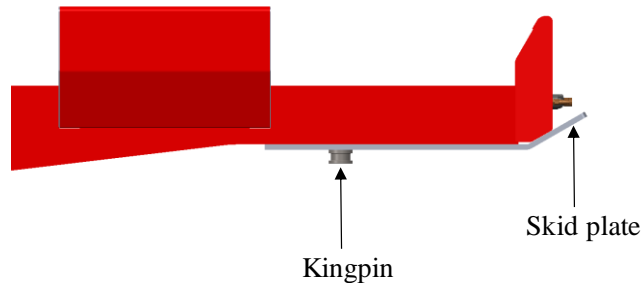


Figure 5.14: Side view of the kingpin-skid plate assembly



Figure 5.15: Aerial view of the kingpin-skid plate assembly

5.4.5 Auxiliary Structures

5.4.5.1 Lower Cross-Bracing

Cross-bracing of the chassis between the pair of longitudinal beams is a method employed in trailer design to reduce twisting of the structure due to the torsional effects created by lateral loads. Trailer manufacturers have implemented the use of different standard structural sections as cross-braces, predominantly channels and round tube sections. A study by Yura [86] on the fundamentals of beam bracing showed that cross-bracing of beams using channel sections attached between the bottom tension flanges reduces the angle of twist of the structure while also increasing the buckling strength of the beam webs when exposed to torsional loads. This suggested approach is used for cross-bracing the MTSs semi-trailers longitudinal beams in this design. Channel sections are welded to the top surface of the longitudinal beams' bottom flanges, spanning the distance between the two longitudinal beams' webs along the beams' length, each spaced 1.2 m apart. The container-supporting cross members provide the bracing required towards the top flange of the beams. While the primary function of the cross braces is to provide added stiffness to a trailer structure, they are also commonly used as a platform

for mounting the components of a trailer's subsystems and for added bracing between the suspension brackets [62].

5.4.5.2 Towing Hitch Mounting

A towing hitch is a device attached to the rear of a trailer chassis to enable additional trailers to be coupled to the set. The hitch, which allows for lateral and vertical articulation of the connection during turning manoeuvres, is designed by manufacturers to be bolted onto the rear end of the chassis at a suitable height for levelled coupling purposes. For this MTS, the semi-trailers are designed with an extension to the rear of the chassis to accommodate the fitment of the towing hitch. A 30 mm plate braced with channel sections, recommended by the towing hitch manufacturers, is bent and profiled to be welded onto the underneath surface of the longitudinal beams bottom flanges with bolt holes at the required distance to ensure levelled coupling to the converter dolly. The method used to select the appropriate towing hitch is presented in Chapter 5.4.7. Figure 5.16 shows the orientation of the towing hitch assembled to the chassis.

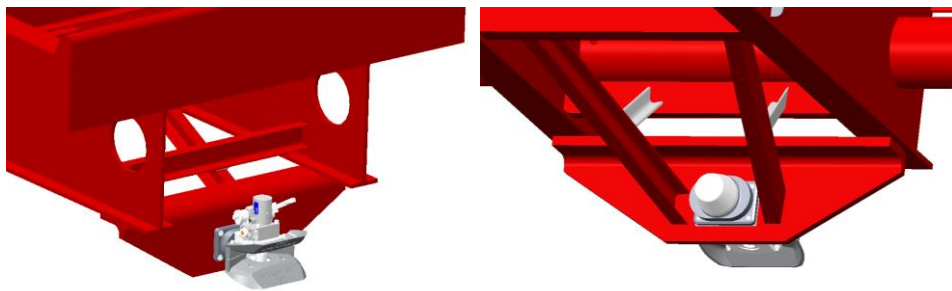


Figure 5.16: Mounting of the towing hitch to the semi-trailer chassis (left) front view (right) rear view

5.4.5.3 Landing Gear

A landing gear is used to support a semi-trailer when it is uncoupled from the prime mover. The gear is fitted at a distance away from the front of the trailer to ensure that interference with the prime mover's chassis does not occur during turning. The A402 model landing gear, manufactured by Jost, was selected for the semi-trailer design due to its availability and telescopic design. The telescopic design allows for the height of the legs to be adjusted for ease of coupling to the terminal tractor as well as the converter dolly.

5.4.5.4 Rear-Underrun Protection Device

A rear-underrun protection device, also known as the rear bumper of heavy goods vehicle, is a safety device that prevents an impacting vehicle from becoming lodged underneath the heavy goods vehicle in a rear end collision. The rear-underrun protection device for the semi-trailers in this study was

designed according to the geometric requirements as per SANS 1055, which is a terminal specific requirement for trailers operated at Pier One. The dimensions are given in Table 5.4.

Table 5.4: Rear-underrun protection device dimensions

Parameter	SANS 1055 Requirement	Design Value
Ground clearance	550 mm (maximum)	550 mm
Lateral length (L)	1 730 mm < L < 1 930 mm	1 930 mm
Distance away from rear extremity of the chassis	450 mm (maximum)	220 mm

5.4.6 Bogie Assembly Position

The position of the bogie assembly for a minimum wheel base is dependent on the mass of the chassis carrying the maximum payload and the position of the kingpin relative to their respective centre of gravities. The structural mass of the chassis, inclusive of the longitudinal centre beams, container supporting cross members and auxiliary structures was found to be 4 277 kg obtained using the computer aided drawing (CAD) software Creo 2.0, however this does not include the mass added to the structure from welding and painting. This additional mass is approximated using the findings from [62] where the welding and paint work for the existing trailers used at the Durban Container Terminal was found to be 5% of the chassis total mass. This resulted in a mass of 4 492 kg for the chassis. Using this mass and the maximum payload of two 20 ft. containers, the position of the bogie assembly was calculated such that it would be loaded to 90% of its rated maximum load capacity. This was done based on recommendations from the axle manufacturer to account for containers that may be overloaded and for irregular load distribution of its contents that may cause the axles to be loaded beyond its rated capacity of 22 700 kg. Figure 5.17 shows the load transfer analysis conducted to determine the position of the bogie, resulting in the semi-trailer having a wheelbase of 8.909 m.

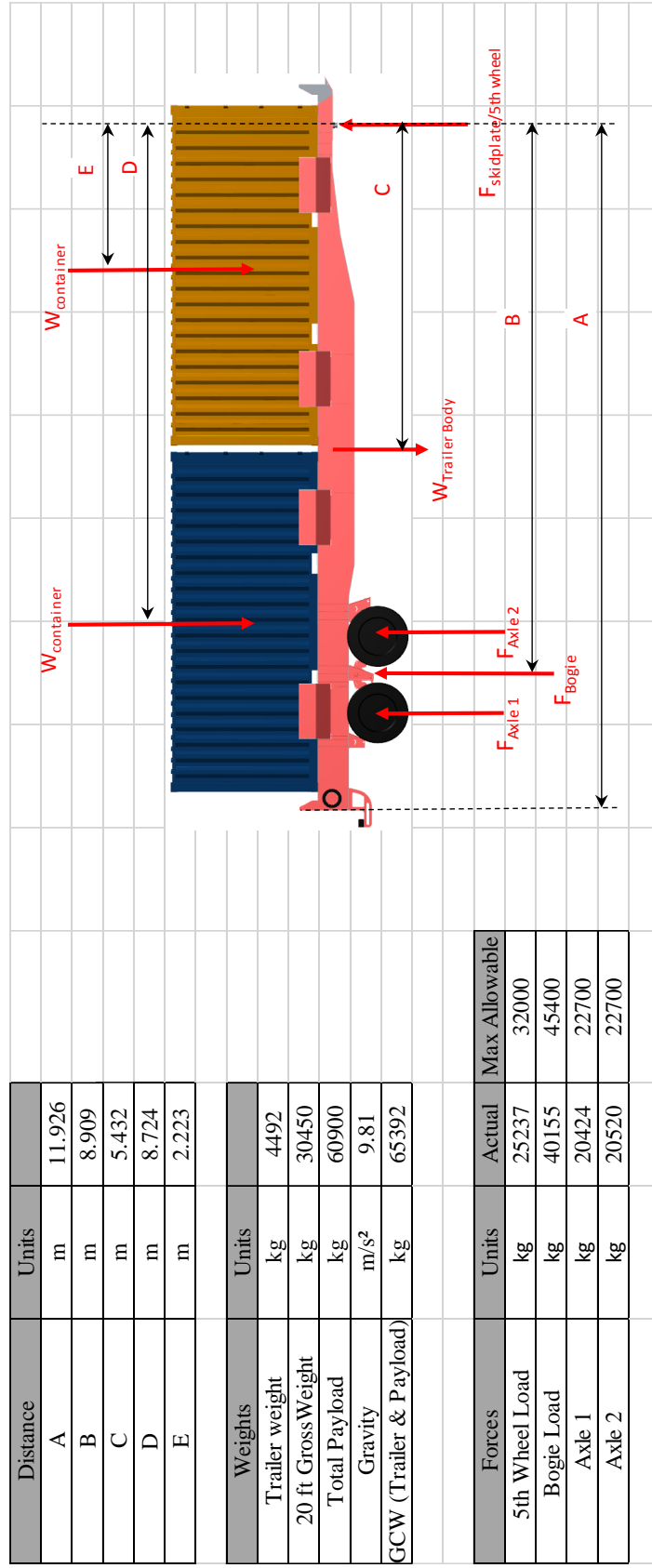


Figure 5.17: Load transfer analysis for bogie positioning

5.4.7 Coupling D-Values

The strength requirement for mechanical couplings used in trailer equipment is determined using the D-value formula [87], shown by Equation (5.4), which represents the theoretical reference value for the horizontal force between the towing vehicle and the trailer [69]. Equation (5.4) was used to select an appropriate kingpin for the leading semi-trailer since it experiences the greatest horizontal force from all the couplings in the MTS as a result of being connected directly to the terminal tractor. Figure 5.18 shows the reaction loads pertaining to the variables used in Equation (5.4) [87]:

$$D = 0.5g \frac{(B + U_T)(T + 0.08B)}{T + B - U_T} \quad (5.4)$$

where D is the theoretical horizontal reference force between the towing vehicle and the trailer, U_T ($=U_d$) is the fifth wheel load imposed by the semi-trailer, T is the sum of the ground axle loads of the tractor as a result of the imposed load U_T , R_{1b} ($=R_{2b}$) is the sum of the ground axle loads of the semi-trailers, C_d is the sum of the ground axle loads of the converter dolly as a result of the imposed load U_d and B ($= R_{1b} + C_d + R_{2b}$) is the sum of the axle loads of the MTS.

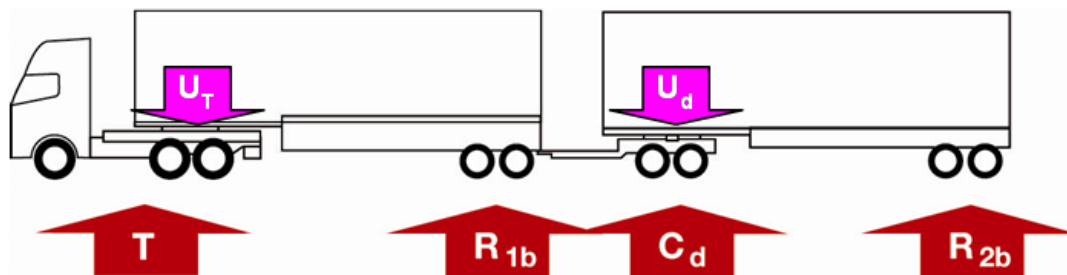


Figure 5.18: Reaction loads for the MTS [87]

The sum of the axle loads for the tractor was obtained by adding the imposed fifth wheel load of the trailer to the mass of the selected terminal tractor (14 000 kg tare mass for the Kalmar TR626i terminal tractor), while the ground axle loads of the trailers were determined by adding the mass of the entire bogie assembly (3 580 kg including rims and tyres) to the sum of the imposed loads on the axles as a result of the chassis mass and the payload. The imposed fifth wheel load and the load on the axles are shown in Figure 5.17. The resulting minimum D-value of the kingpin required for this application was found to be 225.92 kN. This led to the selection of the Jost KZ1116 kingpin which has a D-value of 260 kN. For reasons of availability, the RO - 50 flex towing hitch which also has a D-value of 260 kN was selected for the semi-trailers. The towing hitch will experience a lower horizontal force than the kingpin, thus the selection of the RO - 50 flex towing hitch suffices for the design even though it has a higher D-value rating than required.

5.4.8 Semi-Trailer Structural Analysis

5.4.8.1 Finite Element Model

To validate the structural integrity of the semi-trailer for the MTS, finite element analyses (FEA) of the chassis using the load cases discussed in Chapter 4.3.2.4 were conducted to ensure that the stresses induced in the materials resulted in the desired safety factor range of 1.2-2.5 for the design. Linear static analyses were conducted using ANSYS®.

Using a mid-surfaced geometry, the model was automatically meshed with predominantly shell elements of the quadrilateral type. This was for improved accuracy as compared to other element types such as triangular elements [88, 89]. The meshed geometry is shown in Figure 5.19, together with the orientation of the global coordinate system. A mid-surfaced model was used for reduced solution times without negatively affecting the accuracy of the results since through-the-thickness variations in strain would be minimal due to the dimensions of the structural components [90]. The kingpin was modelled as a solid body rather than a mid-surfaced body since it did not conform to the requirements for using shell elements [90].

The effect of the semi-trailer's suspension system and its spring configuration were incorporated in the analyses by means of multi-point rigid connections with deformable contact behaviour, as well as 1D bar and spring elements to represent the axles and leaf springs respectively [54, 62]. A similar setup was used to simulate the effects of the tractor's and converter dolly's suspension when the semi-trailer is coupled to the fifth wheel. Spring constants equivalent to the manufacturer's specifications for the suspensions were used for defining the spring elements in the model. The container payloads were incorporated into the model using two mass elements weighing 30 450 kg each as the highest payload scenario, located at the geometric centre of the containers and applied as a uniformly distributed load to the surfaces of the chassis that supports the load. The mass of the semi-trailer was also included in the analyses. Figure 5.20 depicts these features of the model together with the orientation of the global coordinate system. The X, Y and Z axes are taken as the longitudinal, vertical and lateral directions respectively.

The von-Mises stress criterion was used in the FEA analyses to evaluate the design stresses, similar to previous studies [54, 57, 61, 83, 85]. This criterion is commonly used by design engineers as it is a theoretical measure of stress used to estimate yield failure in isotropic, ductile materials such as mild steel, making it suitable for the structural analyses in this study. While the use of maximum principle and shear stress as the criteria for evaluating the safety of structures designed from ductile materials can be found in literature [91], the use of the von-Mises stress criterion is the most appropriate for determining the structural safety for materials in their elastic range [92].

As mentioned in Chapter 4.4.3, grade S355 steel has been selected as the material for the design of the semi-trailers. The mechanical properties of this steel grade, shown in Table 4.5, was used in the analyses.

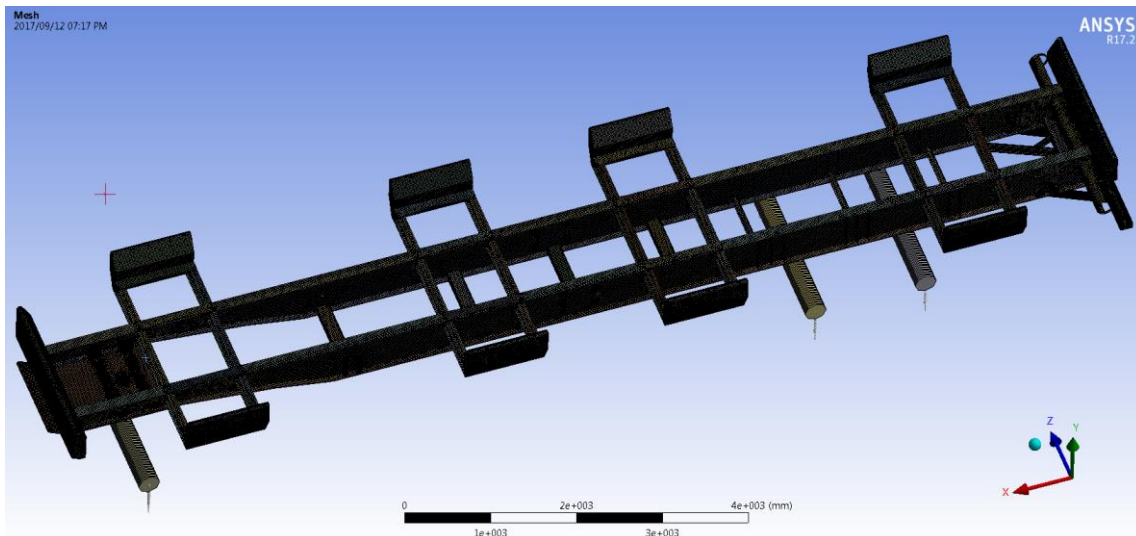


Figure 5.19: Meshed semi-trailer geometry

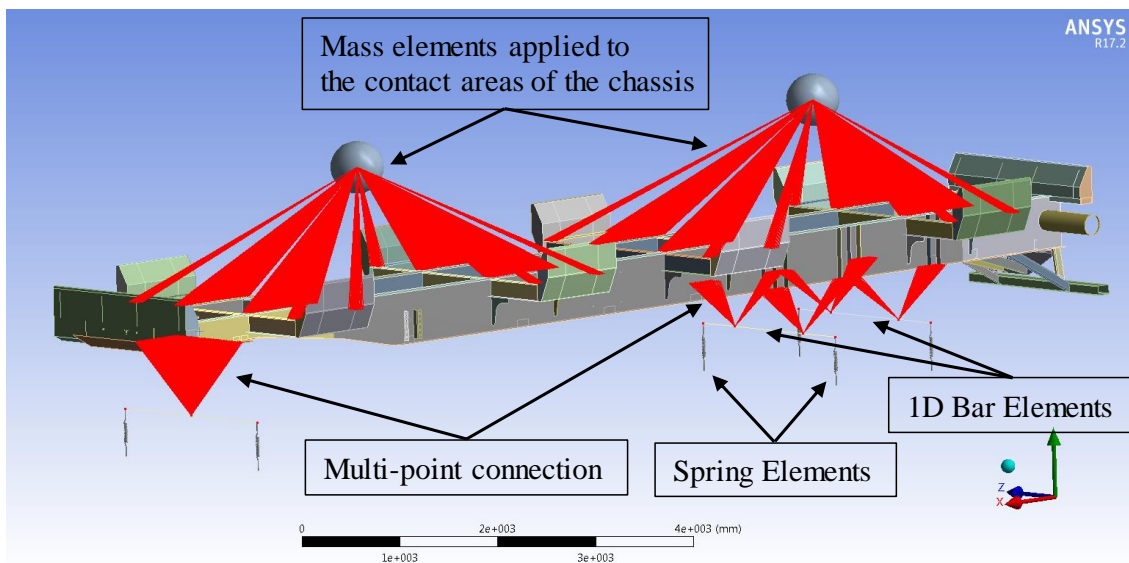


Figure 5.20: Full finite element model representation

5.4.8.2 Vertical Load Case

The vertical load case consists of the payload, together with an acceleration equivalent to two times gravity in the vertical direction (negative Y axis direction of the global coordinate system) applied to the entire model. The model was constrained in at the kingpin and the suspension to prevent rigid body motion, while replicating the actual restraints on the structure during real life usage. Translational constraints in the direction of the global X and Y axes were applied to top and bottom of the springs respectively, while the translational constraint in the direction of the global Z axis was applied to the surface of the kingpin and the top of the springs [62]. The von-Mises stress plots for this load case are shown in Figure 5.21 and Figure 5.22.

The results of this load case initially showed non-compliance to the design criterion of a maximum allowable non-localised peak stress of 296 MPa for a minimum safety factor of 1.2 against yielding [64]. Apart from the stress concentrations in the model which generate high stress values at localised points [93], the von-Mises stress results for the skid plate in the region around the kingpin as well as the front section of the longitudinal beam webs were found to be within the range of 352 to 395 MPa. These results are shown in Figure 5.23.

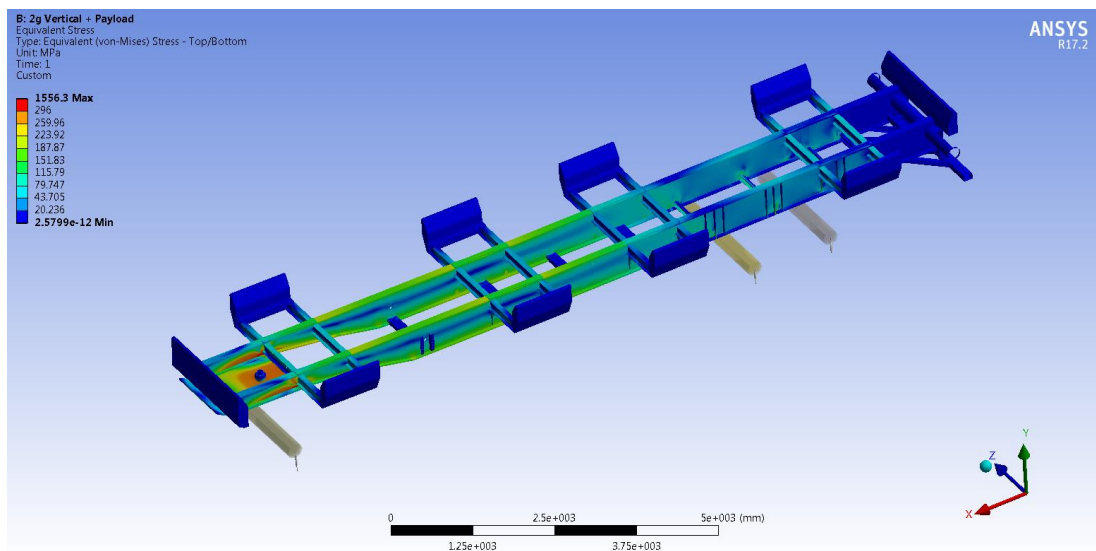


Figure 5.21: von-Mises stress plot for the semi-trailer vertical load case – top view

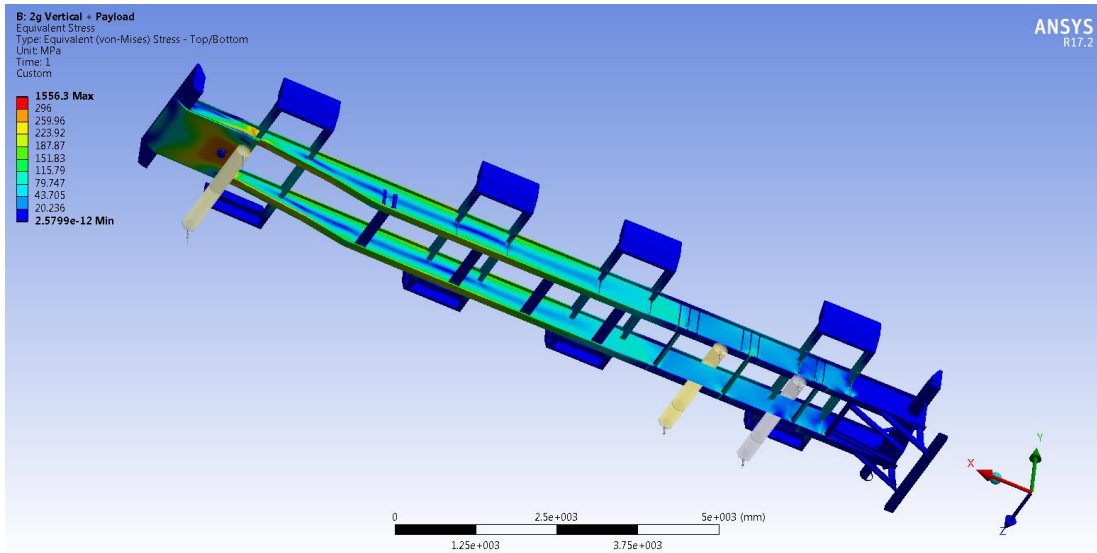


Figure 5.22: von-Mises stress plot for the semi-trailer vertical load case – bottom view

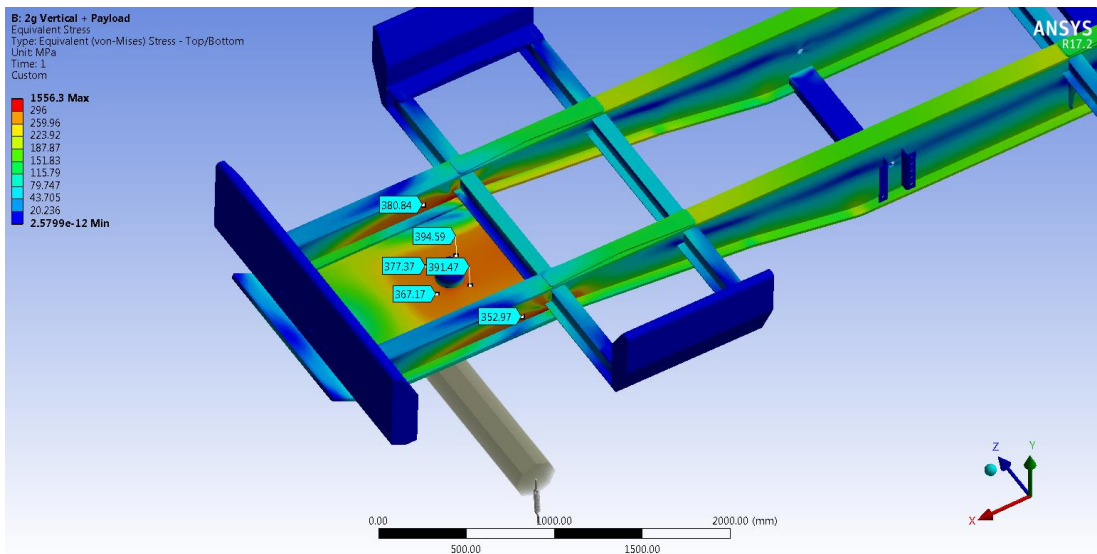


Figure 5.23: High stress regions on the skid plate and the longitudinal beams webs

The high stress in these regions are caused by the vertical load on the skid plate at the support area representing connection to the fifth wheel of the tractor/convertor dolly. This support area lies between the span of the 2 longitudinal beams, causing the skid plate to experience high bending stresses. The deformation of the skid plate is transferred to the front end of the longitudinal beams due to the contact area between them, causing the bottom flanges to bend inward which generates high stresses on the web region. This can be seen in Figure 5.24 where the deformation in this region is scaled by a factor of 5 for visual purposes.

To reduce the high stresses experienced at these regions, the skid plate was braced using fabricated channel sections with a 20 mm plate thickness, with due regard for space limitations, in an effort to minimise bending of the plate and the web of the longitudinal beams. The design modification is shown

in Figure 5.25, with the corresponding stress results for this region incorporating the added bracing shown in Figure 5.26 and Figure 5.27. The modification proved to be successful in reducing the von-Mises stress in this area below the allowable value of 296 MPa, with stresses found within the range of 147 to 287 MPa.

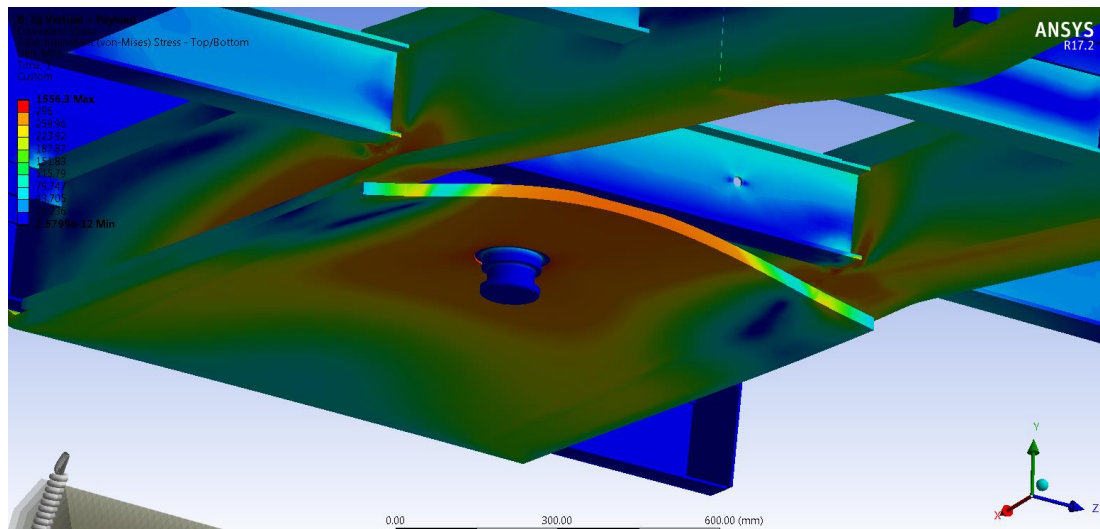


Figure 5.24: Scaled deformation of the high stress region

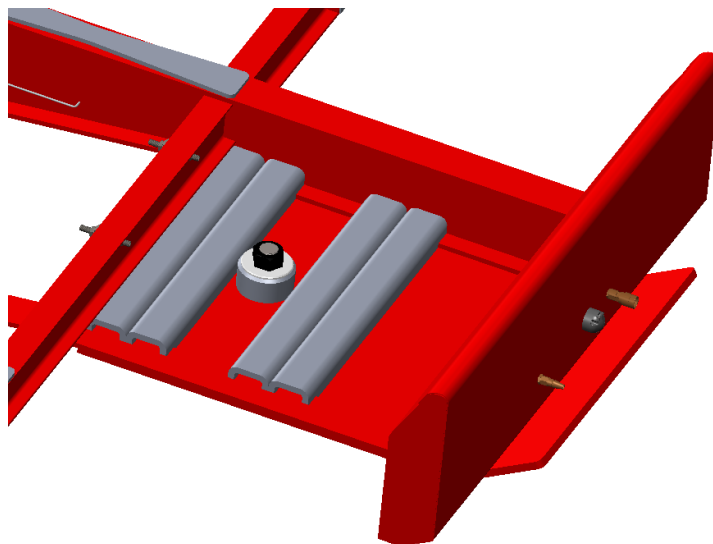


Figure 5.25: Additional bracing of the skid plate to minimise bending (left longitudinal beam hidden)

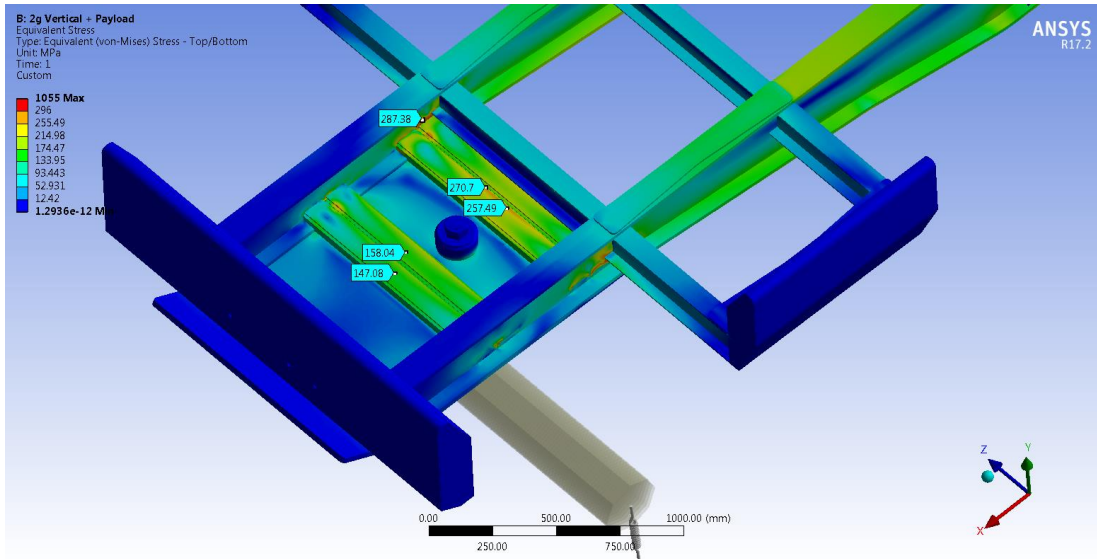


Figure 5.26: von-Mises stress plot of the skid plate with the added bracing – top view

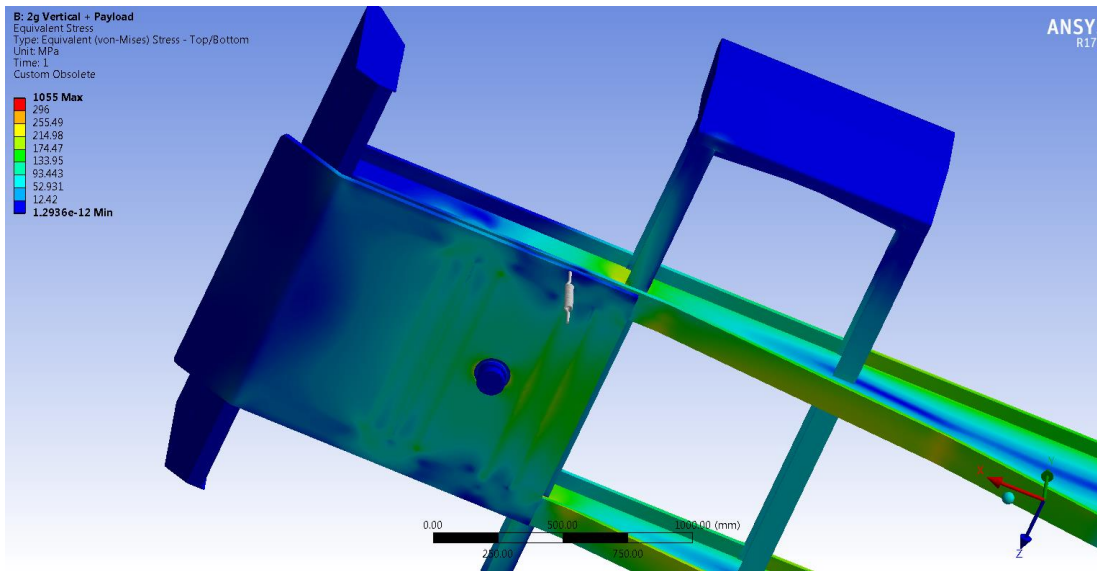


Figure 5.27: von-Mises stress plot of the skid plate with the added bracing – bottom view

On inspection of the stress on the longitudinal beams, the location of the maximum stress was found to occur in the region where one of the support plates is positioned on the top flange. This support plate effectively increases the thickness of the top flange in that area, consequently reducing the stress results at that point when compared to the analytical calculations for the maximum stress presented in Chapter 5.4.2. The stress from the FEA at the location which coincided with the maximum bending moment calculated in Chapter 5.4.2, was found to be 205 MPa. Since this stress was considerably lower than the maximum allowable value of 296 MPa an opportunity existed to reduce the thickness of the longitudinal beams flanges as a potential mass saving modification. Subsequent analyses resulted in the top and bottom flange thickness being reduced from 20 mm to 16 mm, pending verification in other load cases. This decreased the mass of the longitudinal beams by 210 kg in total. The final von-Mises stress plots

for this load case are shown in Figure 5.28 and Figure 5.29. The non-localised peak stress for this load case was found to be 287 MPa (see Figure 5.26), resulting in a safety factor of 1.24. This value falls within the allowable safety factor range discussed in Chapter 4.3.2.4.

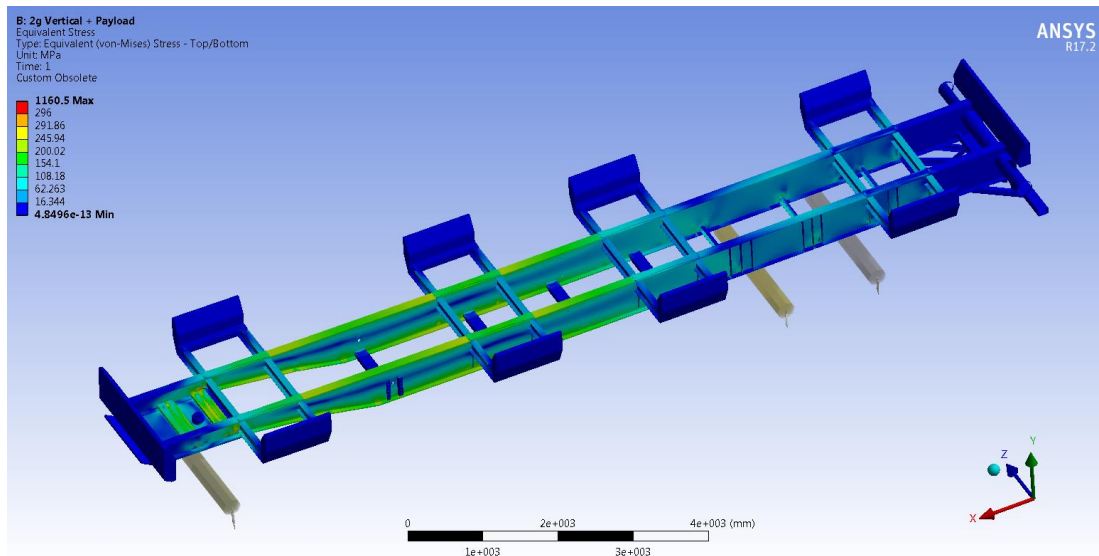


Figure 5.28: Finalised von-Mises stress plot for the semi-trailer vertical load case – top view

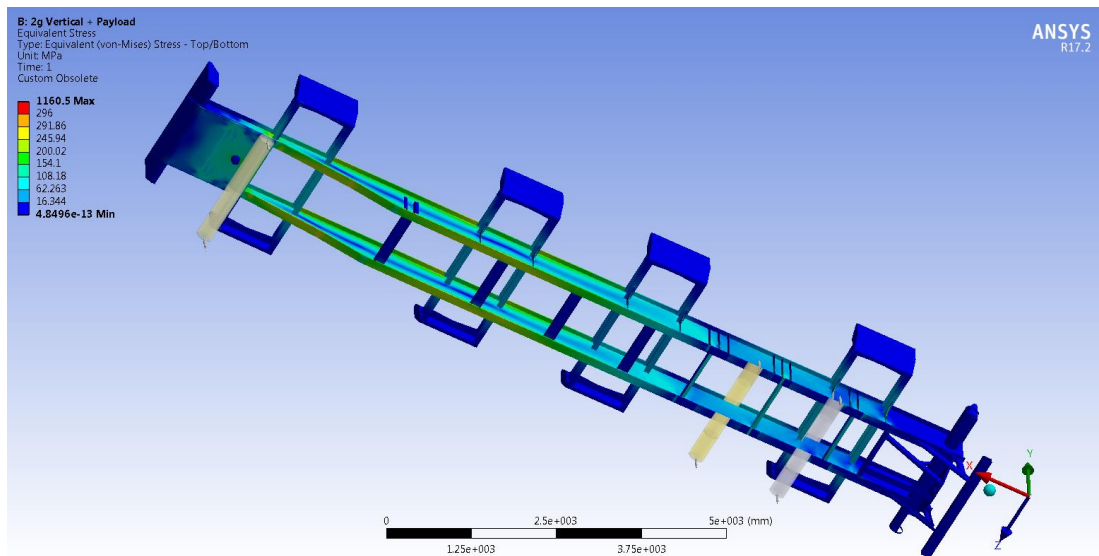


Figure 5.29: Finalised von-Mises stress plot for the semi-trailer vertical load case – bottom view

5.4.8.3 Longitudinal Braking Load Case

The longitudinal braking load case consists of the payload coupled with an acceleration of 0.52g applied to the entire model in the positive X direction of the global coordinate system. Gravity was applied to the model in the negative Y direction of the global coordinate system. Similar to the vertical load case, the model was constrained in the respective directions at the kingpin and the suspension to prevent rigid body motion, while replicating the actual restraints on the structure during braking of the semi-trailer. A translational constraint in the direction of the global Y axis was applied to the bottom of the springs respectively, while the translational constraint in the direction of the global Z axis was applied to the surface of the kingpin and the top of the springs [62]. The surface of the kingpin was also constrained in the direction of the global X axis. The von-Mises stress plots for this load case are shown in Figure 5.30 and Figure 5.31.

The results of this load case complied with the design criteria for the chassis with a maximum stress of 258 MPa occurring on the skid plate in the region of the kingpin, resulting in a safety factor of 1.38. This value falls within the allowable safety factor range defined in Chapter 4.3.2.4. Localised high stress points exceeding the yield stress of the material were found in the longitudinal beam's webs at the corner regions of the skid plate braces (see Figure 5.32), however this is due to modelling approximations used in the FEA process and is not considered a true representation of the stress distribution in those areas [93]. This is discussed further in Chapter 8.

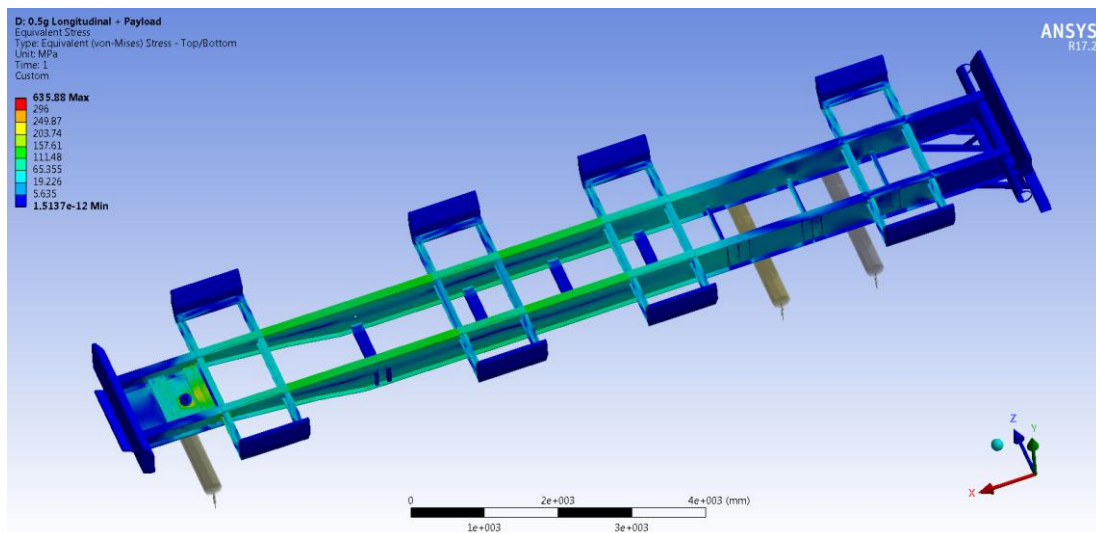


Figure 5.30: von-Mises stress plot for the semi-trailer braking load case – top view

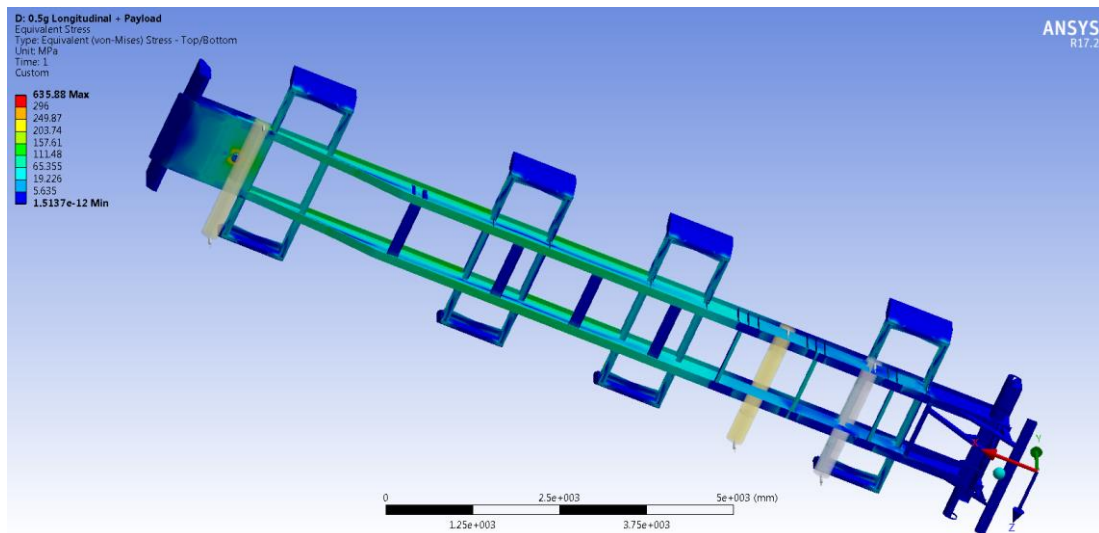


Figure 5.31: von-Mises stress plot for the semi-trailer braking load case – bottom view

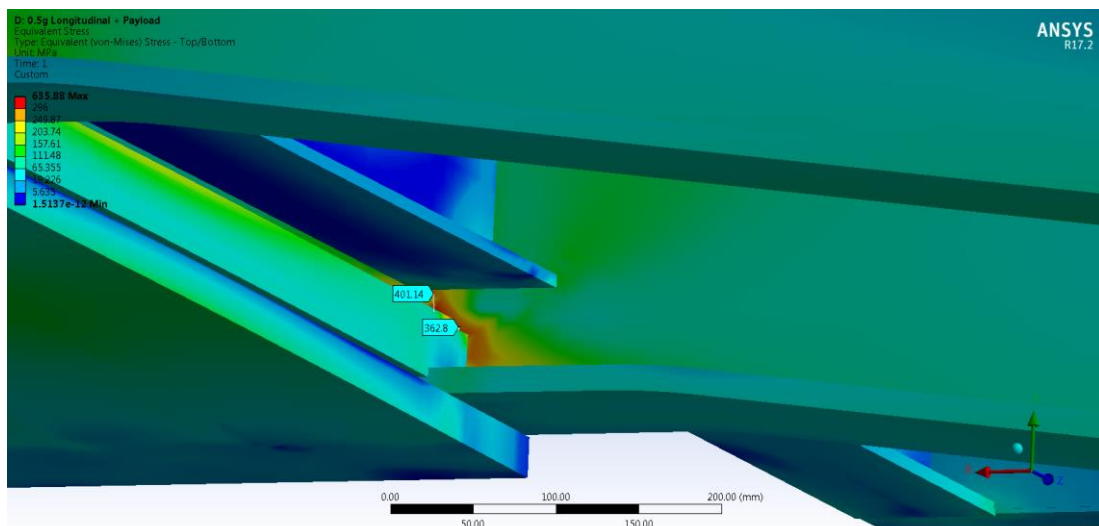


Figure 5.32: Localised high stress region at the web-skid plate bracing interface

5.4.8.4 Longitudinal Acceleration Load Case

The longitudinal load case simulating the maximum tractive force of the terminal tractor transferred to the kingpin of the semi-trailer was conducted by applying this force directly onto the kingpin in the positive X direction of the global coordinate system. The D-value of the kingpin, described in Chapter 5.4.7, is a theoretical reference force calculation used to determine the strength requirements of the coupling and is based on the mass of the vehicles concerned, however it does not represent the actual tractive force provided by the terminal tractor used, as Equation (5.4) is independent of the tractive performance of the prime mover. The maximum tractive effort of the Kalmar TR626i terminal tractor was calculated as 256 kN, using the performance data shown in Appendix B. This maximum tractive effort is available between 1000-1400 rpm in the first gear, which is during take-off. This force value was applied directly to the kingpin, simulating the tractor pulling the MTS. Together with the tractive

force, this load case consisted of the mass of the payload and gravity applied to the model in the negative Y direction of the global coordinate system. Translational constraints in the direction of the global Z and Y axes were applied to the top and bottom of the springs respectively, while the translational constraint in the direction of the global X axis was applied to the surface where the towing hitch is connected to the chassis. The von-Mises stress plots for this load case are shown in Figure 5.33 and Figure 5.34.

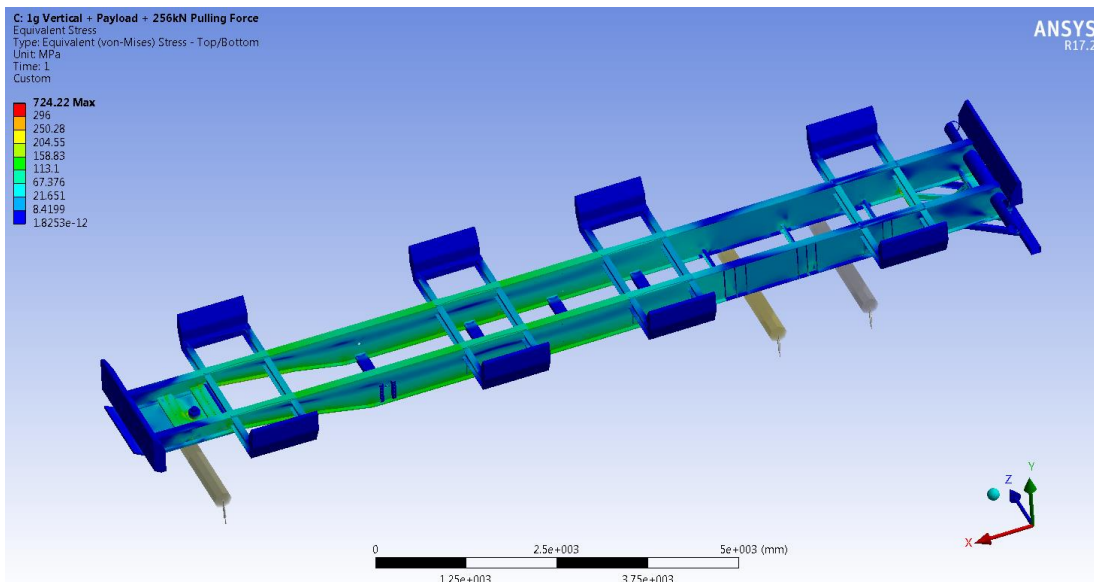


Figure 5.33: von-Mises stress plot for the semi-trailer accelerating load case – top view

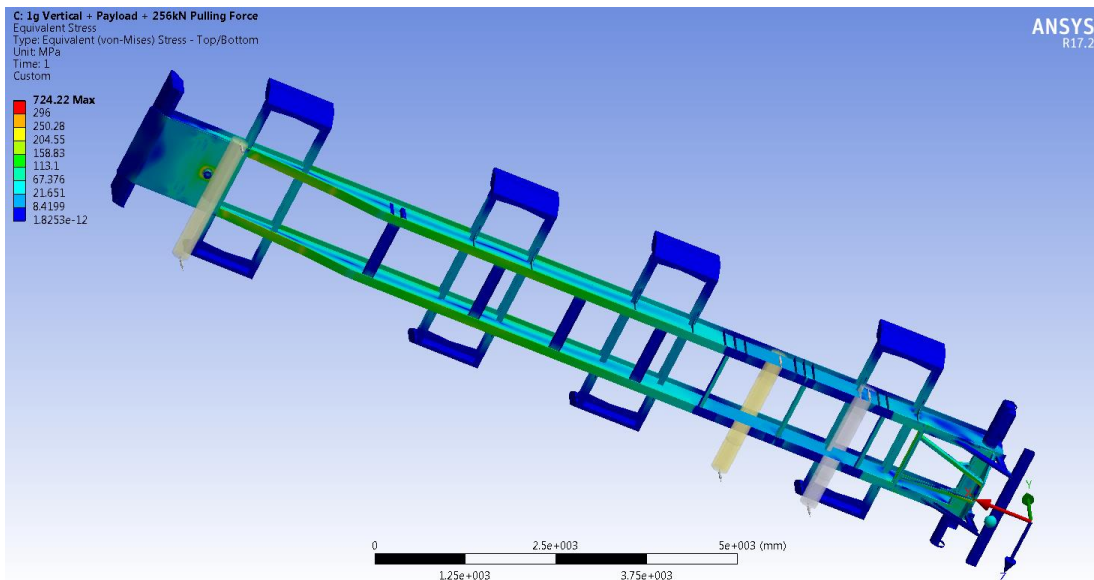


Figure 5.34: von-Mises stress plot for the semi-trailer accelerating load case – bottom view

The non-localised peak stress in this load case was found to be 190 MPa on the bottom flange of the longitudinal beams, resulting in a safety factor of 1.86. This falls within the allowable safety factor range. Localised high stress points exceeding the yield stress of the material were found at the corners

of the cross members used to brace the towing hitch mounting plate, shown in Figure 5.35. These localised high stresses are discussed further in Chapter 8.

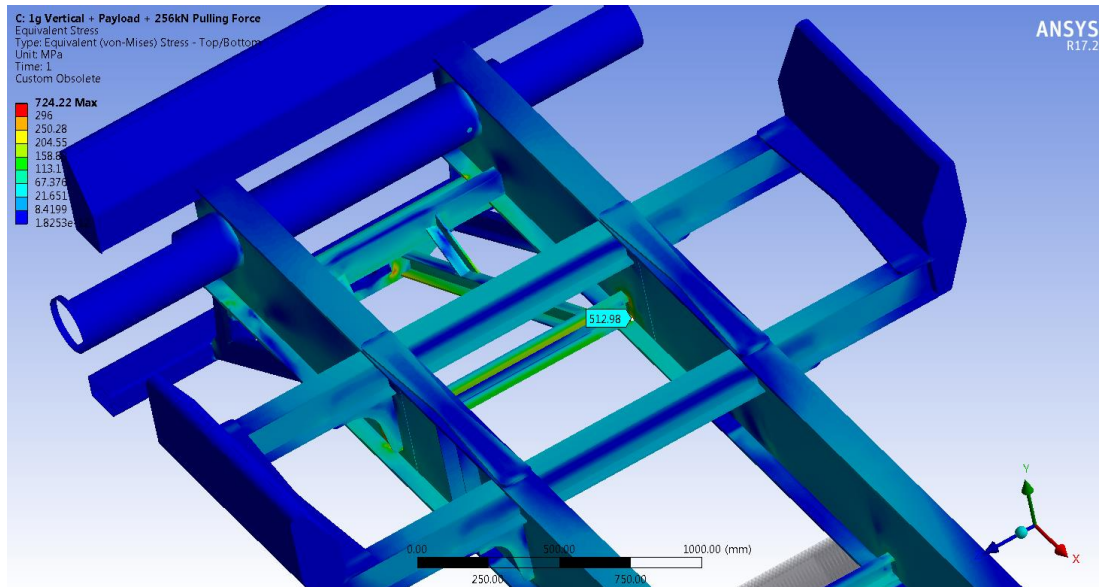


Figure 5.35: Localised high stress at the corners of the cross member

5.4.8.5 Lateral Load Case

The lateral load case was conducted to simulate the effects on the chassis during cornering. This load case consists of the payload together with an acceleration of 0.25g applied to the entire model in the negative Z direction of the global coordinate system, while gravity was applied to the model in the negative Y direction. Similar to the previous load cases, the model was constrained at the kingpin and the suspension to prevent rigid body motion, replicating the actual restraints on the structure during real life cornering. Translational constraints in the direction of the global X and Y axes were applied to the top and bottom of the springs respectively, while the translational constraint in the direction of the global Z axis was applied to the surface of the kingpin [62]. The von-Mises stress plots for this load case are shown in Figure 5.36 and Figure 5.37.

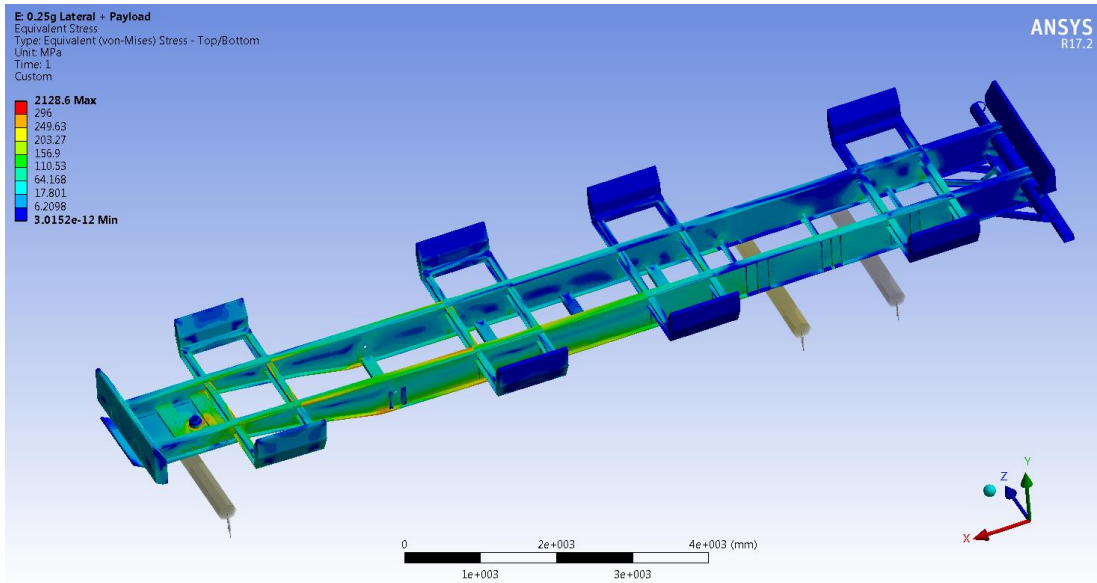


Figure 5.36: von-Mises stress plot for the semi-trailer lateral load case – top view

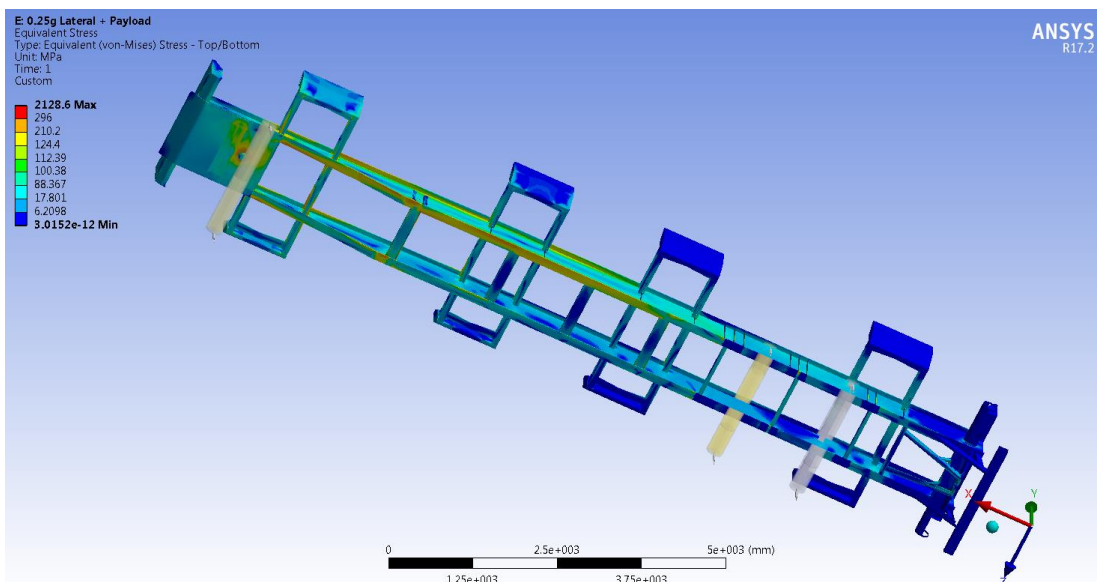


Figure 5.37: von-Mises stress plot for the semi-trailer lateral load case – bottom view

The results of this load case complied with the design criteria for the chassis with a maximum stress of 272 MPa occurring on the top flange of the right longitudinal beam (when viewed from the front), resulting in a safety factor of 1.31. This value falls within the allowable safety factor range discussed in Chapter 4.3.2.4. Localised high stress points exceeding the yield stress of the material occurred in the longitudinal beams webs at the corner regions of the skid plate braces as well as at the corners of the channel section cross braces due to modelling approximations used in the FEA process [93] and these are discussed in further Chapter 8.

5.4.9 Semi-Trailer Final Design

On completion of the structural analysis, the CAD model of the semi-trailer was updated with the longitudinal beams flanges reduced to 16 mm and the cross bracing addition to the skid plate, described in Chapter 5.4.8.2. These modifications resulted in a final chassis mass of 4 410 kg, 82 kg less than the initial mass as sized via the analytical analysis. The semi-trailer design for the MTS was carried out with the intention of having a reduced mass and improved manoeuvrability when compared to the existing semi-trailers at the terminal that could have been used to form the MTS (Chapter 4.2.2). Preliminary comparisons of the mass of each chassis showed that the semi-trailer designed in this study is 2260 kg lighter than the existing semi-trailers, representing a 33.9% mass reduction which directly leads to a lower product cost. A detailed mass and cost comparison is given in Chapter 7 and discussed further in Chapter 8. Figure 5.38 shows the CAD model of the finalised semi-trailer design for use in the MTS.

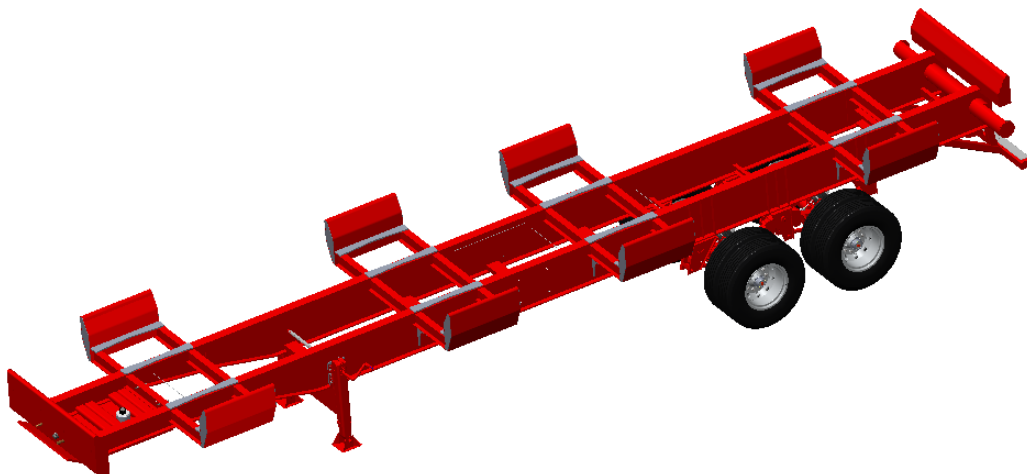


Figure 5.38: Finalised semi-trailer design

5.5 Converter Dolly Design

5.5.1 General Structural Arrangement

The structural arrangement of a converter dolly, similar to a semi-trailer, consists of a steel chassis constructed from two longitudinal centre beams joined together using cross members. The length of the beams were determined based on the geometry of the suspension fitted onto the bottom of the lower flanges, while the height of the beams is based on the overall height requirement of the converter dolly for levelled coupling to a semi-trailer [45]. The distance between the beams is governed by the centre mounting distance of the axles used. A fifth wheel coupling is fitted onto a mounting plate that is positioned on the upper surface of the longitudinal beams top flanges, directly in line with the centre of the bogie assembly for even load distribution and reduced tyre wear when turning [94, 95]. In operation, this fifth wheel couples to the kingpin of a semi-trailer.

There are two configurations of the drawbar arrangement which distinguishes the converter dolly types. An A-type converter dolly, which is used in the MTS design for this study, has a single point towing connection which allows articulation in yaw (steering), pitch (fore/aft rotation), and roll (side-to-side rotation) of the dolly with respect to the towing vehicle [95]. A C-type converter dolly has a double draw bar arrangement, resulting in two parallel towing connections to the leading semi-trailer. This connection type eliminates yaw, improving the vehicles stability at speeds above 45 km/hr., however this reduces the low speed manoeuvrability of the trailer system and produces extreme towing hitch forces as well as tyre scrubbing during small radius turns at low speeds [95]. The A-type converter dolly was chosen for the MTS in this study since it is used for low speed applications and does not require added stability for higher speed usage.

The structural arrangement detailed above is highlighted in Figure 5.39 and used as a guideline for the geometrical setup of the structural members which form the converter dolly designed for the MTS.

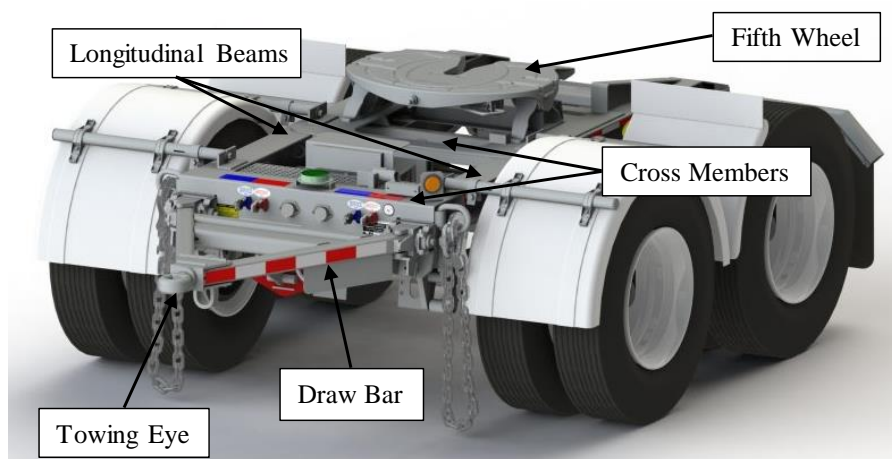


Figure 5.39: Converter dolly – structural arrangement

5.5.2 Chassis Structure

The chassis of the converter dolly consists of two I-section longitudinal beams of length 2 597 mm to accommodate the fitment of the GO underslung bogie. The height of the longitudinal beams was determined from the required overall height of the converter dolly, taking into consideration the height of the bogie which fits underneath the bottom flange of the longitudinal beams and the fifth wheel which fits onto the top flange. The webs of the beams have a varying height between 346 mm and 140 mm, while the flanges have a width of 130 mm based on the size required for mounting the suspension onto the beam. Similar to the semi-trailer design, the cross-sectional shape selected for the longitudinal beams of the converter dolly was that of an I-section due to its efficacy with supporting bending loads and its resistance to flexure [62, 81]. The initial material thickness used for the webs and flanges was preselected to be 10 mm and verified using FEA in Chapter 5.5.6 to achieve the required safety factor range of 1.2 - 2.5 [64].

To reduce twisting of the structure due to the torsional effects created by lateral loads, the chassis of the converter dolly is braced using a combination of standard channel and square tube sections towards the bottom flange of the longitudinal beams based on the recommendations from [86], similar to the semi-trailer design. These cross braces were positioned strategically such that they could also be used as the platform for additional bracing between the suspension brackets.

The front end of the chassis has two brackets spaced 870 mm apart for connecting the A-frame drawbar, discussed further in Chapter 5.5.5. Figure 5.40 below shows the chassis of the converter dolly with the longitudinal beams and cross members in position.

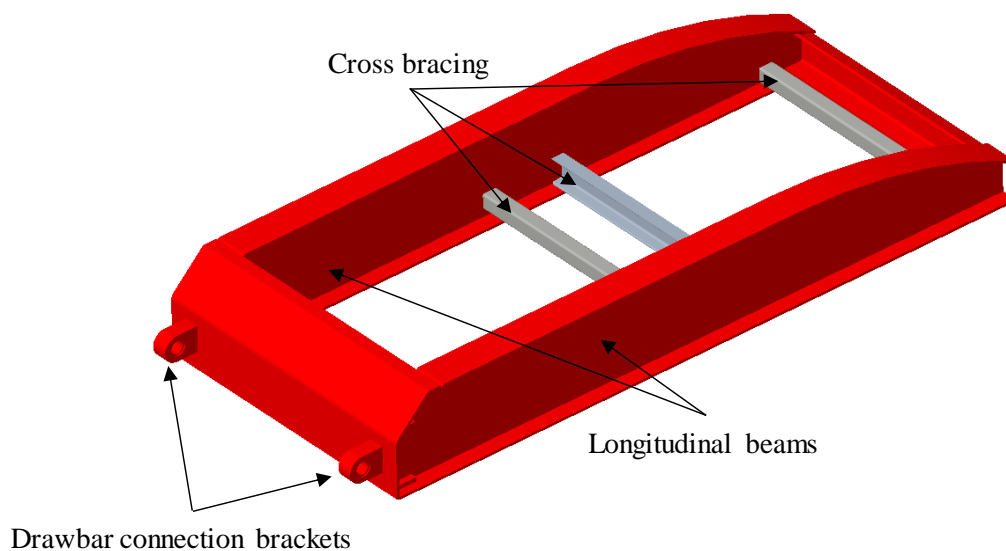


Figure 5.40: Converter dolly chassis

5.5.3 Fifth Wheel Assembly

The fifth wheel assembly selected for the converter dolly was the Jost JSK 38C-1 heavy duty coupling suitable for connection to the 3 ½” kingpin used in the semi-trailer design. This selection was based on the imposed vertical load from the skid plate of the semi-trailer, as well as the fifth wheels strength requirement determined using the D-value calculation for selecting mechanical couplings used in trailer equipment [69, 87]. The results of the D-value calculation used for selecting the appropriate fifth wheel are given in Chapter 5.5.6.

The fifth wheel is designed to be bolted onto a mounting plate that is fastened to the top flanges of the longitudinal beam using eight M20x1.5 bolts of strength class 10.9 as per ECE R55-01 regulations [96]. As mentioned in Chapter 5.5.1, it is recommended in [94, 95] that the fifth wheel coupling used in converter dollies be directly in line with the centre of the bogie assembly for even load distribution to the axles and reduced tyre wear when turning. This recommendation has been factored into the converter dolly design. Figure 5.41 displays the fifth wheel and mounting plate which is bolted onto the top flange of the longitudinal beams.

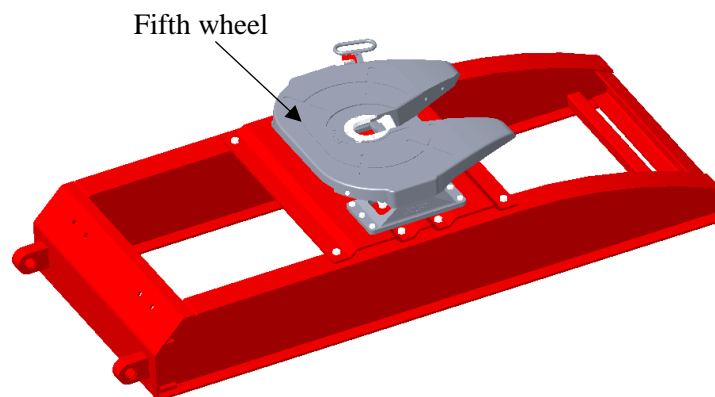


Figure 5.41: Fifth wheel assembly fitted to chassis

5.5.4 Bogie Assembly

The under slung bogie selected for the converter dolly requires a minimum clearance of 220 mm between the centre line of the axles and the underneath surface of the longitudinal beams bottom flanges as per the specifications from the manufacturer [74]. This clearance is required to prevent the axles from colliding with the chassis when loaded to its maximum allowable capacity of 22 700 kg. To achieve this, trailer equipment manufacturers use boxed steel structures called pedestals which are welded onto the suspension brackets for an increased clearance between the axles and the longitudinal beams. This approach is adopted for the converter dolly design and is shown in Figure 5.42. The pedestals are designed with a height of 100 mm to achieve the minimum required clearance. Figure 5.42 shows the bogie assembled to the chassis with the pedestals in position.

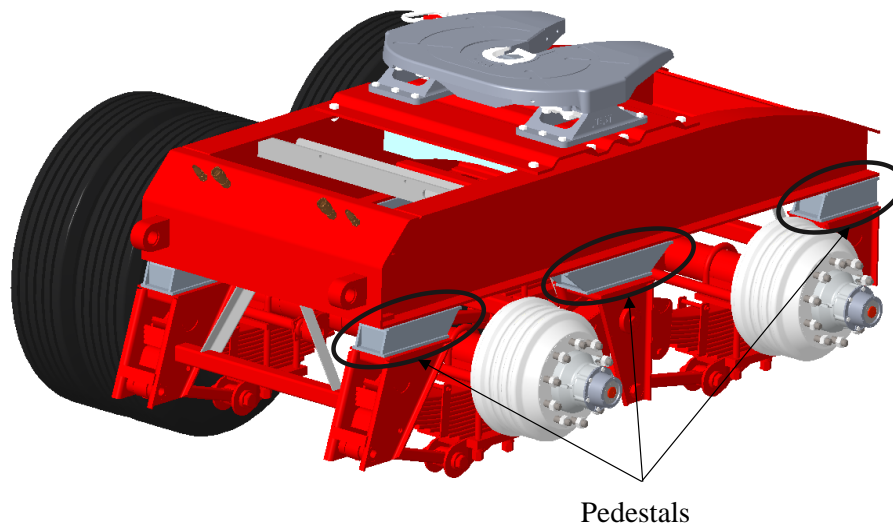


Figure 5.42: Bogie assembly utilising pedestals for connection to the chassis (tyres hidden)

5.5.5 Drawbar Arrangement

The single point drawbar used for the converter dolly was designed with a length of 1 650 mm to ensure that the rear end of the leading semi-trailer in the MTS set clears the front container guides of the second semi-trailer during turning manoeuvres, preventing collisions during tight turns. The connection points of the drawbar to the chassis of the converter dolly were designed to be as far apart as possible, taking into account manufacturing considerations, in order to reduce the bending moment on the front members of the chassis during movement. M36x4 shanked bolts were used to connect the drawbar to the chassis of the converter dolly. The towing eye selected for the design was the Jost Heavy Duty Towing Eye (Part number: 57005) which is mounted at the front end of the drawbar and used to connect the converter dolly to the leading semi-trailer. The selection of the towing eye was based on the strength requirement determined using the D-value calculation for selecting mechanical couplings used in trailer equipment [69, 87]. The results of the D-value calculation used for selecting the towing eye are detailed in Chapter 5.5.6. Figure 5.43 shows the drawbar designed from standard square steel sections and fabricated steel plates to form the structure, together with the towing eye assembled in position.



Figure 5.43: Drawbar design

5.5.6 Coupling D-Values

The D-value rating for the coupling equipment used in the converter dolly design was obtained from the equations presented in ISO 12357-3 [87] which details the strength requirements of mechanical coupling used in multiple vehicle combinations. Variations of Equation (5.4) were used to determine the minimum D-value for selecting the appropriate couplings. The results of the calculations yielded D-values of 249 kN for both the towing eye and fifth wheel couplings, leading to the selection of the Jost JSK 38C-1 fifth wheel and Heavy-Duty Towing Eye which had D-values of 250 kN and 314 kN respectively. These selections were also based on local availability.

5.5.7 Converter Dolly Structural Analysis

5.5.7.1 Finite Element Model

Finite element analyses (FEA) of the chassis were conducted to ensure that the stresses induced in the materials resulted in the desired safety factor range of 1.2-2.5 using the load cases discussed in Chapter 4.3.2.4. Linear static analyses were conducted using ANSYS®. A similar approach to the semi-trailer FE model was used for the converter dolly.

A mid-surfaced geometry was meshed with predominantly shell elements of the quadrilateral type for improved accuracy, as compared to alternate types such as triangular elements [88, 89]. The meshed geometry is shown in Figure 5.44, together with the orientation of the global coordinate system. A mid-surfaced model was used for reduced solution times, assuming minimal through-the-thickness variations in strain [90]. The towing eye was modelled as a solid body rather than a mid-surfaced body since it did not conform to the requirements for using shell elements [90].

The effect of the converter dollie's suspension system and its spring configuration were incorporated in the analyses by means of multi-point rigid connections with deformable contact behaviour, as well as 1D bar and spring elements to represent the axles and leaf springs respectively [54, 62], similar to the semi-trailer model. Spring constants equivalent to the manufacturer's specifications for the suspensions were used for defining the spring elements in the model. The load imposed onto the fifth wheel connection by the semi-trailer was incorporated into the model using a remote force located at a position representing the fifth wheel-kingpin interface. The mass of the converter dolly was included in the analyses. For reduced solution times, the fifth wheel geometry was excluded from the model since the imposed loads could be directly applied to the mounting plate at the areas of contact.

Figure 5.45 depicts these features of the model together with the orientation of the global coordinate system. The X, Y and Z axes are taken as the longitudinal, vertical and lateral directions respectively.

Similar to the structural analyses for the semi-trailers, the von-Mises stress criterion was used to evaluate the design stresses for the converter dolly [54, 57, 61, 83, 85] as it is most appropriate for determining the structural safety of materials showing elastic properties [92].

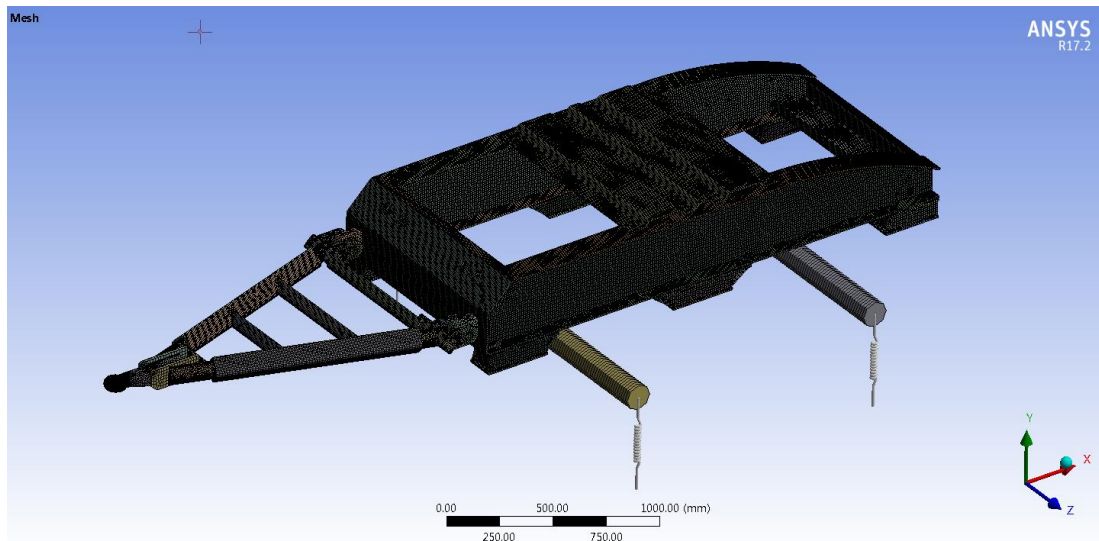


Figure 5.44: Meshed converter dolly geometry

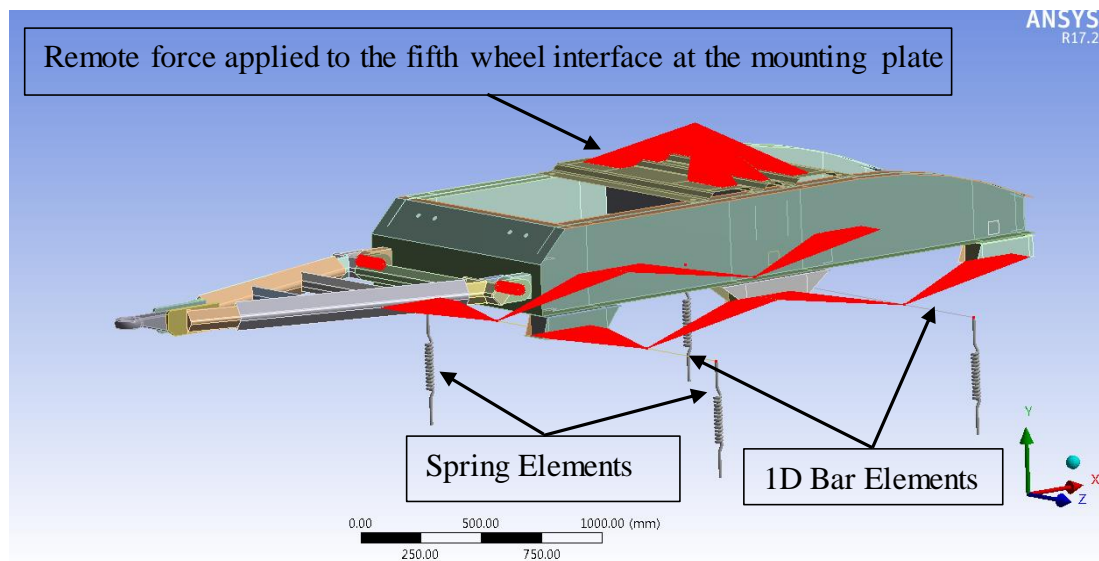


Figure 5.45: Finite element model representation

5.5.7.2 Vertical Load Case

This load case consists of the vertical force applied to the mounting plate, together with an acceleration equivalent to two times gravity in the vertical direction (negative Y axis direction of the global coordinate system) applied to the entire model. The vertical force applied to the mounting plate was equal to twice the actual vertical load transferred from the semi-trailer to the fifth wheel of the converter dolly in order to maintain a design factor of 2 (see Chapter 4.3.2.4). The model was constrained in the respective directions at the suspension and the towing eye to prevent rigid body motion, while

replicating the actual restraints on the converter dolly during real life usage. Translational constraints in the direction of the global X and Y axes were applied to top and bottom of the springs respectively, while the translational constraint in the direction of the global Z axis was applied to the inner surface of the towing eye and the top of the springs. The von-Mises stress plots for this load case are shown in Figure 5.46 and Figure 5.47.

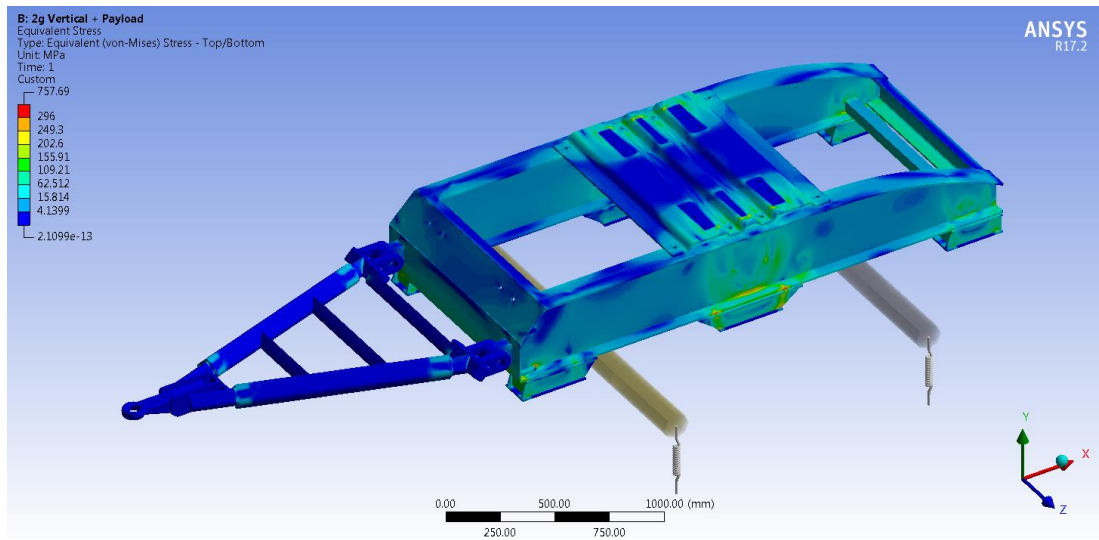


Figure 5.46: von-Mises stress plot for the converter dolly vertical load case – top view

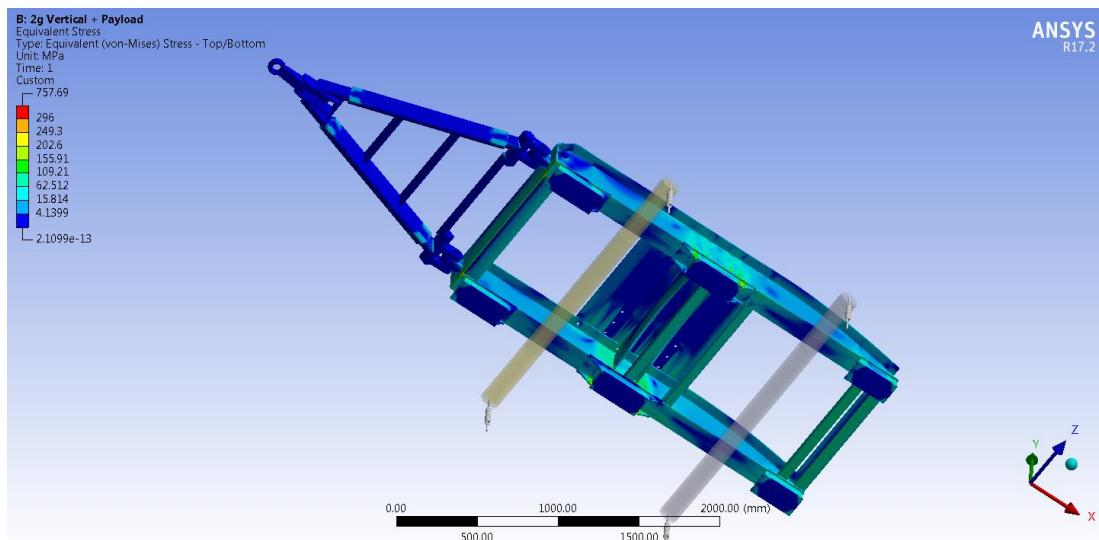


Figure 5.47: von-Mises stress plot for the converter dolly vertical load case – bottom view

The results of this load case complied with the design criteria for the converter dolly with a non-localised peak stress of 266 MPa occurring on the web of the longitudinal beam in the region of the bottom flanges, resulting in a safety factor of 1.33. This falls within the allowable safety factor range discussed in Chapter 4.3.2.4. Localised high stress points exceeding the yield stress of the material were found in the longitudinal beams webs at the corner regions of the front cross member and at the interface

between the longitudinal beams and the foremost pedestal (see Figure 5.48), discussed further in Chapter 8.

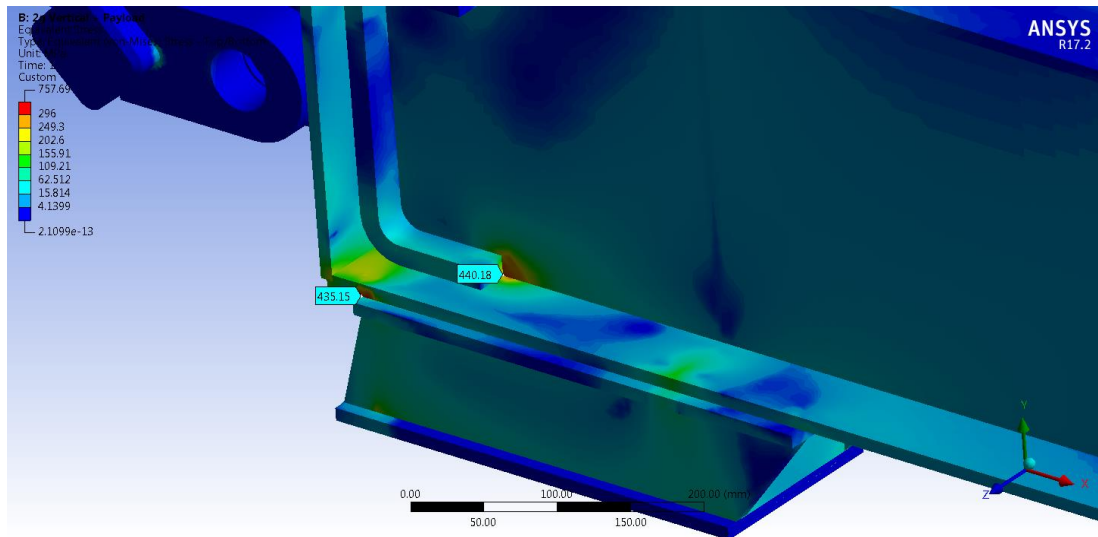


Figure 5.48: Localised high stress regions for the vertical load case

5.5.7.3 Longitudinal Braking Load Case

The longitudinal braking load case consists of the vertical force applied to the mounting plate which is equivalent to the actual vertical load transferred from the semi-trailer to the fifth wheel of the converter dolly, coupled with an acceleration of 0.52g applied to the entire model in the negative X direction of the global coordinate system. The force component on the fifth wheel due to the longitudinal acceleration was included in the model, equivalent to the imposed vertical load on the fifth wheel multiplied by the longitudinal acceleration magnitude. This force was applied in the negative X direction of the global coordinate system.

Gravity was applied to the model in the negative Y direction of the global coordinate system. Similar to the vertical load case, the model was constrained in the respective directions at the towing eye and the suspension to prevent rigid body motion, while replicating the actual restraints on the structure during real life usage which resembled braking of the converter dolly. Translational constraints in the direction of the global Y and Z axes were applied to the bottom and top of the springs respectively, while the translational constraint in the direction of the global X axis was applied to the inner surface of the towing eye. The von-Mises stress plots for this load case are shown in Figure 5.49 and Figure 5.50.

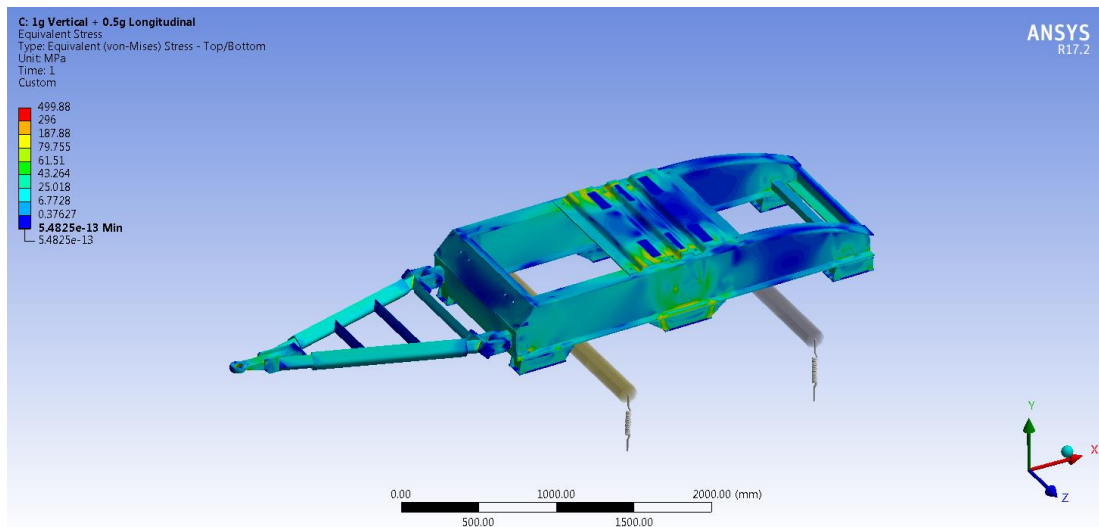


Figure 5.49: von-Mises stress plot for the converter dolly braking load case – top view

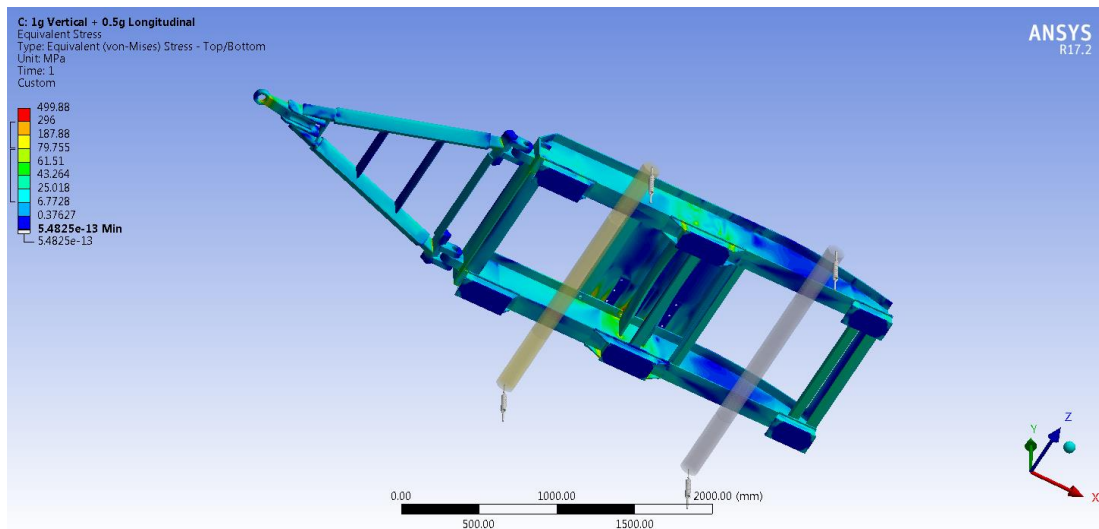


Figure 5.50: von-Mises stress plot for the converter dolly braking load case – bottom view

The results of this load case complied with the design criteria for the converter dolly with a non-localised peak stress of 174 MPa occurring on the bottom flange of the longitudinal beams in the region of the centre pedestal, resulting in a safety factor of 1.7. This falls within the allowable safety factor range. Localised high stress points exceeding the yield stress of the material were found at the corners of the members supporting the mounting plate (see Figure 5.51), however this is due to modelling approximations used in the FEA process and is not deemed a true representation of the stress distribution in those areas [93], as discussed further in Chapter 8.

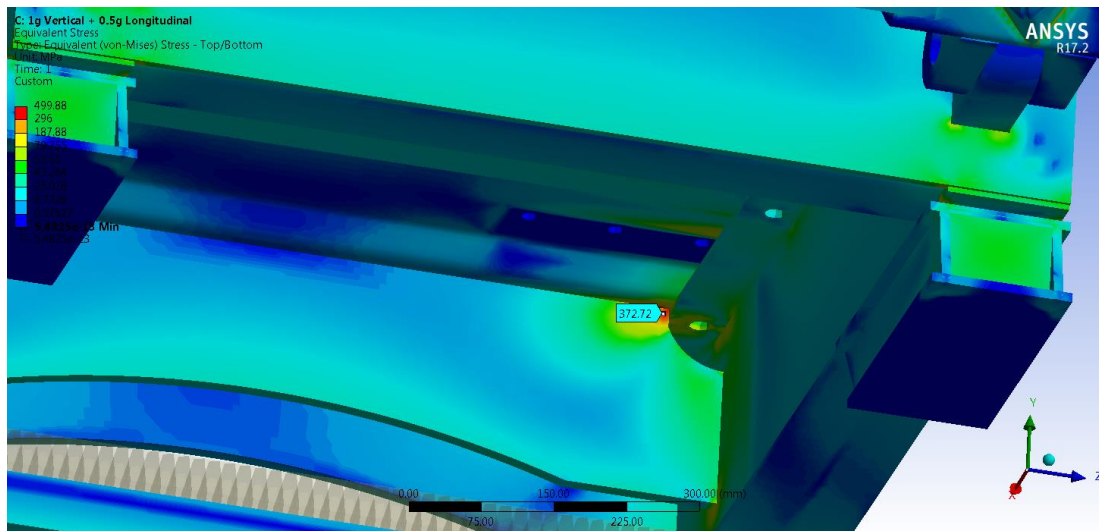


Figure 5.51: Localised high stress regions at the corner of the mounting plate support members

5.5.7.4 Longitudinal Acceleration Load Case

The longitudinal load case simulating the maximum horizontal force on the drawbar of the converter dolly due to the tractive force of the terminal tractor was conducted by applying this force directly onto the towing eye in the negative X direction of the global coordinate system. As previously mentioned, the D-value is a theoretical reference force calculation used to determine the strength requirements of the coupling and is based on the mass of the vehicles concerned, however it does not represent the actual horizontal force on the couplings due to the tractive performance of the prime mover.

Similar to the longitudinal acceleration load case for the semi-trailer design where the maximum calculated tractive force was applied to the kingpin, the maximum horizontal force on the towing eye during take-off was calculated as 120 kN and applied onto the towing eye for the analysis using the performance data shown in Appendix B.

Together with the horizontal force, this load case consisted of the vertical force applied to the mounting plate equivalent to the actual vertical load transferred from the semi-trailer to the fifth wheel of the converter dolly in the negative Y direction of the global coordinate system. Translational constraints in the direction of the global Z and Y axes were applied to the top and bottom of the springs respectively, while the translational constraint in the direction of the global X axis was applied to the mounting plate in the areas which contact the fifth wheel. The von-Mises stress plots for this load case are shown in Figure 5.52 and Figure 5.53.

The non-localised peak stress in this load case was found to be 213 MPa on the front end of the bottom flange of the longitudinal beams, resulting in a safety factor of 1.67, that falls within the allowable safety factor range discussed in Chapter 4.3.2.4. Localised high stress points exceeding the yield stress

of the material were found at the corners of the square sections used to form the drawbar hinge, shown in Figure 5.54. These localised high stresses are discussed further in Chapter 8.

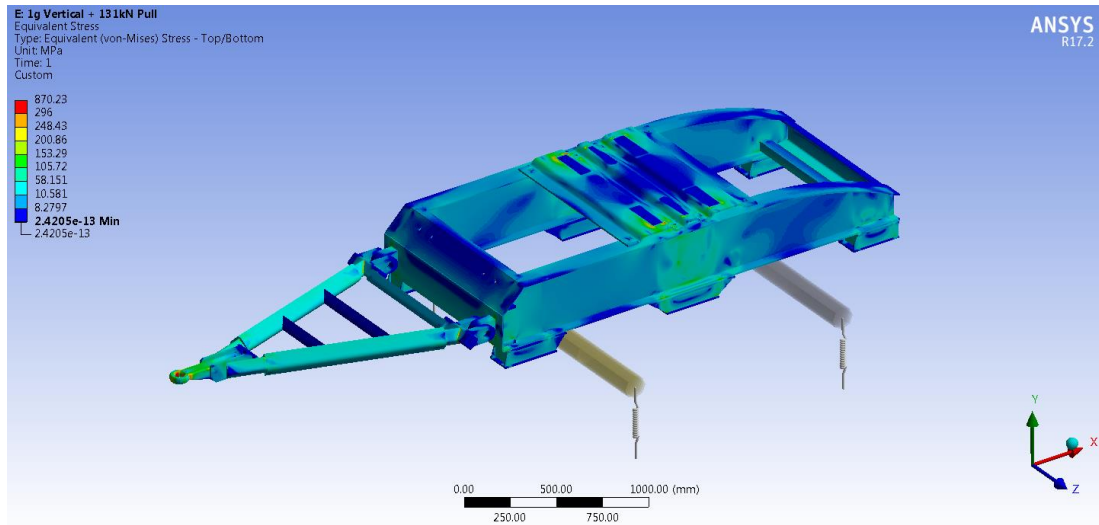


Figure 5.52: von-Mises stress plot for the converter dolly accelerating load case – top view

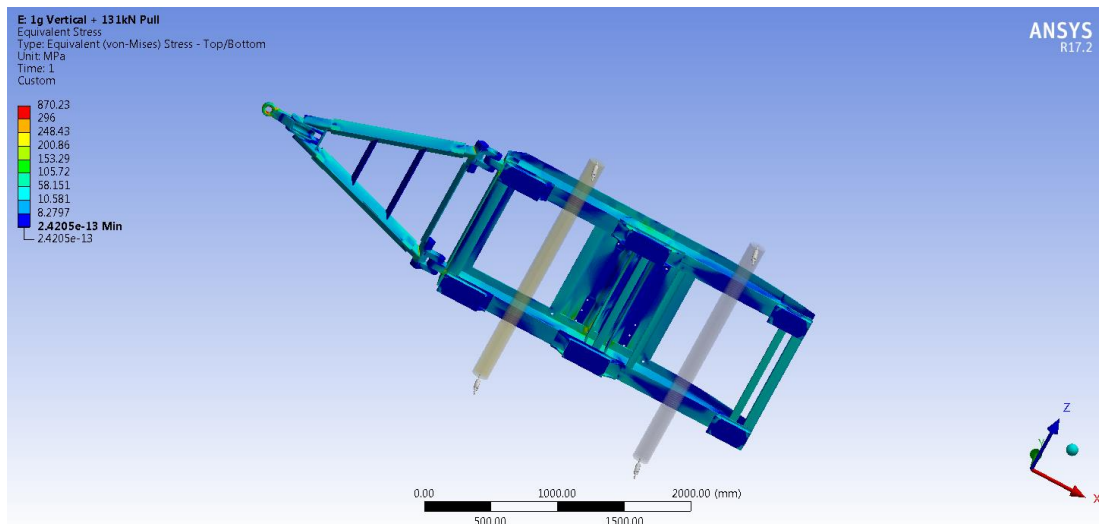


Figure 5.53: von-Mises stress plot for the converter dolly accelerating load case – bottom view

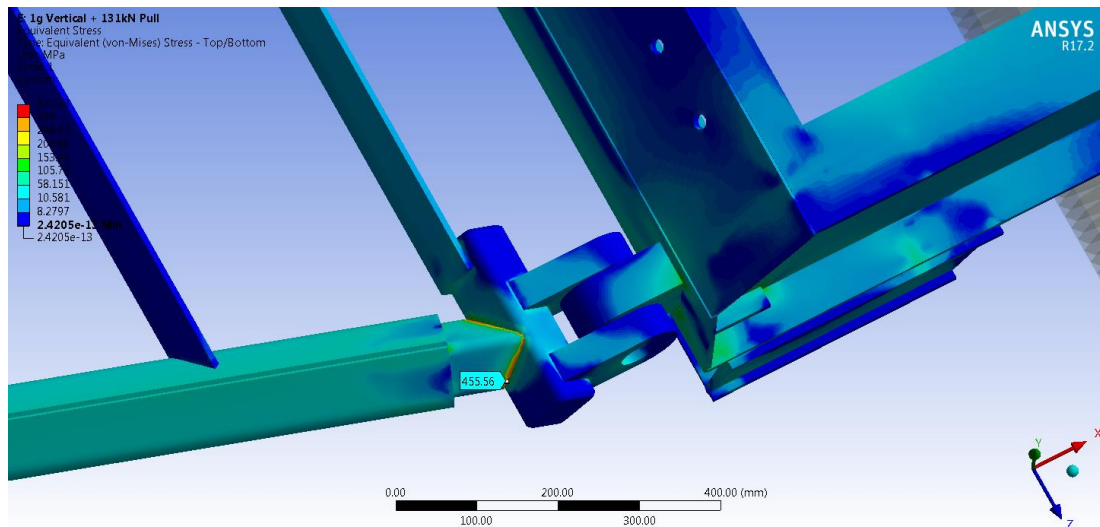


Figure 5.54: Localised high stress at the corners of the square sections of the drawbar hinge

5.5.7.5 Lateral Load Case

The lateral load case was conducted to simulate the cornering effects on the converter dolly during turning manoeuvres of the MTS. This load case consisted of the vertical force on the mounting plate together with an acceleration of 0.25g applied to the entire model in the negative Z direction of the global coordinate system. Gravity was applied to the model in the negative Y direction. The force component on the fifth wheel due to the lateral acceleration was included in the model, equivalent to the imposed mass on the fifth wheel multiplied by the lateral acceleration of 0.25g. This force was applied in the negative Z direction of the global coordinate system.

Similar to the previous load cases, the model was constrained at the towing eye and the suspension to prevent rigid body motion, replicating the actual restraints on the structure during real life cornering. Translational constraints in the direction of the global X and Y axes was applied to the top and bottom of the springs respectively, while the translational constraint in the direction of the global Z axis was applied to the inner surface of the hole in the towing eye. The von-Mises stress plots are shown in Figure 5.55 and Figure 5.56.

The non-localised peak stress in this load case was found to be 286 MPa on the webs of the longitudinal beams, resulting in a safety factor of 1.24. This value falls within the allowable safety factor range. Localised high stress points exceeding the yield stress of the material were found at the corners of the square sections used to form the drawbar hinge, shown in Figure 5.57 and discussed further in Chapter 8.

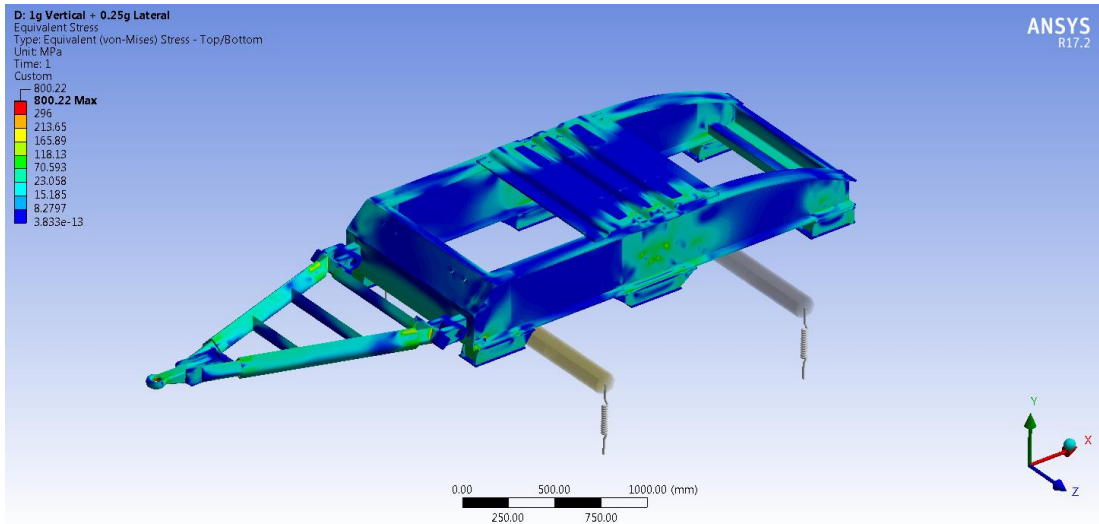


Figure 5.55: von-Mises stress plot for the converter dolly lateral load case – top view

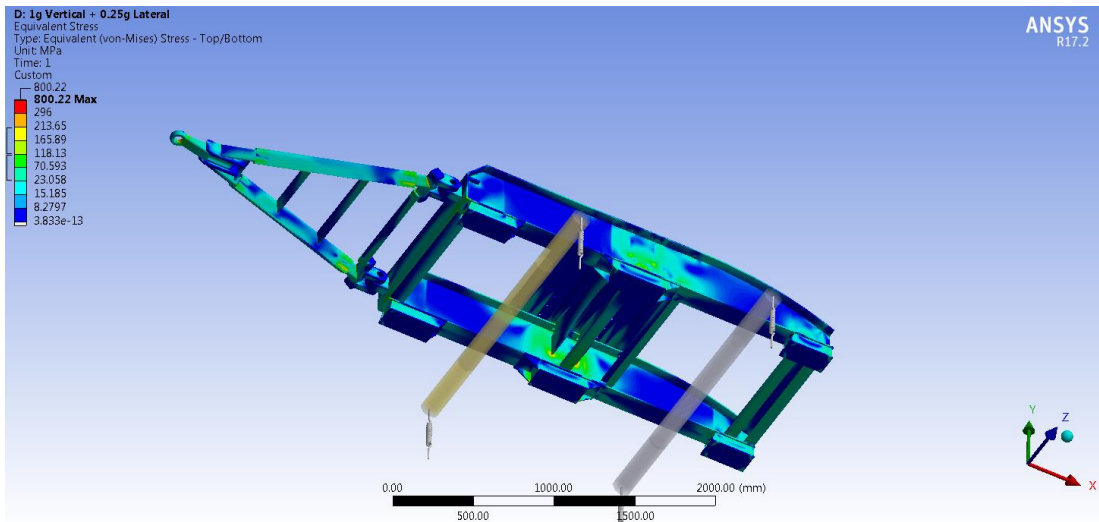


Figure 5.56: von-Mises stress plot for the converter dolly lateral load case – bottom view

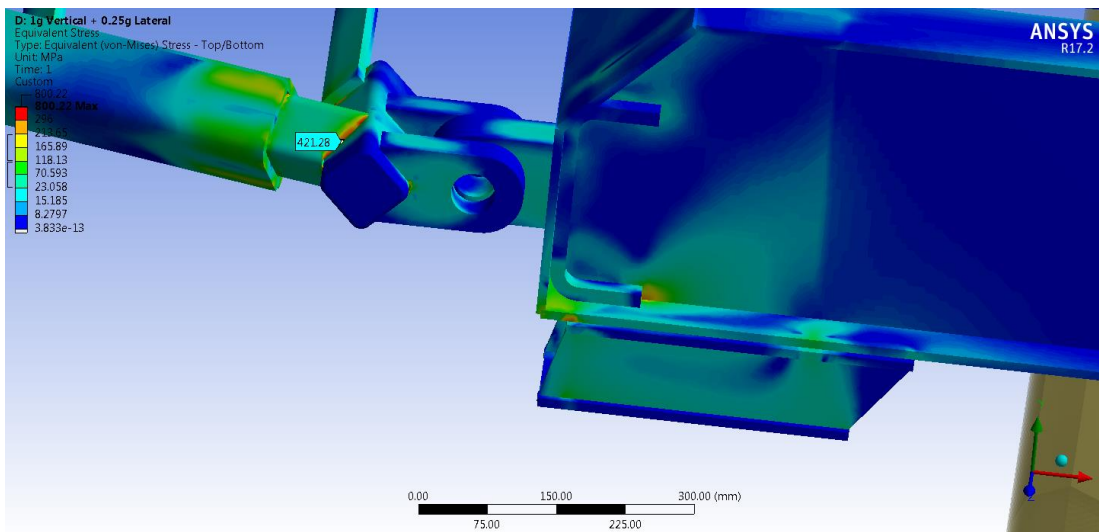


Figure 5.57: Localised high stress at the drawbar hinge corners

5.5.8 Converter Dolly Final Design

The results of the structural analysis showed that the initial design of the converter dolly was within the limits of the safety factor range detailed in Chapter 4.3.2.4. Subsequent analyses of the structure allowed for the reduction in the thickness of certain members which experienced low stress in order to reduce the mass of the converter dolly's chassis, resulting in a mass reduction of 148 kg when compared to the initial chassis design. On completion of the structural analysis the CAD model of the converter dolly was updated with the reduced material thicknesses. The modifications resulted in a final structural mass of 1 045 kg. Figure 5.58 shows the CAD model of the finalised converter dolly designed for use in the MTS.

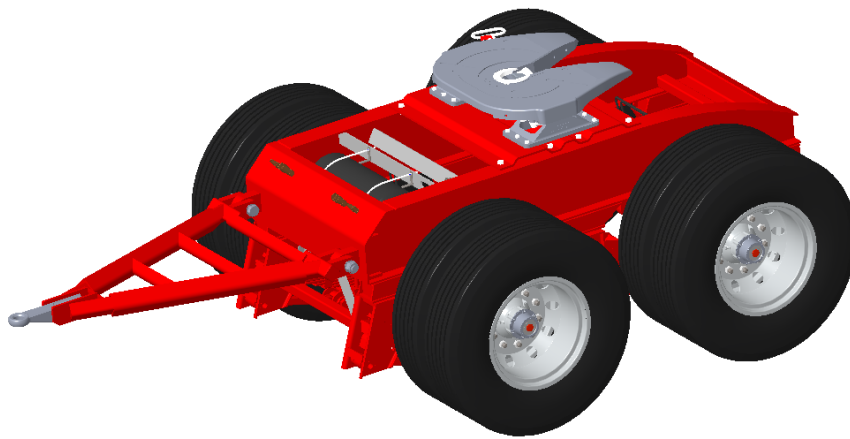


Figure 5.58: Finalised converter dolly design

5.6 Complete Multi-Trailer System

The completed MTS design is shown in Figure 5.59 with the identical semi-trailers connected using the converter dolly. The MTS has a total tare mass of 20 571 kg (including the mass of the suspensions, axles and tyres) and a length of 27.8 m with the two semi-trailers in the set.



Figure 5.59: Completed MTS design

5.7 Chapter Summary

A detailed design of the MTS was provided, beginning with the design of the semi-trailers and thereafter the converter dolly. The Kalmar TR626i terminal tractor was selected as the prime mover for the MTS such that the appropriate geometrical features and clearances could be implemented into the design to allow it to function without structural interference from the prime mover. The MTS was designed in accordance with the technical and functional requirements presented in Chapter 4.3.1 and was verified structurally using FEA based on the criteria presented in Chapter 4.3.2.4. An iterative design process was adopted where the mass of both the semi-trailer and converter dolly was reduced based on the results of the structural analyses. This was done to reduce the manufacturing cost of the product in order to increase the operational cost benefit of using MTSs at Pier One.

6 Turning Analysis

6.1 Introduction

This chapter details the turning analyses of the MTS for the container movement operations undertaken at the Durban Container Terminal. The investigation was conducted to ensure that the vehicle is able to complete the typical turning manoeuvres required for container movement within the confinement of Pier One. The turning software BricsTurn[®] was used to conduct the analyses for the expected turning activities. The results of the analyses were used to confirm that the MTS was able to be manoeuvred around the quayside and within the available space between the stacking areas using the Kalmar TR626i terminal tractor.

6.2 Equivalent Wheelbase for the Tractrix Method

BricsTurn[®] utilises the geometric tractrix method to predict the low speed swept path of a vehicle combination as the steering axle traverses a predefined curve. The method is based on the passive following of the trailing axle groups in the vehicle combination, with the curves tracking the path followed by the geometric centre of the trailing axle groups during a turn known as the “tractrix” curve [97]. To obtain the swept path of the vehicle combination, the tractrix curve is offset using the geometry of the vehicle, considering the change in perpendicularity of the steering axle to the prescribed path being followed [98]. BricsTurn[®] relies on the following geometric parameters to generate the tractrix curves and hence the swept path of a multi-unit vehicle combination:

1. The wheelbase of each vehicle in the set. For multiple axles, this is measured to the geometric centre of the axle group.
2. The distance from each coupling point to the centre of the preceding axle group.
3. The width of the vehicles and each axle group.
4. A predefined path followed by the centre of the steering axle.

During turning manoeuvres, vehicles with multiple fixed trailing axles do not experience pure rolling motion due to tyre scrub which creates lateral forces generated by the tyres at the ground interface [98], reducing the turning performance of the vehicle by inducing a larger swept path. Effectively, a vehicle with multiple fixed trailing axles would not exhibit the same turning behaviour as that of a vehicle with a single fixed trailing axle. This is an effect that BricsTurn[®] does not automatically take into consideration. To model the turning performance of vehicles with multiple axles, an “equivalent wheelbase” principle was developed by Winkler and Aurell [99] on the basis that a vehicle with multiple fixed trailing axles with wheelbase WB may be reduced to having one fixed axle with equivalent wheelbase WB_{Eq} , producing the same turning behaviour at low speeds. Figure 6.1 depicts this relationship for a three-axle rigid truck (two fixed rear axles and one steering axle). The broken lines represent the bicycle model of the three-axle vehicle with wheelbase WB and an axle spacing of 2Δ .

The lateral forces at the tyre-ground interface due to the slip angles created is denoted by F_y . The solid lines represent the two-axle vehicle with equivalent wheelbase WB_{Eq} (one fixed rear axle and one steering axle).

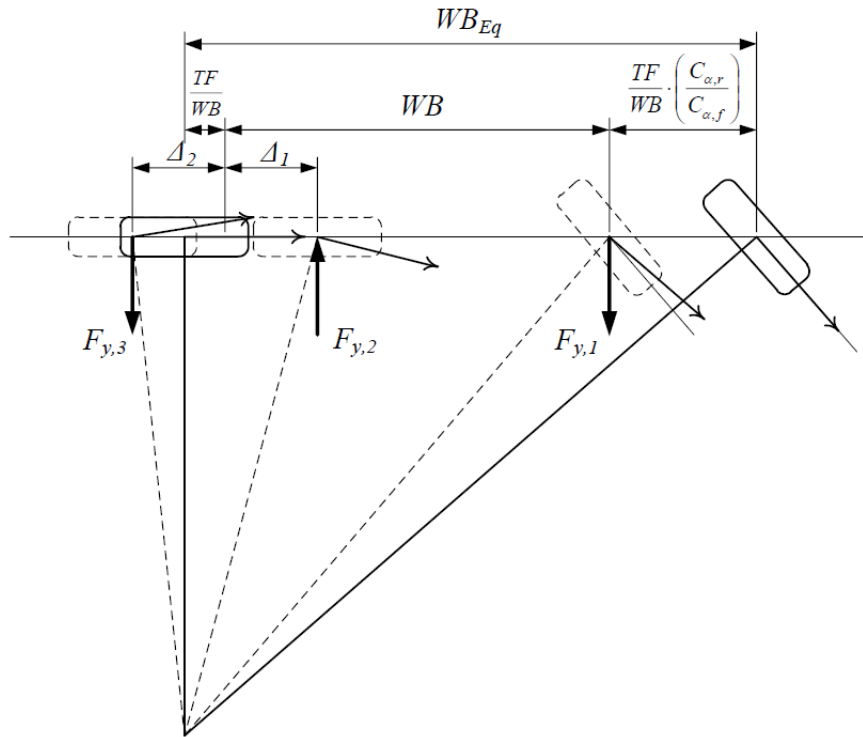


Figure 6.1: Equivalent wheelbase for a three-axle rigid truck [98]

Winkler and Aurell [99] defined the wheelbase of the equivalent two axle vehicle, WB_{Eq} , shown in Figure 6.1 using Equation (6.1) where C_α is the sum of the cornering stiffness of the front and rear tyres, denoted by subscript f and r , and TF the tandem factor. The cornering stiffness is a proportionality constant characterised by the ratio of a tyre's slip angle and the resulting lateral force developed [98].

$$WB_{Eq} = WB + \frac{TF}{WB} + \frac{TF}{WB} \left(\frac{C_{\alpha,r}}{C_{\alpha,f}} \right) \quad (6.1)$$

The tandem factor, TF , is obtained from Equation (6.2) for a vehicle with n fixed axles.

$$TF = \left(\sum_{i=1}^n \Delta i^2 \right) \div n \quad (6.2)$$

For the particular case of low speed turning, the equivalent vehicle model develops small slip angles and the third term in Equation (6.1) can be omitted [98, 99], making the equivalent wheelbase independent of the tyre's cornering stiffness at low speeds.

While the study conducted by Winkler and Aurell in [99] was for that of a rigid truck, the same theory can be applied to trailer systems by substituting the hitch points as the steering axle [98]. Although lateral hitch forces are not present in the case of a rigid truck around which the theory was developed, de Saxe [98] showed that the effect of lateral hitch forces on the equivalent wheelbase model can be neglected, which was also in line with the findings of Morrison [100]. Equations (6.1) and (6.2) were utilised to find the equivalent wheelbase for each vehicle in the MTS for use as inputs into the turning models implemented in BricsTurn®.

6.3 BricsTurn® Simulation

6.3.1 Method Validation

To validate the results yielded by BricsTurn®, the swept path plots of the double and triple-trailer combination vehicles used for the geometric design of highways, as shown in the governing AASHTO policy of 2001 [101], were compared to the plots yielded by BricsTurn® for the same vehicles and turn using its geometric parameters presented in [101]. This approach was necessitated by the lack of other publicly available swept path plots of vehicles for particular turning manoeuvres, including data of the vehicle's geometric parameters and information on the turn radius. The AASHTO policy is used for the design of roads in the United States of America, in part to ensure that all vehicle types are catered for with regard to the space requirements for turning. Figure 6.2 and Figure 6.3 shows the swept paths of a double-trailer (called a 33D) and triple-trailer (called a 30T) adapted from the AASHTO road design guideline, each for a 180° turn at their respective centreline turn radii (CTR). The replicated scenarios using BricsTurn®, shown in Figure 6.4 and Figure 6.5, yielded results within 2.5% for the minimum and maximum radii of the swept paths when compared to the plots from the AASHTO policy, validating the results produced by BricsTurn®. Table 6.1 shows the results comparison for the models implemented in BricsTurn® to the data obtained from the AASHTO road design guideline.

Table 6.1: Comparison of BricsTurn® and AASHTO swept path radii for the 33D and 30T trailers

Parameter	Data Source	33D Double-Trailer	30T Triple-Trailer
Maximum outer radius of the swept path	AASHTO	18.4 m	13.87 m
	BricsTurn®	18.4 m	13.86 m
% Difference		0 %	0.07 %
Minimum inner radius of the swept path	AASHTO	4.54 m	3 m
	BricsTurn®	4.43 m	2.93 m
% Difference		2.43 %	2.33 %

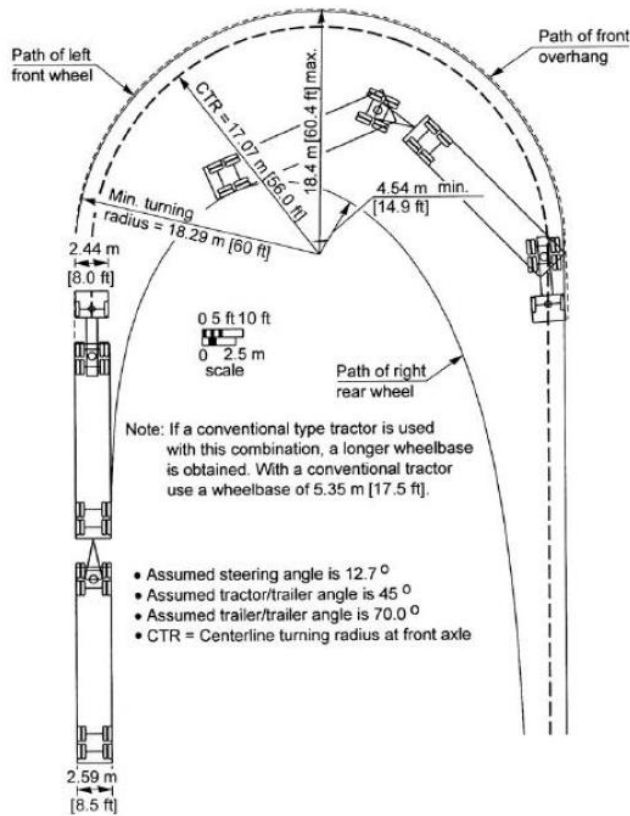


Figure 6.2: Turning path for 33D double-trailer combination [101]

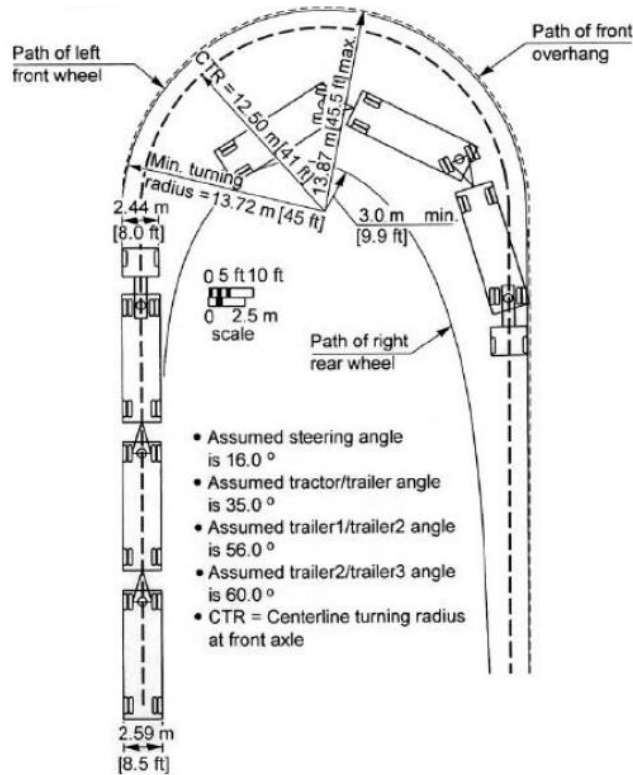


Figure 6.3: Turning path for 30T triple-trailer combination [101]

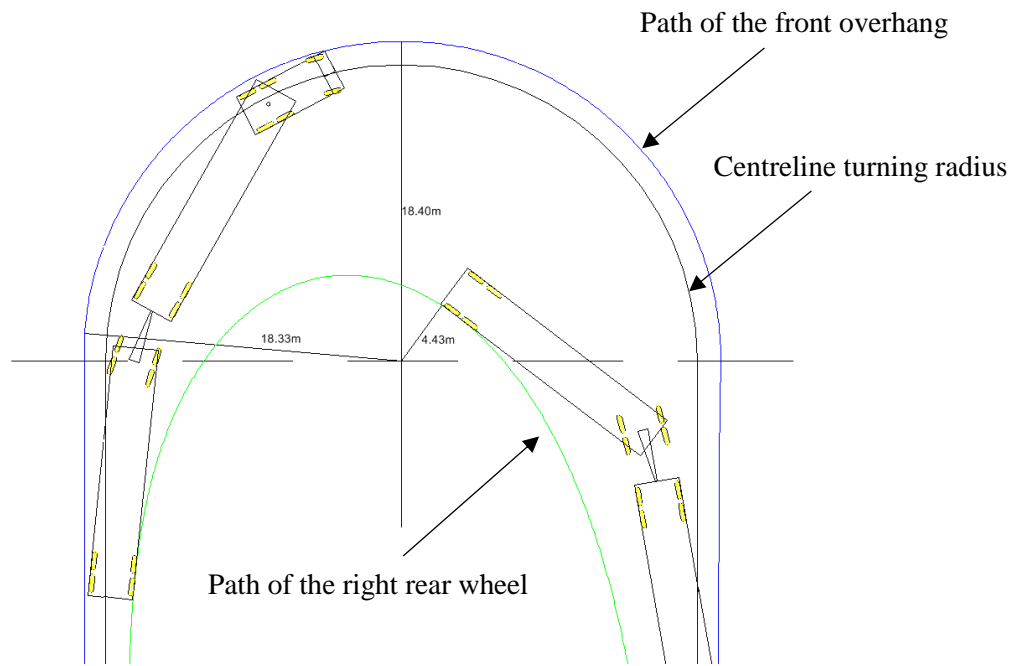


Figure 6.4: BricsTurn[®] swept path plots for the for 33D double-trailer combination

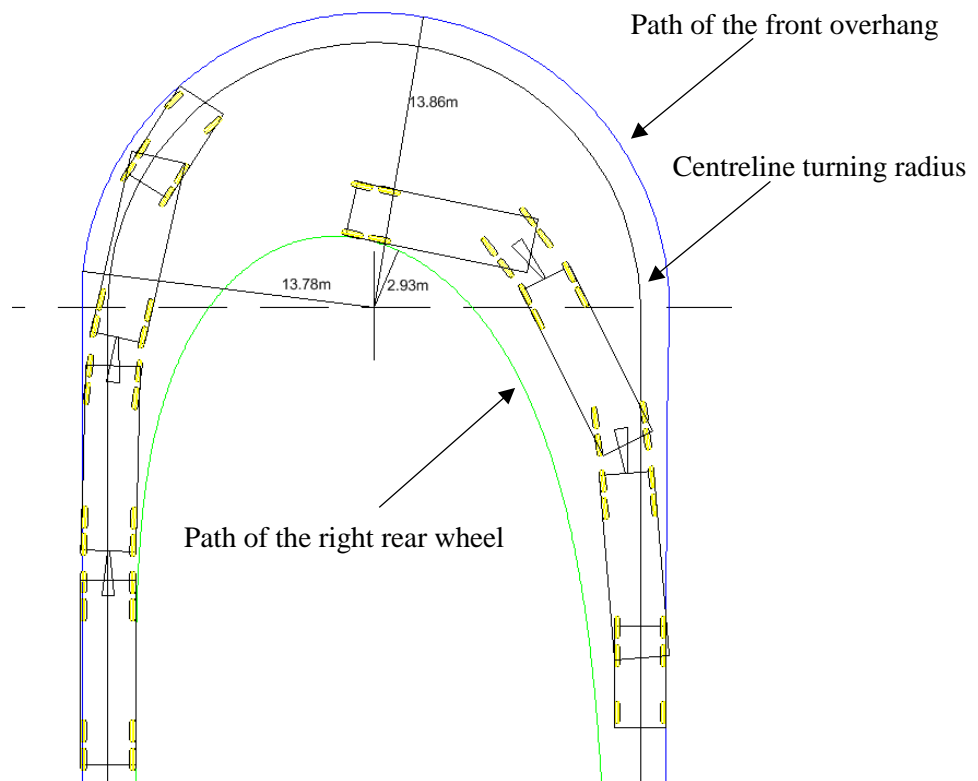


Figure 6.5: BricsTurn[®] swept path plots for the for 30T triple-trailer combination

6.3.2 Input Data

BricsTurn[®] requires the wheelbase lengths of each vehicle in the MTS set as well as the various hitch point distances to the relevant bogie centres to carry out the analyses. Steering and geometry data for the prime mover was obtained from the respective product data sheets for the Kalmar TR626i terminal tractor. The steering lock-to-lock time for the tractor, defined as the time taken to turn the steering wheel from full left lock to full right lock (or vice versa), was approximated as 3.5 seconds for the analyses. This was determined from physical lock-to-lock time measurements of the existing tractors at the Durban Container Terminal where the average time for multiple drivers was obtained. The time measurement activity was required since this information for the TR626i model was not readily available. All simulations were conducted at the maximum terminal operating speed of 30 km/hr., together with the equivalent wheelbase (see Chapter 6.2) of each individual vehicle in the set. Figure 6.6 shows the user interface of BricsTurn[®] and the input data for the MTS's turning analyses.

The screenshot displays the BricsTurn software interface for inputting vehicle data for an MTS. The interface is divided into several sections:

- Vehicle List:** A list of vehicle models including AASHTO A-BUSM, AASHTO BUS-40, AASHTO BUS-45, AASHTO P, AASHTO P-T, AASHTO WB-100T, AASHTO WB-40, AASHTO WB-50, AASHTO WB-62, AASHTO WB-65, AASHTO WB-67, AASHTO WB-67D, and DRAWBAR, FTA 98 (UK). The MTS model is selected and highlighted in blue.
- Vehicle data:** Fields for Name (MTS), Type (Double Trailer), and Units (Meter).
- Vehicle Path Units and Direction:** A dropdown menu set to 'Meter' and a checkbox for 'Reverse direction'.
- Speed:** A dropdown menu set to '30 km/h (Kilometers/Hour)'.
- Output Settings:** Checkboxes for 'Plot Vehicle', 'Plot only First and Last', 'Plot Swept Path', and 'Plot Vehicle Swept Envelope'. The 'Max Vehicle Plot Spacing' is set to 2.
- Vehicle Details:** A section with tabs for 'Vehicle Details', 'Turning Report', and 'Lock to lock Report'. It features a diagram of the vehicle with dimensions labeled (F, WB, B, H, H2, H3, F2, F3, WB2, WB3, B2, B3) and a table of values.

Total Length: 32.217 meter

Width	#1	#2	#3	Lock to lock time (seconds)	3.5		
Wheel	2.5	2.578	2.578	Max wheel turning angle (seg #1)	25.95		
Vehicle	2.5	2.789	2.789	Max angle between Segments	70		
F=	1.65	H=	-0.292	F2=	1.122	F3=	1.277
WB=	3.4	H2=	2.964	WB2=	8.96	WB3=	8.96
B=	0.825	H3=	3.169	B2=	3.185	B3=	3.185

Figure 6.6: BricsTurn[®] input data for the MTS's turning analyses

6.3.3 Turning Manoeuvres

The turning simulations implemented in BricsTurn® to validate the manoeuvrability of the MTS within the confinement of Pier One was carried out by replicating the expected turns which the MTS would need to complete for container movement between the vessel and stacking areas during the vessel loading and unloading operations. Each simulation required the intended path of the centre of the tractor's steering axle to be sketched and used as an input for the path to be followed by the tractor. Rectangular blocks representing the size of the stacking areas were included in the layout of the simulation output area to visualise the MTS manoeuvring within the terminal. Each turn was simulated using radii equal to the minimum turn radius of the TR626i terminal tractor (7.77 m) so as to not violate its turning capabilities. Figure 6.7 shows the tractrix curves of a common double 90° turn where the MTS exits and enters adjacent storage blocks (e.g. exiting between blocks F and G and entering between blocks D and E) centrally, while Figure 6.8 depicts the worst case, highly uncommon, scenario of the MTS both exiting and entering a storage block directly underneath an RTG.

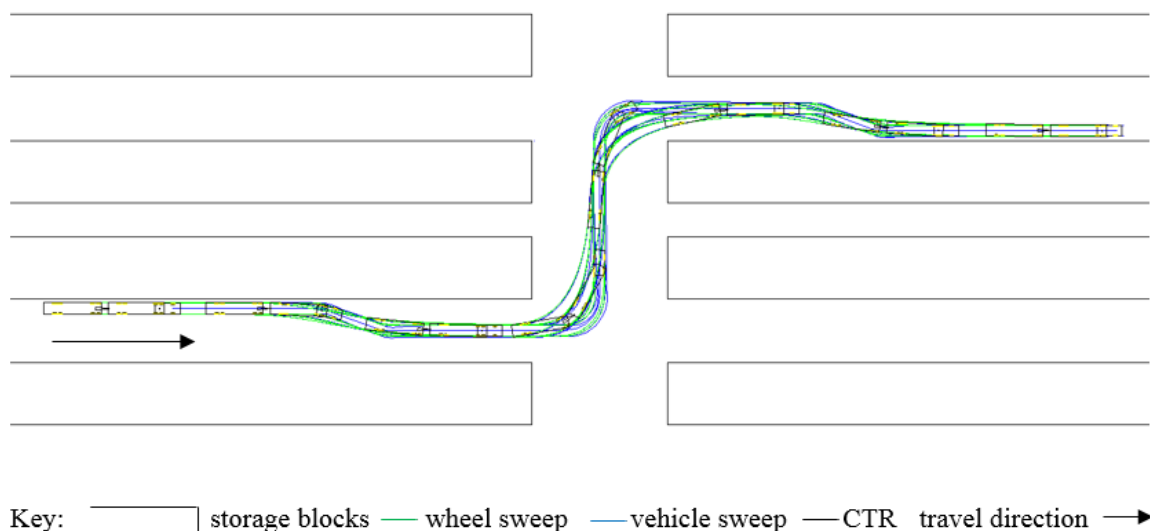
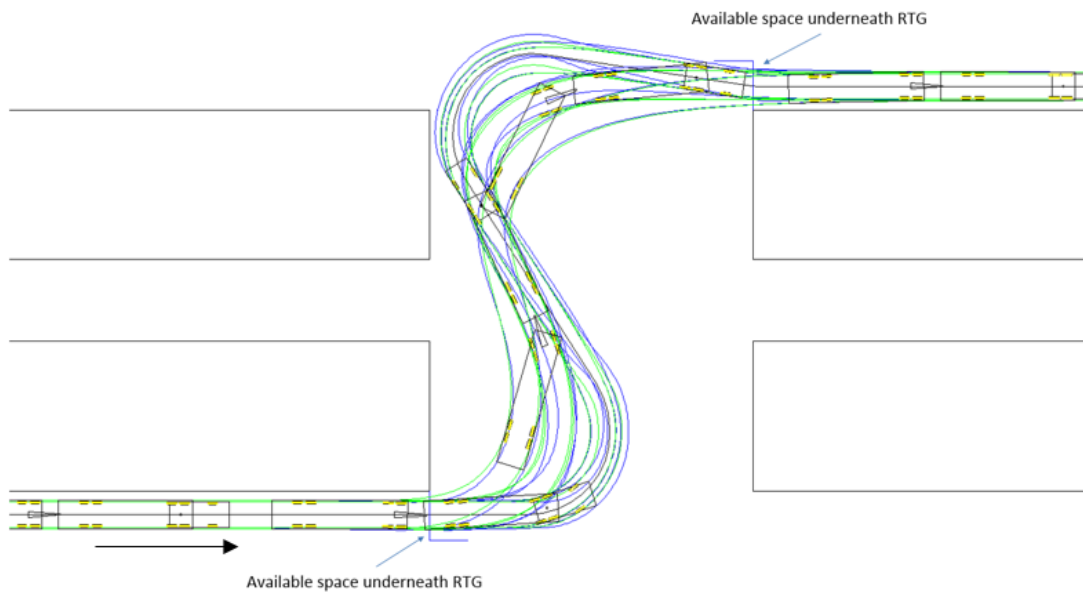


Figure 6.7: Double 90° turn with central exit-entry of storage blocks

For the worst case scenario shown in Figure 6.8, the MTS needs to complete a 123° turn at the minimum turning radius when exiting the storage block, followed by a 131° turn also at the minimum turning radius in order to enter the next storage block without colliding with the RTG. The angles and lengths of this turn were determined using an iterative approach since BricsTurn® does not automatically suggest a path to be followed for the completion of a turn.

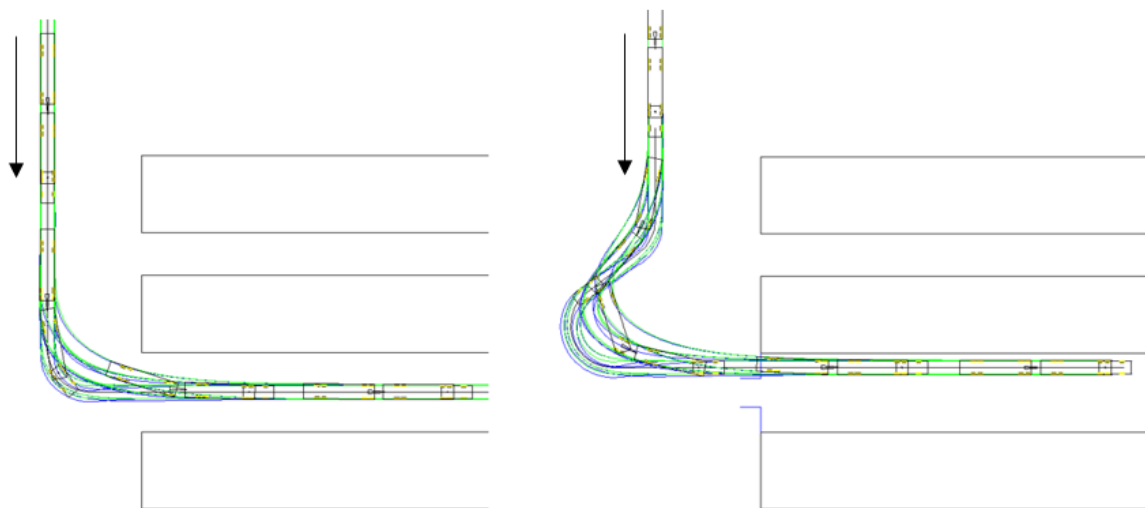
Figure 6.9 shows the MTS entering the stacking area of block 1 for each area designation (blocks A1, B1, C1..., G1) for the scenario of entering centrally and the worst case of having to enter the block underneath an RTG. For the case of entering underneath an RTG, the MTS would have to complete a 127° turn moving away from the storage block for approximately 12 m and thereafter complete a 142°

turn to enter the block. An iterative approach was used to determine these parameters, similar to that described for the turns between adjacent storage blocks.



Key: storage blocks — wheel sweep — vehicle sweep — CTR travel direction →

Figure 6.8: Worst case exit-entrance of adjacent storage blocks (underneath RTG)



Key: storage blocks — wheel sweep — vehicle sweep — CTR travel direction →

Figure 6.9: Entering a stacking area (blocks A1 to G1) centrally (left) vs. underneath an RTG (right)

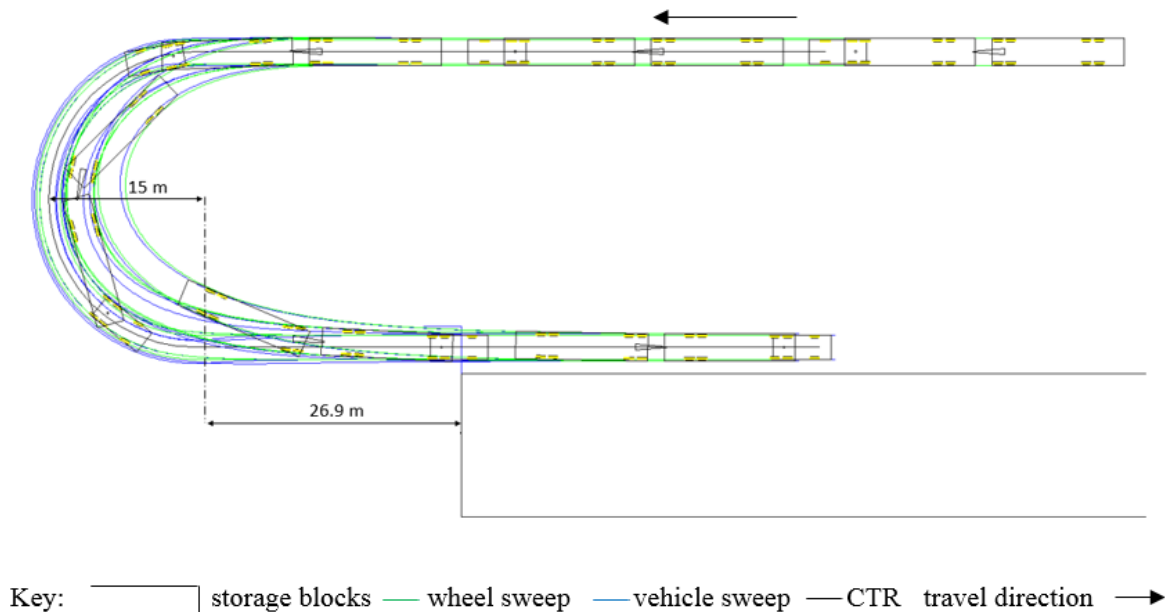


Figure 6.10: Entering blocks A1, A2 and A3 underneath an RTG during vessel loading

Figure 6.10 depicts the worst case turning manoeuvre (entering the storage block underneath an RTG) which the MTS would complete between the QCs and storage blocks A1 to A3 for the case of using the MTS for the vessel loading procedure. For this scenario, the entire available space between the QCs and blocks A1 to A3 can be used to perform the 180° turn. Using a 15 m turning radius for the tractor, the start of the turn must occur at a minimum horizontal distance of 26.9 m away from the entrance point of the RTG to ensure that a collision between the two does not occur. Again, an iterative approach was used to determine these parameters

The above analyses using BricsTurn® validates the ability of the MTS to be manoeuvred within Pier One for container movement between the vessel and the stacking areas using the Kalmar TR626i terminal tractor.

6.4 Chapter Summary

This chapter presented the turning analyses conducted for the MTS using BricsTurn®. Background information on the effect which multiple axles have on the turning performance of a vehicle was provided, together with the equivalent wheelbase method which is used to model these effects. The results yielded by BricsTurn® for an 180° turn of the 33D double-trailer and the 30T triple-trailer was validated using the AASHTO road design guideline prior to the analyses being conducted for the MTS. The turning analyses for the MTS included the worst case scenarios which could be encountered during container movement at Pier One, with the results of the analyses verifying that the designed MTS can be operated by any competent driver within the confinement of Pier One.

7 System Comparison

7.1 Introduction

This chapter presents a comparative analysis for the scenarios of using the semi-trailer designed in this study versus Pier One's existing semi-trailer design as the vehicles in the MTS configuration. As mentioned in Chapter 4.2.2, the existing semi-trailer design currently used by the terminal could be modified by adding towing hitches at the rear of each trailer, and used with the converter dolly designed in this study to form the MTS configuration, however, an opportunity existed for a better designed semi-trailer with regards to mass, cost and manoeuvrability, since the Port of Durban recapitalises its trailer fleet in 5 year cycles. The mass, product cost and turning performance for both semi-trailer designs, when used in the MTS arrangement, is compared together with its influence on reducing the operational cost of the waterside horizontal-transport system at Pier One. The preliminary operational cost comparison presented in Chapter 3.4 is refined in Chapter 7.3, using the results from Chapter 7.2, factoring in the actual cost of the MTS designed in this study.

7.2 Comparison

7.2.1 Mass

Table 7.1 shows the mass comparison of the semi-trailer designs, with the tare mass consisting of the respective chassis and bogie masses combined. The data for the existing semi-trailers was obtained from the study conducted by Dwarika [62] for the analysis. While the bogie mass for the semi-trailer designed in this study was marginally greater than the bogie used on the existing trailers due to the different tyres utilised, the comparison of the chassis masses revealed that the semi-trailer chassis designed in this study had a significantly lower mass than that of the existing semi-trailers, with a saving of approximately 34%. When comparing the tare masses, the saving was found to be approximately 21%. The larger chassis mass of the existing trailers can be attributed to the increased material thicknesses used when compared to the chassis designed in this study, as well as a greater number of cross members and other structural members. This is further discussed in Chapter 8.

Table 7.1: Mass comparison of the semi-trailer designs

Assembly	Existing Semi-trailer	New Semi-trailer	Mass Saving
	kg	kg	%
Chassis	6 670	4 410	33.9
Bogie	3 490	3 580	-2.6
Total Tare	10 160	7 990	21.4

7.2.2 Product Manufacturing Cost

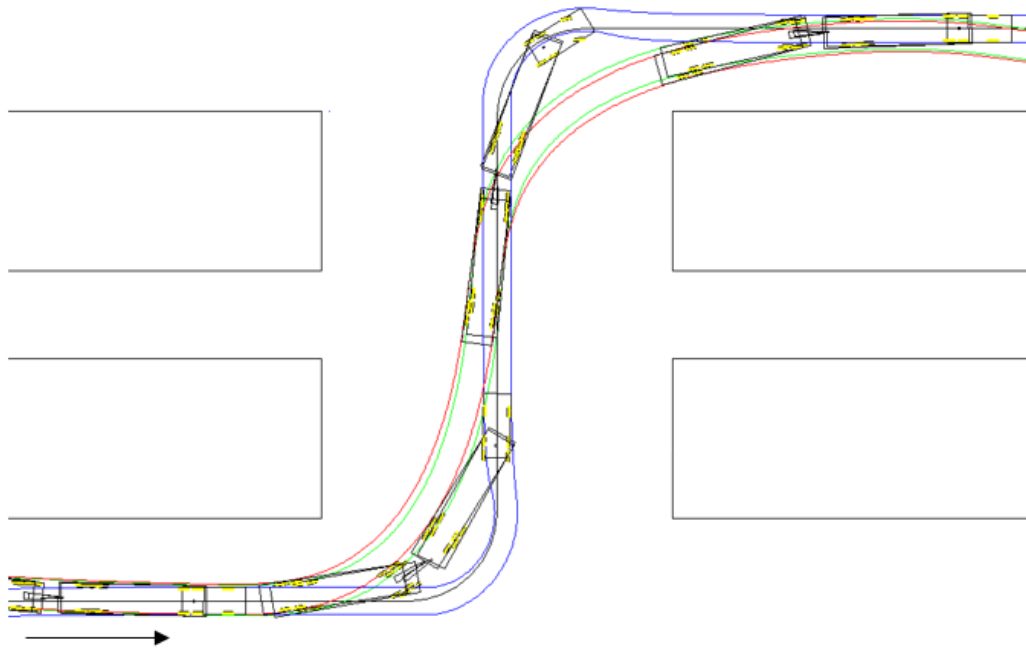
The product cost for the MTS using each semi-trailer design was determined by approximating the material and auxiliary system cost for the semi-trailers as well as the converter dolly. The raw material cost for the chassis of each vehicle was determined using the average steel cost by mass for S355 structural steel, which was R22 823.61 per 1000 kg as of October 2017 [102]. The fabrication cost for these steel items (cutting, bending, machining etc.) was approximated as 50% of the material cost for each respective vehicle. The raw material and fabrication cost approximation was obtained from discussions with steel suppliers on the costs associated with the semi-trailer and converter dolly chassis designed in this study. The cost of the auxiliary systems (bogie, kingpin, towing eyes, fifth wheel and so on) for each vehicle was determined from suppliers within South Africa. Table 7.2 gives the product cost comparison for the MTS when using the two different semi-trailer designs, with a detailed cost breakdown shown in Appendix C. This analysis excluded determining the exact labour costs for manufacturing as it falls outside the scope of this study, however a mark-up on the manufacturing cost to account for labour costs and a suitable profit margin is included in Chapter 7.2.4 when analysing the effect of the equipment cost on the operational cost of the waterside horizontal-transport system. As can be seen in Table 7.2, the cost of the MTS is projected to be 15.1% lower when using the semi-trailer designed in this study than when using the existing semi-trailers. This cost saving can be attributed to the lower mass of the new chassis design, resulting in a cheaper semi-trailer when compared to the existing vehicle.

Table 7.2: Product manufacturing cost comparison for the MTS using each semi-trailer design

Semi-Trailer	Semi-Trailer Cost	Converter Dolly Cost	MTS Cost
Existing	R 457 399	R 293 021	R 1 207 819
New design	R 392 675		R 1 025 679

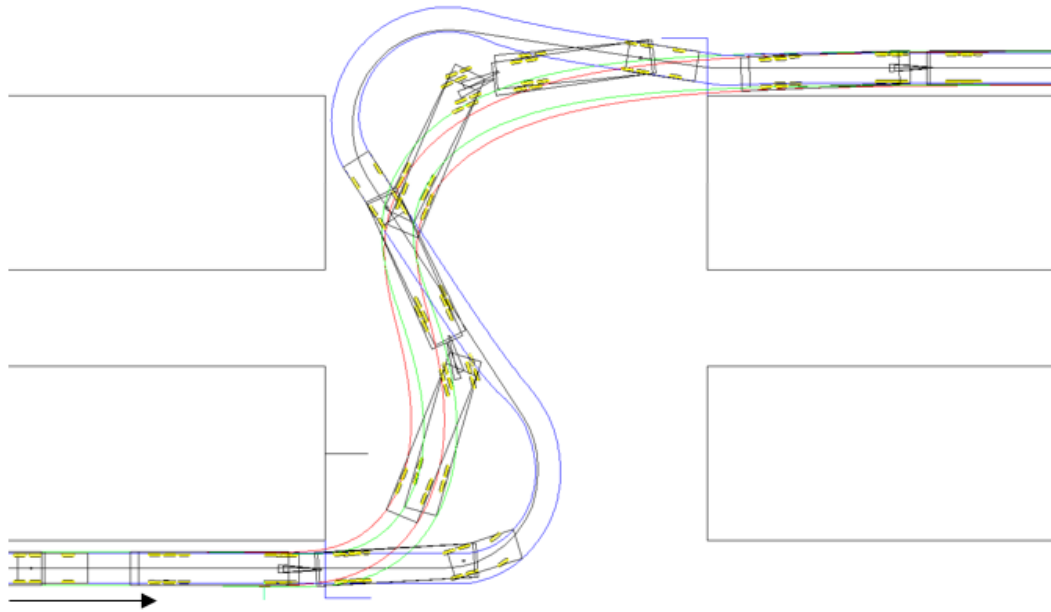
7.2.3 Turning Performance

A comparison of the turning performance for the MTS using each semi-trailer type was conducted for the worst case turning scenarios presented in Chapter 6 to analyse the swept paths of each combination. The maximum width of the swept path (see Figure 4.8) for each manoeuvre was used to compare the turning performance of the MTS combinations as this directly relates to the amount of off-tracking which occurs during a turn. The path followed by the centre of the tractor's steering axle in each case is the same, represented by the black curves in Figure 7.1 to Figure 7.3. The blue tractrix curves represent the front left and right corners of the tractor, while the green and red curves represent the innermost path followed by new and existing semi-trailer designs respectively for the second trailer in the MTS set. The tractrix curves for each combination was superimposed such that the difference in the swept paths during a turn could be visualised.



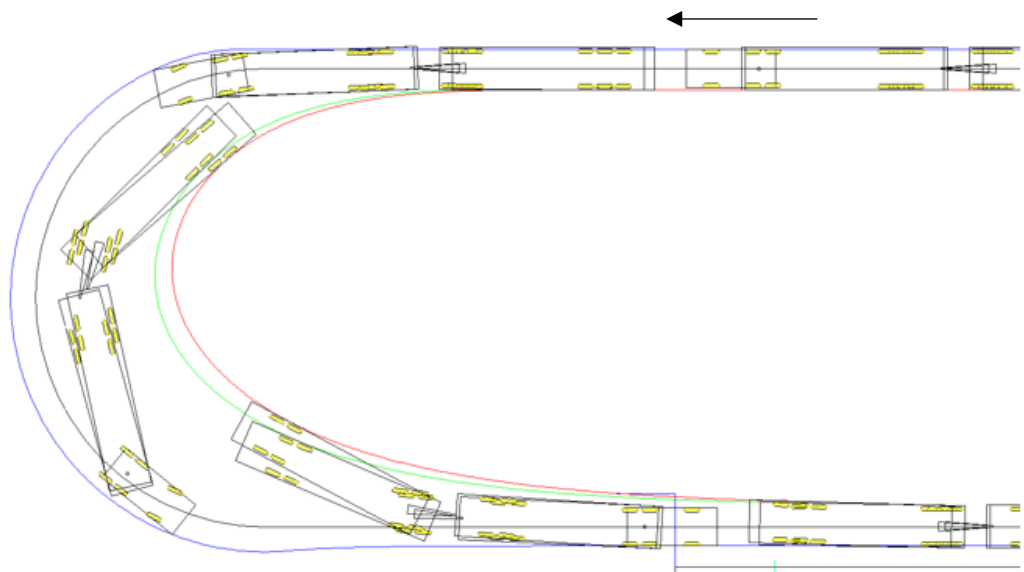
Key: storage blocks — rear wheel sweep (new semi-trailer) — CTR
 — rear wheel sweep (existing semi-trailer) — front path of the tractor → direction

Figure 7.1: Double 90⁰ turn – central exit and entry showing the swept path difference



Key: storage blocks — rear wheel sweep (new semi-trailer) — CTR
— rear wheel sweep (existing semi-trailer) — front path of the tractor → direction

Figure 7.2: Double 90° turn – exit and entry underneath RTG showing the swept path difference



Key: storage blocks — rear wheel sweep (new semi-trailer) — CTR
— rear wheel sweep (existing semi-trailer) — front path of the tractor → direction

Figure 7.3: 180° turn – Entry into block A underneath RTG showing the swept path difference

Table 7.3: Swept path comparison for the MTS using each semi-trailer design

Turning scenario	Maximum width of the swept path		% Improvement using new semi-trailer design
	MTS using new semi-trailer design	MTS using existing semi-trailer design	
Double 90° turn – central exit and entry. (See Figure 7.1)	11.9 m	12.9 m	7.7 %
Double 90° turn – exit and entry underneath RTG. (See Figure 7.2)	9.8 m	10.6 m	7.5 %
180° turn – entry into block A underneath RTG. (See Figure 7.3)	9.9 m	11.2 m	11.6 %

The reduction in the maximum width of the swept path using the semi-trailer designed in this study was found to be within the range of 7.5% to 11.6% when compared to the MTS configuration using the existing semi-trailers. This is attributed to the smaller wheelbase of the new semi-trailer design (8.909 m vs. 9.635 m), as well as a greater kingpin setback which reduces the overall length of the vehicle when coupled to the tractor, which results in lower off-tracking and hence a reduced maximum swept path width when compared to the existing design. Reduced off-tracking allows the MTS to complete turns in a smaller available area (since the swept area is smaller), increasing its manoeuvrability and reducing the chances of collision with stationary objects due to off-tracking.

7.3 Operational Cost Comparison

The preliminary operational cost comparison conducted for the waterside horizontal-transport system for the two vehicle types (MTSs and TTUs), documented in Chapter 3.4, was refined using the data from Chapter 7.2 in order to determine the impact of the designed MTS on reducing these operational costs.

Table 7.4 shows the updated equipment cost per shift for each vehicle type. The unit cost for the existing TTUs at Pier One was determined using the most recent equipment prices available. The unit cost for the MTS was determined using the cost of the TR626i terminal tractor, together with a mark-up on the product manufacturing cost for the MTS designed to account for labour costs and a suitable profit margin. This mark-up was determined by comparing the existing semi-trailers actual selling price to its product manufacturing cost approximated in this study, shown Table 7.2. This mark-up was calculated to be 85.4% of the semi-trailers manufacturing cost which was factored into the unit cost for the MTS. The TTU and MTS unit costs used for this comparison were found to be consistent with the findings of Goussiater in [13]. The equipment cost per shift to operate each vehicle type showed minimal

difference due to the now higher than initially predicted unit cost (see Chapter 3.4) for the MTS. This higher unit cost directly impacts the maintenance costs per shift, shown in Table 7.5, with the maintenance cost difference between the two vehicles also being minimal due to the higher MTS unit cost than initially predicted.

Table 7.4: Equipment cost per shift (loading and unloading)

Type	Unit Cost	Required Fleet Size	Total Equipment Cost	Cost Per Shift
TTU	R 2 347 809	15	R 35 217 135	R 7 091
MTS	R 3 899 406	9	R 35 094 654	R 7 067

Table 7.5: Maintenance cost per shift (loading and unloading)

Type	Total Equipment Cost	%	Annual Maintenance Cost	Cost Per Shift
TTU	R 35 217 135	10.00	R 3 521 714	R 709
MTS	R 35 094 654		R 3 509 465	R 707

The preliminary fuel cost calculation for the MTS, shown earlier in Table 3.5, was refined using the average fuel consumption of the TR626i terminal tractor and presented in Table 7.6. The current fuel price (as of October 2017) was included in the cost calculations. The fuel consumption of this tractor was lower than the CVS Ferrari FR270 which was used in the preliminary fuel cost calculations, resulting in a larger saving in fuel costs than initially predicted for the MTS. Table 7.6 shows that a saving of 11.1% in fuel costs can be achieved when using the suggested fleet size of MTSs for the vessel loading and unloading procedure due to a smaller fleet size when compared to the existing TTUs for equal QC productivity.

Table 7.6: Fuel cost per shift (October 2017)

Type	Total Distance Covered in 1 Shift (km)		Prime Mover Fuel Consumption (km/litre)	Fuel Cost per Litre	Cost Per Shift	
	Loading	Unloading			Loading	Unloading
TTU	266.2	885	1.079	R 13.74	R 2 625	R 8 727
MTS	133	442	0.606		R 2 541	R 8 443

The labour cost per shift for operating a fleet of MTSs versus that of a fleet of TTUs for the vessel loading and unloading procedures, previously shown in Table 3.7, remains the same since the fleet size

of each vehicle required for equivalent QC productivity has not changed. Table 7.7 below shows the finalised total operating cost per shift for the container movement procedures at Pier One when using a fleet of the MTSs designed in this study versus the existing TTUs.

Table 7.7: Total operating cost per shift

Type	Vehicles Required		Total Operating Cost Per Shift	
	Unloading	Loading	Unloading	Loading
TTU	15	9	R 43 291	R 25 657
MTS	9	9	R 32 392	R 25 248

The main saving contributor when using a fleet of MTSs, as initially observed in the preliminary cost comparisons, emanates from a reduction in labour costs for the unloading procedure. The labour cost saving when using the required fleet size of MTSs for vessel unloading makes up 88% of the overall 25% saving in operating costs shown in Table 7.7. The savings when using MTSs for the loading procedure, similar to the preliminary cost exercise, was found to be marginal; an approximate saving of 1% in operating costs is still expected when compared to the TTU fleet.

8 Discussion

The discrete event simulation created to replicate the existing operations at Pier One proved to be an accurate method for benchmarking the terminal's current performance for the use of TTUs as the transport medium for container movement, with the results found to be within 7% of the physically measured TTU cycle times and within 3% of the current quay crane productivity. The modified version of the benchmark model, created to understand the influence that an MTS fleet would have on port productivity and operational costs, revealed that using MTSs at Pier One has a significantly greater effect on reducing operational costs than it does on improving productivity. Even though the use of MTSs has only shown benefit for the vessel unloading operation, the financial savings are considerable. The initial operational cost comparison for the system types (TTUs and MTSs) revealed that this cost can be reduced by up to 25% for the vessel unloading operation when using nine MTSs with a carrying capacity of four TEUs instead of the existing two TEU capacity tractor-trailer units. This creates an opportunity to reduce the charges levied to container vessel operators and hence improve the Port's competitiveness. Determining the actual influence which the waterside horizontal-transport systems operational costs have on the charges imposed to vessel operators falls outside the scope of this study, however studies have shown that the costs associated with container movement between the vessel and storage area form a large part of the total cost of a vessel calling at a port [10], making them a key component in determining the service tariffs levied to container vessel operators.

A detailed survey of the literature surrounding the simulation of port terminal activities revealed that most of the available literature focused on port performance and its associated activities from a macroscopic level. This work, which built on the study conducted by Goussiater [13], is one of the few available dedicated analyses of the waterside horizontal-transport system and creates a platform for future studies in this regard. The models could be used to understand how changes in the fleet size and carrying capacity of the other container handling equipment (RTGs and QCs) at Pier One influences productivity and operational costs. Port layout changes could also be analysed by using the model to assess potential benefits.

The ArenaTM models in this study focused on the movement of the trailers in the system and can benefit from additional improvements. An improvement would be the incorporation of traffic created using MTSs to understand if this has any effect on trailer availability at the quay cranes. This could be done by modelling the MTSs using guided transporters (as opposed to the conventional transporters utilised for this work) that account for the position of the other vehicles in their vicinity, however this increases the complexity, size and solution time of the model due to the complex logic implementation required. The probability distributions used in this study were obtained from data sets containing manual time measurements. An additional improvement would be to refine these distributions by creating data sets using the time logs associated with container movements that are recorded by the terminal's logistic

system. This will allow for larger data sets to be used to which suitable distributions could be assigned, yielding improved mathematical representations for the processing time of the activities in the system.

A preliminary operational cost comparison to run each system type, based on the fleet sizes as per the DES results for equivalent QC productivity, was conducted to determine the financial benefit of using MTSs at Pier One instead of the existing TTU fleet. The equipment, fuel, maintenance and labour costs, which in totality make up the operational cost for using each trailer system type, were calculated and compared on a “per shift” basis. For each individual cost, the preliminary comparison showed that a fleet of MTSs for equivalent QC productivity was cheaper to operate than TTUs due to the reduced fleet size for the vessel unloading procedure with lower labour costs being the main contributor. A reduction in labour costs can be viewed in a negative manner by the labour unions representing the terminal’s workforce as it could signify job losses, however the use of MTSs can create an opportunity for the terminal’s management to re-skill these staff for other influential positions within the organisation. This is beneficial to both the workforce and the terminal’s management since these individuals will be developing new skills to aid the operations of the terminal.

Multiple MTS types were investigated to select an appropriate configuration for the proposed design that met the technical and functional requirements for trailer equipment intended for container movement at Pier One. From the types investigated, the semi-trailer lead MTS configuration incorporating the use of a converter dolly was deemed the most suitable due to its ability to decouple its semi-trailers for use as TTUs, its semi-trailer interchangeability in the MTS set, as well as its kingpin feature which allows it to be connected to a tractors fifth wheel for coupling purposes. For this system type, the terminal’s existing semi-trailers could in theory be modified for use as the MTS, however, an opportunity exists for a better designed semi-trailer with regard to mass, cost and manoeuvrability as the terminal replaces its trailer equipment every five years. For this reason, an MTS incorporating a newly designed semi-trailer and converter dolly was pursued using locally available materials and components.

A major component of the MTS design process, apart from the investigation into locally available materials and standard components, involved a detailed review of the available literature and information from trailer manufacturers on the strength requirements for the semi-trailer and converter dolly chassis. A review of the applicable trailer design standards, publications on trailer design studies as well as the design methods employed by trailer manufacturers was conducted to determine appropriate load cases and safety factors for the structural design of the respective chassis. An examination of the available SANS, ISO and ADR standards revealed that while there are various guidelines detailing the design requirements for individual trailer components, there is no comprehensive standard that details the strength requirements for a chassis with regards to the load cases and safety factors employed during the design phase for a given payload. A review of the literature

applicable to the theoretical design and field testing of trailers was conducted to gain an insight into the static and dynamic forces acting on the chassis of a trailer which could be potentially adopted for the MTS load cases. The literature showed varying load cases and safety factors employed by various authors, supporting the notion of a lack of a general structural design standard for trailer equipment.

Information on the load cases and safety factors used by trailer manufacturers was obtained from the study conducted by Cowling [54] and revealed that manufacturers have developed their own design standards through experience, based on the requirements for each type of trailer and its operating environment. While a few manufacturers make use of dynamic models incorporating fatigue effects, the more common approach was found to be the application of a design factor to the static load cases to account for fatigue loading using a static analysis. The same approach was adopted in this study. The study describing the forces experienced by trailer equipment operating in a port terminal environment, conducted by Dwarika [62], revealed the maximum accelerations which the existing semi-trailers experience during container movement operations. His study was of interest to the author as it gave an insight into the actual loads that might be experienced by the MTS. The load cases proposed by Dwarika [62] were marginally lower than those adopted in this study, suggesting that the load cases and safety factors used here are adequate to ensure that fatigue failure does not occur. The load cases selected for the present MTS can be used for future trailer designs intended for port use.

Finite element analyses of the entire semi-trailer and converter dolly chassis were conducted for the load cases chosen using ANSYS® software to validate the structural integrity of the design for the required safety factor range. The structural components which were mid-surfaced were chosen based on their length-to-thickness ratio where a minimum value of 10 was used as the deciding criteria [90]. A combination of shell and solid elements was used to mesh the geometry, with local mesh controls applied to certain areas to provide a finer mesh for improved accuracy. The models were constrained in the relevant directions to prevent rigid body motion that creates solution errors, while replicating the real-world constraints on the structure. The von-Mises stress criterion was used to evaluate the stresses for each load case, similar to the studies conducted in [54, 61, 83, 85], due to its accuracy when estimating yield failure in ductile isotropic materials [92]. Modifications to the chassis were made in certain regions where the yield stress of the material did not correspond to a minimum safety factor of 1.2 until the results from all load cases satisfied the design safety factor requirements. In order to reduce the weight of the chassis, an iterative approach was adopted where the initial design was refined by reducing the material thicknesses of the structure during the subsequent FEA analyses where stresses below the threshold value of 296 MPa was found. This resulted in a final mass saving of 82 kg for the semi-trailer and 148 kg for the converter dolly over the initial design prior to the analyses.

Localised high stress points exceeding the yield stress of the material were regularly found during the analysis of the stress results for the semi-trailer and the converter dolly, this was due to modelling approximations within the software simulation. Inaccurate stress concentrations, as well as singularity points, frequently arise in the FEA process due to geometry features such as sharp re-entrant corners, fillet corners and at the corners of bodies in contact [93]. While the stress results in those areas may not be an accurate representation of the actual stresses present in reality, the stress fields away from those local concentrations provides credible results based on St. Venant's principle [93]. The results yielded by the FEAs were scrutinised at the high stress regions to determine if the stresses were erroneous and could be disregarded, or if they were real stresses that needed to be reduce by redesigning the structural members. A method employed to check this was the use of the Structural Error Tool in ANSYS® which highlights the regions of the geometry where the stress errors are present. The tool represents the error associated with the discrepancy between the calculated stress field in a region and the model's globally continuous stress field [103], highlighting the regions where discontinuous stress results are present. An example is shown in Figure 8.1 below for the isolated high stress point occurring in the longitudinal acceleration load case, validating the notion that the results in that region are not a true representation and can be disregarded.

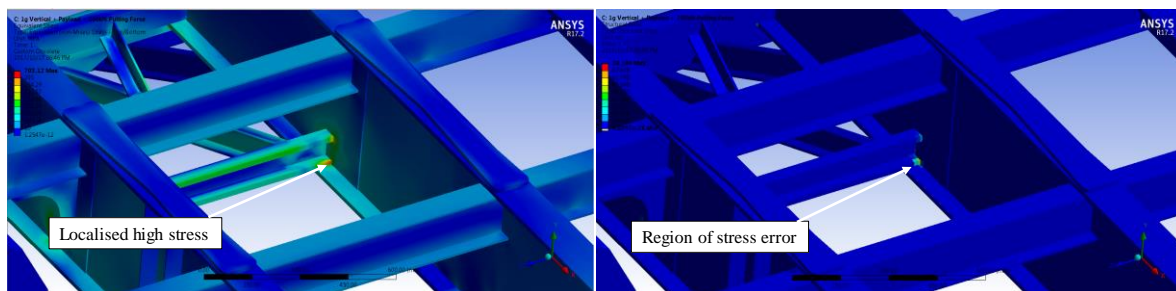


Figure 8.1: Localised high stress error confirmed using the Structural Error Tool in ANSYS®

The D-value equations used to determine the strength requirement for mechanical couplings were adopted in this study for selecting appropriate kingpins, towing eyes and hitches as well as the fifth wheel for the converter dolly. The D-value can be viewed as a “blanket” method for selecting trailer couplings with the appropriate strength as the equations do not take into consideration the tractive effort provided by the prime mover in a trailer system. This is useful to trailer designers as this tractive effort information is rarely available. While this method has been proven in industry to be a successful approach for selecting trailer couplings without having data on the tractive performance of the prime mover, it must be noted that the results yielded by the D-value equations do not represent the actual maximum horizontal force on the coupling as a result of the tractive effort provided by the prime mover. For the case of the MTS, the D-value equations under-predict the horizontal force on the kingpin of the lead semi-trailer compared to what is provided by the tractor (225.92 kN vs 256 kN), however a kingpin with a safe rating relative to both (260 kN) was selected.

The turning analyses conducted using BricsTurn[®] validated the MTSs ability to be manoeuvred within the terminal yard for the typical turns it would need to complete during container movement operations. This incorporated the equivalent wheel base methodology for multi-axle vehicles proposed by Winkler and Aurell [99]. It was necessary to consider the application of this theory in the turning analyses since the software does not automatically take the influence of multiple axles into account. The simulation results for the worst case turns show that MTS can complete such movements, but the MTS will be more difficult to manoeuvre accurately when compared to the existing TTUs due to it being much longer. For successful implementation of the MTS at Pier One, driver training for long vehicle combinations will need to be conducted, as well as the addition of road markings which could guide drivers to complete the more difficult turns without relying on their judgement alone.

Future improvements to the design of the MTS proposed in this study can be made to enhance the manoeuvrability of the vehicle. One method is by incorporating the use of steerable axles in the design of the semi-trailers. Available steering systems in the market, such as the Tridec[®] system from Jost, can be fitted to reduce the off-tracking of the semi-trailers in the MTS. Disadvantages of this type of system is that they will increase the tare mass and cost of the MTS, with most of the systems not being designed to safely bear the high axle loads of these semi-trailers.

The system comparison conducted between the existing semi-trailers and the semi-trailer designed in this study when used in the MTS configuration showed that the new design is lighter, cheaper and had better manoeuvrability than the existing trailer. The mass comparison revealed that the newly designed chassis is 33.9% lighter than the existing semi-trailers, with a saving of 21.4% on the overall tare mass. The heavier chassis of the existing semi-trailers can be attributed to the higher load cases utilised for the design which results in a stronger, heavier design than is required. This was confirmed in a study conducted by Dwarika [62] who showed that lower load case acceleration values could be used for the design of those semi-trailers without compromising their structural integrity. The lower chassis mass directly results in a reduced product cost for the newly designed semi-trailer since both designs utilise the same steel grade; a 15.1% lower product cost for the MTS is expected when using the semi-trailer designed in this study compared to the existing semi-trailers. The manoeuvrability comparison of the MTS when using each semi-trailer design was conducted by superimposing the swept paths of each system for identical paths followed by the tractor. Comparisons of the maximum width of the swept paths for each manoeuvre confirmed that the smaller wheelbase and the greater kingpin setback of the new semi-trailer design results in reduced off-tracking for identical turns of the MTS, allowing the MTS to complete turns in a smaller available area than if the existing semi-trailers had to be used in the set.

The finalised operational cost comparison of the waterside horizontal-transport system for the currently used TTUs versus the proposed MTS design was conducted by refining the product costs determined for each system type, as well as accounting for the use of the TR626i terminal tractor as the prime mover in the MTS. The product cost of the MTS designed in this study was found to be 5.4% higher than what was first predicted, in Chapter 3.4, resulting in the equipment and maintenance costs per shift for each system being almost identical. The savings in fuel costs, due to a lower fleet size of MTSs, is higher than initially predicted due to the lower fuel consumption of the chosen tractor. Even though the actual fuel usage of the tractors in reality rarely matches the average consumption values reported by manufacturers (used in this study for all setups), the average values give a useful relative indication of the amount of fuel used for each vehicle for costing purposes. Labour costs still account for the largest influence on the overall cost savings when using a fleet of MTSs; 88% of the overall 25% saving in operating costs is due to the reduction in the number of tractor drivers required. While the use of MTSs has only shown financial benefit when used for the vessel unloading procedure, the cost saving for the terminal over a 12 month period (for the 458 unloading shifts only) is substantial; the savings would be approximately R5 million if the suggested fleet of MTSs is implemented.

9 Conclusion

The objectives of this study have been met through the following:

1. The existing container movement operations at Pier One was benchmarked using discrete event simulation models for the vessel loading and unloading procedures. The simulation results were validated against the current performance of the terminal, with the results being within 7% of the physically measured TTU cycle times and within 3% of the current measured quay crane productivity.
2. The container movement operations using MTSs as a replacement for the existing TTUs was modelled and the resulting effects showed a 25% reduction in operational costs for the unloading procedure when using an MTS fleet. An MTS fleet with nine vehicles could replace the existing fifteen TTUs while maintaining the current productivity levels of the terminal.
3. Based on the results from (2) which revealed the requirement of an MTS that could have its trailers uncoupled and used as TTUs, a semi-trailer lead MTS design incorporating a converter dolly was proposed.
4. The MTS design was carried out using locally available components and materials. The design was conducted with a view to a reduced mass and cost, and improved manoeuvrability over the existing semi-trailers, which in theory could also be used in the MTS configuration with the converter dolly designed in this study. The semi-trailer designed here was shown to have a 21.4% lower tare mass and a 14.1% lower product cost over the existing semi-trailers. Up to an 11.6% improvement in the turning performance of the MTS is expected when using the semi-trailers designed in this study.

The use of MTSs for quayside container movement operations has been successfully implemented in many major international port terminals as a method of reducing the operational costs associated with the waterside horizontal-transport system and this study has shown that the use of MTSs at Pier One of the Durban Container Terminal also creates operational cost reduction opportunities. Even though the use of an MTS fleet only shows marginal QC productivity improvements for the vessel unloading operations and almost no benefit (nor detriment) to the vessel loading procedure, the reduction in fleet size in comparison to the existing TTUs used for the unloading procedure results in considerable operational cost savings for the terminal which can be achieved while maintaining current levels of productivity.

The MTS design provided here, suits the technical and functional requirements for trailer equipment operated at Pier One. This design, which incorporated locally available materials and components, would fulfil the South African Government's policies on localisation during manufacture. The vehicle provides a method for the Durban Container Terminal to reduce operational costs and can potentially

result in lower tariffs being offered to container vessel operators, thus improving the competitiveness of the Port.

The reduction in labour costs could potentially be viewed in a negative manner by the respective labour unions representing the tractor drivers, with opposition against implementing MTSs. The implications of reducing labour therefore needs to be addressed by the terminal and respective labour representatives so as to determine how multi-trailer systems can be implemented at the terminal for the benefit of both the port operator and the workforce.

This study focused only on Pier One since Pier Two utilises straddle carriers instead of TTUs, however a similar study can be conducted for Pier 2 to determine if there is any benefit to the terminal in switching to the use of MTSs. Further research into the influence of multiple vessels berthed at Pier One, varying the stacking areas for container storage, as well as using QCs and RTGs with greater lifting capacities (more than one TEU) could be conducted to determine the resulting influence on operational costs and port productivity for the Durban Container Terminal. This study is intended to inspire further research into the applicability and benefit of MTSs for container movement at other major ports within South Africa.

10 References

- [1] A. E. Branch, *Export Practice and Management*, Springer, 2013.
- [2] D. Steenken, S. Voß and R. Stahlbock, “Container terminal operation and operations research – a classification and literature review,” *OR Spectrum*, vol. 26 , no. 2004, p. 3–49, 2004.
- [3] Maersk Liner, “Transport & Trade,” The Maersk Group, 2016. [Online]. Available: <http://www.maersk.com/en/industries/transport>. [Accessed 19 June 2017].
- [4] M. Bell, K. Bichou and A. Evans, “Developing and implementing global interoperable standards for container security,” in *Risk Management in Port Operations, Logistics and Supply Chain Security*, CRC Press, 2013, 2007.
- [5] L. A. R. Hulten, “Container logistics and its management. PhD thesis,” Chalmers University of Technology: Department of Transportation and Logistics, 1997.
- [6] G. Muller, *Intermodal freight transportation*, 3rd Edition., Westport: Eno Foundation for Transportation, 1995.
- [7] K. Glenn, Interviewee, *Terminal costs pose a big challenge for ship operators*. [Interview]. 17 September 2015.
- [8] M. H. Nur, “Port Pricing and Cargo Handling in Port of Portland and Implications for Somalia's Port System, Master of Science Dissertation,” School of Oceanography, Oregon State University, 1982.
- [9] Korea Maritime Institute, ESCAP, “Comparative Analysis of Port Tariffs in the ESCAP Region,” United Nations, New York, 2002.
- [10] D. Seedah, R. Harrison, L. Boske and J. Kruse, “Container Terminal and Cargo-Handling Cost Analysis Toolkit,” Texas Department of Transportation Research and Technology Implementation, 2013.
- [11] D. Nazari, “Evaluating Container Yard Layout, MSc Thesis,” Maritime Economics and Logistics, Erasmus University, Rotterdam, 2005.
- [12] N. Kemme, “Container-Terminal Logistics,” in *Design and Operation of Automated Container Storage Systems*, Springer, 2013, pp. 26-27.
- [13] A. Goussiatiner, “Efficiency of multi-trailer systems for ship to stacks container transportation,” *Port Technology International*, pp. 78-82, 2012.
- [14] Port Strategy, “Mafi Rolls Along Nicely in Manila,” 7 May 2012. [Online]. Available: <http://www.portstrategy.com/news101/products-and-services/mafi-rolls-along-nicely-in-manila>. [Accessed 26 March 2017].

- [15] Transnet Port Terminals, “Durban Container Terminal,” 2013. [Online]. Available: https://www.transnetportterminals.net/Ports/Pages/Durban_Container.aspx. [Accessed 23 October 2016].
- [16] Port Strategy, “Keeping Durban Competitive,” 12 November 2014. [Online]. Available: <http://www.portstrategy.com/news101/world/africa/keeping-durban-competitive>. [Accessed 21 June 2017].
- [17] T. Hutson, “Ports & Ships Maritime News,” 5 April 2016. [Online]. Available: http://ports.co.za/news/news_2016_04_05_01.php. [Accessed 21 June 2017].
- [18] Centre for Competition, Regulation and Economic Development, “Review of regulation in the Ports Sector,” 2014.
- [19] Ports Regulator of South Africa, “Global Port Pricing Comparator Study - Research Summary,” 2012.
- [20] J. Simpson, “The Competitive Edge of the Port of Durban: Challenges and Opportunities,” Durban, 2015.
- [21] Portfolio Committee on Public Enterprises, “The Role of State Owned Companies in Supporting Localisation and Local Procurement in South Africa,” Department of Trade and Industry South Africa, 2016.
- [22] T. Govender, M. Brooks and C. Bemont, “The effect of multi-trailer systems on the efficiency of container movements between the ship and stacks at the Durban Container Terminal,” *South African Journal of Industrial Engineering*, vol. 28, no. 4, pp. 80-94, 2017.
- [23] Y.-M. Park, “Berth and crane scheduling of container terminals,” PhD Thesis, Pusan National University., 2003.
- [24] Conductix Wampfler, “Container Handling Photo Gallery,” 2017. [Online]. Available: <http://www.conductix.com/en/markets/container-handling>. [Accessed 22 June 2017].
- [25] Port Technology, “Port of Santos orders 12 of Cargotec’s Kalmar RTG cranes,” 5 May 2011. [Online]. Available: https://www.porttechnology.org/news/port_of_santos_orders_12_of_cargotecs_kalmar_rtg_cranes. [Accessed 22 June 2017].
- [26] N. Murugan, Interviewee, *Operation of the Durban Container Terminal*. [Interview]. 15 May 2016.
- [27] K. Ramani, “An interactive simulation model for the logistics planning of container operations in seaports,” *Simulation* 66, pp. 291-300, 1996.
- [28] A. Carteni and S. de Luca, “Simulation of a container terminal through discrete event approach,” Department of Civil Engineering – University of Salerno, 2009.

- [29] S. Robinson, *Simulation- The practice of model development and use*, Wiley, 2004.
- [30] S. Adam, "Simulation and Analysis of Port Bottlenecks: The Case of Male," Lincoln University, 2009.
- [31] M. Kotachiav, G. Rabadib and M. F. Obei, "Simulation Modeling and Analysis of Complex Port Operations with Multimodal Transportation," *Procedia Computer Science*, vol. 20, p. 229 – 234, 2013.
- [32] O. Kulaka, O. Polata and H.-O. Guentherb, "Performance Evaluation of Container Terminal Operations," 2011.
- [33] S. Gori and M. Petrelli, "A microsimulation model for real time management of port activities," 2015.
- [34] A. Kulatunga, R. Mekala and M. A. L. , "Determining the Best Fleet Sizing of a Container Terminal for a Given Layout," in *Proceedings of the 2011 International Conference on Industrial Engineering and Operations Management*, Kuala Lumpur, Malaysia, 2011.
- [35] S. Gibilisco, "Discrete event simulation (DES)," Techtarget, July 2012. [Online]. Available: <http://whatis.techtarget.com/definition/discrete-event-simulation-DES>. [Accessed 3 September 2017].
- [36] D. Kelton, R. Sadowski and D. Sadowski, *Simulation with Arena*, Second Edition, McGraw Hill.
- [37] W. Y. Yun and Y. S. Choi, "A simulation model for container-terminal operation analysis using an object-oriented approach," *International Journal of Production Economics*, vol. 59, pp. 221-230, 1999.
- [38] C. Chen, S.-Y. Huang and W.-J. Hsu, "Simulation and optimization of container yard operations:A survey," 2007.
- [39] S. Robinson, *Simulation; The practice of model development*, John Wiley & Sons Ltd, 2004.
- [40] L. Schroder, "Port of Durban Container Terminal - Final Project Report," University of Pretoria, 2013.
- [41] A. Isalgue, J. Martinez and M. Eguren, "Containers movements cost analysis in a marine terminal," Universitat de Barcelona, Barcelona, 2014.
- [42] Prime Creative Media, "Prime Mover Magazine," Prime Creative Media, 2017. [Online]. Available: <http://www.primemovermag.com.au/uploads/trailer/articles/tm-0414-feat-vawdrey630.jpg>. [Accessed 07 July 2017].
- [43] Max Atlas, "Converter Dolly," 2017. [Online]. Available: <http://max-atlas.com/trailer/d213-2-04/>. [Accessed 26 July 2017].

- [44] State of California, Department of Motor Vehicles, "Section 7: Doubles and Triples," 2017. [Online]. Available: https://www.dmv.ca.gov/portal/dmv/?1dmy&urile=wcm:path:/dmv_content_en/dmv/pubs/cd1_h1m/sec7. [Accessed 26 July 2017].
- [45] Transnet Port Terminals, *Cornerless Bathtub-type Trailers - Technical Specification*, Transnet, 2015.
- [46] South African National Standard, *SANS 1447-2 : Braking (motor and towed vehicles, designed for low speed or use off public roads), Part 2 - Low Speed Trailers*, 2007.
- [47] South African National Standards, *SANS 1046 - Lights and light-signalling devices installed on motor vehicles and trailers. Edition 3*, 1990.
- [48] South African National Standard, *SANS 1376: Lights for motor vehicles, Part 1, 2 and 3.*, 2006-2008.
- [49] South African National Standard, *SANS 1055: Rear underrun protection devices.*, 2007.
- [50] Australian Government: Department of Infrastructure and Regional Development, "Australian Design Rules," 6 November 2015. [Online]. Available: <https://infrastructure.gov.au/roads/motor/design/>. [Accessed 01 August 2017].
- [51] UNECE, "European Agreement concerning the International Carriage of Dangerous Goods by Road," 2011. [Online]. Available: <http://www.unece.org/trans/danger/publi/adr/adr2011/11ContentsE.html>. [Accessed 08 August 2017].
- [52] International Organization for Standardization, *ISO 611: Road Vehicles- Braking of automotive vehicles and their trailers*, 2003.
- [53] International Organization for Standardization, *ISO 4184: Road vehicles - Special warning lamps - Dimensions*, 2004.
- [54] S. L. Cowling, "Design Optimisation of a Cane Haulage Vehicle, Masters Thesis," 2008.
- [55] R. Govender, Interviewee, *Load cases and safety factors used in the design of Transnet Engineering's port trailers*. [Interview]. 06 February 2017.
- [56] British Standard, *BS EN 10025-2: Hot rolled products of structural steel*, European Committee for Standardization, 2004.
- [57] G. Koszalka, H. Debski, M. Dziurka and M. Kaczor, "Design of a frame to a semi low-loader," *Journal of KONES Powertrain and Transport*, vol. 18, no. 2, pp. 215-223, 2011.
- [58] A. Iqbal, S. Oak and S. Kharatmal, "Analytical Optimization of Chassis Frame for 40ft Dual-Axle Flatbed Trailer Design," *IOSR Journal of Mechanical and Civil Engineering*, vol. 7, no. 6, pp. 76-84, 2013.

- [59] D. Martins, J. Cardoso and A. Mourão, “Structural optimisation of a semi-trailer based on performance and industrial cost,” in *3rd International Conference on Integrity, Reliability and Failure*, Portugal, 2009.
- [60] R. A. Rahman and O. Kurdi, “Finite element analysis of road roughness effect on stress distribution of heavy duty truck chassis,” *International Journal of Technology*, vol. 1, pp. 57-64, 2010.
- [61] E. Ebrahimi, A. Borghei, M. Almasi and H. Rabani, “Design, fabrication and testing of a hay bale trailer,” *Research Journal of Applied Sciences, Engineering and Technology*, vol. 2, no. 3, pp. 222-226, 2010.
- [62] Y. Dwarika, “Critical Tracking and Stress Analysis of Transnet Engineering Trailers, Masters Thesis,” University of KwaZulu-Natal, 2017.
- [63] C. Winkler, T. Gillespie and S. Karamihas, *The Mechanics of Heavy-Duty Truck Systems*, 2014.
- [64] A. C. Ugural, “Safety Factors,” in *Mechanical Design of Machine Components, Second Edition*, pp. 12-15.
- [65] D. L. Harkey and C. V. Zegeer, “Operational Characteristics of Longer Combination Vehicles and Related Geometric Design Issues,” *Transportation Research Record*.
- [66] M. W. Sayers, “Vehicle Off-tracking Models,” University of Michigan Transportation Research Institute, Michigan .
- [67] D. Pecchini and F. Giuliani, “Experimental Test of an Articulated Lorry Swept Path,” *Journal of Transportation Engineering*, vol. 139, no. 12, 2013.
- [68] Province of Nova Scotia, “Weights and Dimensions of Vehicles Regulations,” 01 December 2015. [Online]. Available: <https://novascotia.ca/just/regulations/regs/mvwd.htm>. [Accessed 10 August 2017].
- [69] SAF Holland, “About Fifth Wheels,” [Online]. Available: https://www.safbenelux.nl/files_content/SAF-HOLLAND_Fifth_Wheel_Fact_Book_en-DE.pdf. [Accessed 03 March 2017].
- [70] Reliance Foundry, “Steel Grading: Carbon & Mild Steel,” Reliance Foundry Co. Ltd., 2017. [Online]. Available: <http://www.reliance-foundry.com/castings/steel-grades#gref>. [Accessed 21 August 2017].
- [71] ArcelorMittal, “High Strength Steels - Product Catalogues,” 2017. [Online]. Available: <https://flatsteel.arcelormittalsa.com/fspcatalogue/ProdCat.asp>. [Accessed 14 August 2017].

- [72] SSAB International, "SSAB Domex – Optimized for you and structures," 2017. [Online]. Available: <https://www.ssab.com/products/brands/ssab-domex-structural-steel>. [Accessed 20 August 2017].
- [73] W. Schutz, "A history of fatigue," *Engineering Fracture Mechanics*, vol. 54, pp. 263-300, 1996.
- [74] GO Axles & Suspensions, *Heavy Duty Axles - Product Data Sheet*, 2014.
- [75] SA Vehicle Testing Authority, *SANS 1447-2 Test Report - GO Axles Hawk HD 22700 Slow Speed Trailer Axle*, SANAS Testing Laboratory, 2013.
- [76] K. O'Reilly, *GO Axles and Suspensions - CAD Models*, 2016.
- [77] Continental Tyres, *Radial Terminal Tyre For Industrial Vehicles - Product Data Sheet*, Continental Tyres.
- [78] Kalmar Global, *Technical Data Sheet - TR626i Terminal Tractor*, Kalmar.
- [79] Kalmar, "Kalmar TR626i and TR632i terminal tractor," Cargotec, 2017. [Online]. Available: <https://www.kalmarglobal.com/equipment/terminal-tractors/all-terminal-tractors/TR626i-and-TR632i/>. [Accessed 24 August 2017].
- [80] R. Govender, Interviewee, *Port Trailer Design Methods*. [Interview]. 27 February 2017.
- [81] Matthew Sutton, "Why is an I-beam shaped the way it is?," Quora, 28 November 2016. [Online]. Available: <https://www.quora.com/Why-is-an-I-beam-shaped-the-way-it-is-How-did-an-I-beams-eventual-final-design-come-to-fulfill-its-primary-function>. [Accessed 30 August 2017].
- [82] The students of Professor Tatu's Values and Science/Technology Seminar, "Steel & The Lehigh Valley," Wordpress, [Online]. Available: <https://sites.lafayette.edu/vast265-sp12/steelopedia/h-l/h-beam/>. [Accessed 15 09 2017].
- [83] K. Patil and E. Deore, "Stress Analysis of Ladder Chassis with Various Cross Sections," *IOSR Journal of Mechanical and Civil Engineering (IOSR-JMCE)*, vol. 12, no. 4, pp. 111-116, 2015.
- [84] D. Sharma and Y. D. Vora, "Design and Analysis of Heavy Duty Vehicle (Trailer) Chassis through FEM Software," *International Journal of Engineering Technology, Management and Applied Sciences*, vol. 5, no. 4, pp. 574-580, 2017.
- [85] G. S. Datar, R. S. Bindu and D. V. Dandekar, "Design and Analysis of 40 Tonne Trailer Used in Heavy Commercial Vehicles," *International Journal on Theoretical and Applied Research in Mechanical Engineering (IJTARME)*, vol. 1, no. 2, pp. 14-21, 2012.
- [86] J. A. Yura, "Fundamentals of Beam Bracing," *Engineering Journal*, pp. 11-26, First Quater, 2001.

- [87] International Organization for Standardization, *ISO 12357-3 : Commercial Road Vehicles — Coupling equipment between vehicles in multiple vehicle combinations - Part 3: Strength requirements*, International Organization for Standardization (ISO), 2012.
- [88] R. D. Cook, “Further development of a three-node triangular shell element,” *International Journal for Numerical Methods in Engineering* , vol. 36, no. 8, p. 1413–1425, 1993.
- [89] M. Rezaiee–Pajand and M. Yaghoobi, “A Robust Triangular Membrane Element,” *Latin American Journal on Solids and Structures*, ISSN 1679-7825, vol. 11, no. 14, 2014.
- [90] University of KwaZulu-Natal, School of Mechanical Engineering, *Engineering Computational Methods - Course Notes*, 2012.
- [91] W. . S. Najjar and F. DeOrtentiis, *Gusset plates in railroad truss bridges - Finite element analysis and comparison with Whitmore Testing*, New York: WSP ▪ SELLS.
- [92] P. M. Kurowski, “What is calculated in FEA?,” 2012. [Online]. Available: http://debis.deu.edu.tr/userweb/zeki.kiral/MEE5049_2014/Failure_Assesment.pdf. [Accessed 21 08 2017].
- [93] M. Acin, “Stress singularities, stress concentrations and mesh convergence,” Acin.Net, 02 06 2015. [Online]. Available: <http://www.acin.net/2015/06/02/stress-singularities-stress-concentrations-and-mesh-convergence/>. [Accessed 13 08 2017].
- [94] Fontaine Fifth Wheel, “Proper location of the fifth wheel,” 2015. [Online]. Available: <http://www.fifthwheel.com/pdfs/documents/prop-location.pdf>. [Accessed 20 March 2017].
- [95] Independant Trailer and Equipment Company, “Convertor Dollies,” I.T.E.C, 2006. [Online]. Available: <http://www.itec-inc.com/dolly/documnts.html>. [Accessed 02 April 2017].
- [96] Jost, *Mounting Instructions: JSK 38C-1 fifth wheel*, Jost International, 2015.
- [97] T. W. Erkert, J. Sessions and R. D. Layton, “A method for determining offtracking of multiple unit vehicle combinations,” *Journal of Forest Engineering*, vol. 1, no. 1, pp. 9-16, 1989.
- [98] C. C. de Saxe , “Performance Based Standards for South African Car Carriers, Masters Dissertation,” University of the Witwatersrand, Johannesburg, 2012.
- [99] C. B. Winkler and J. Aurell, “Analysis and testing of the steady-state turning of multi-axle trucks,” *5th International Symposium on Heavy Vehicle Weights and Dimensions*, pp. 135-161, 1998.
- [100] W. Morrison, “A swept path model which includes tyre mechanics,” *Proceedings of the 6th Conference of the Australian Road Research Board*, pp. 149-182, 1972.
- [101] American Association of State Highway and Transportation Officials, *A policy on geometric design of highways and streets*, 2001.
- [102] Macsteel Trading, *Coastal Selling Prices for Steel- October 2017*, 2017.

- [103] ANSYS,
“https://www.sharcnet.ca/Software/Ansys/15.0.7/en-us/help/ans_cmd/Hlp_C_PRERR.html,”
SAS IP, [Online]. Available: https://www.sharcnet.ca/Software/Ansys/15.0.7/en-us/help/ans_cmd/Hlp_C_PRERR.html. [Accessed 13 November 2017].
- [104] Jost, *Product Catalogue*, 2017. [Online]. Available: <https://www.jost.co.za>
[Accessed 11 March 2018].

Appendix A - MTS General Assembly

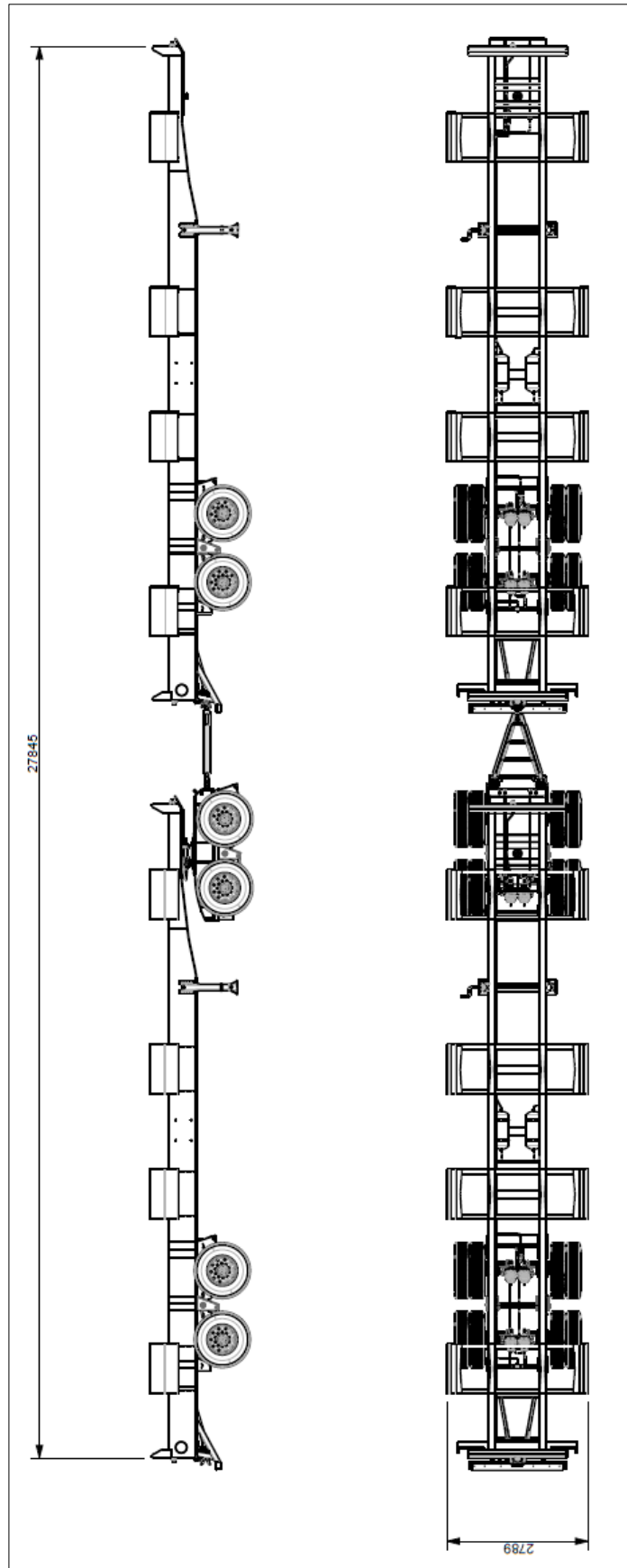


Figure A.1: MTS assembly

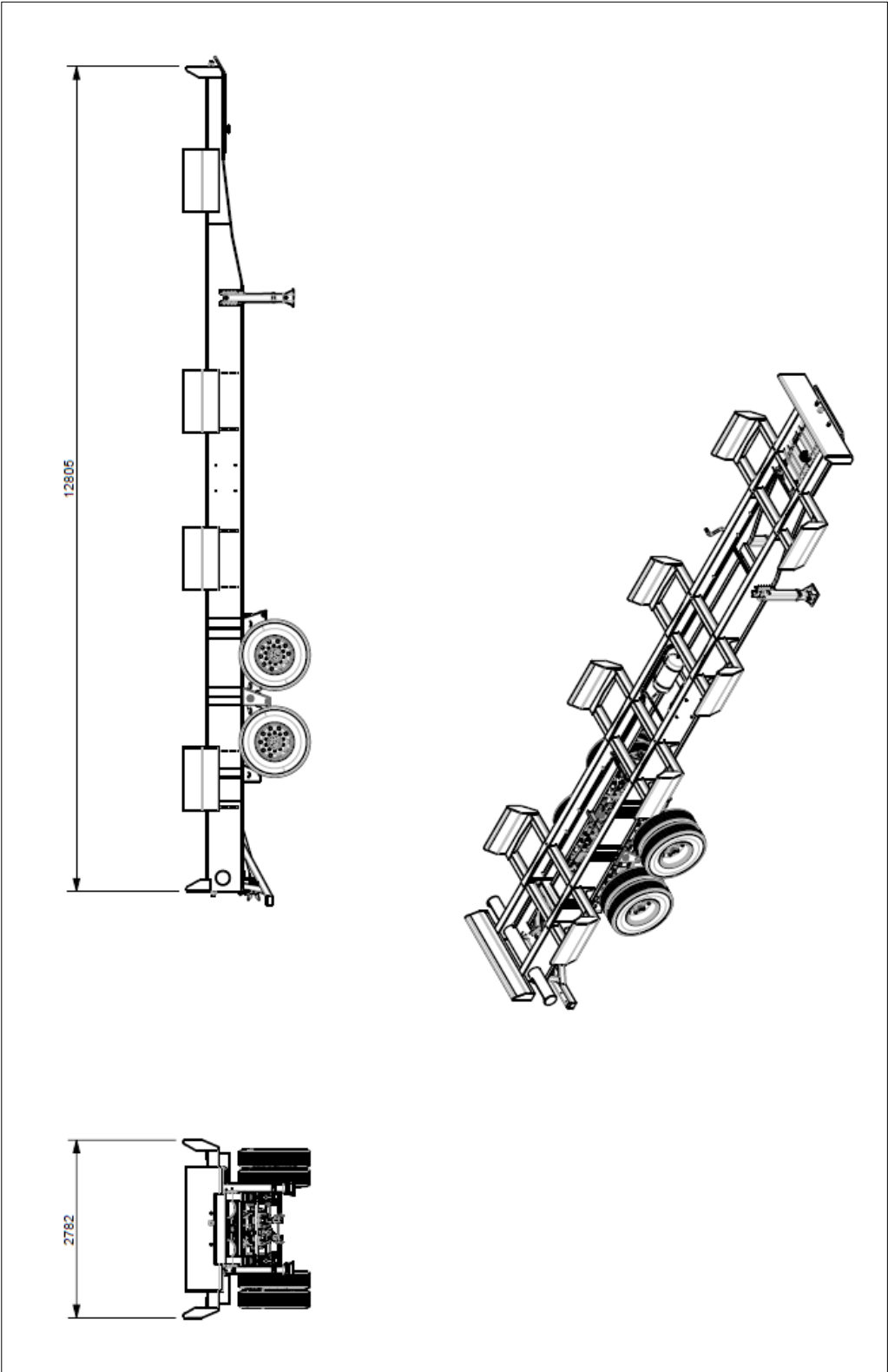


Figure A.2: Semi-trailer assembly

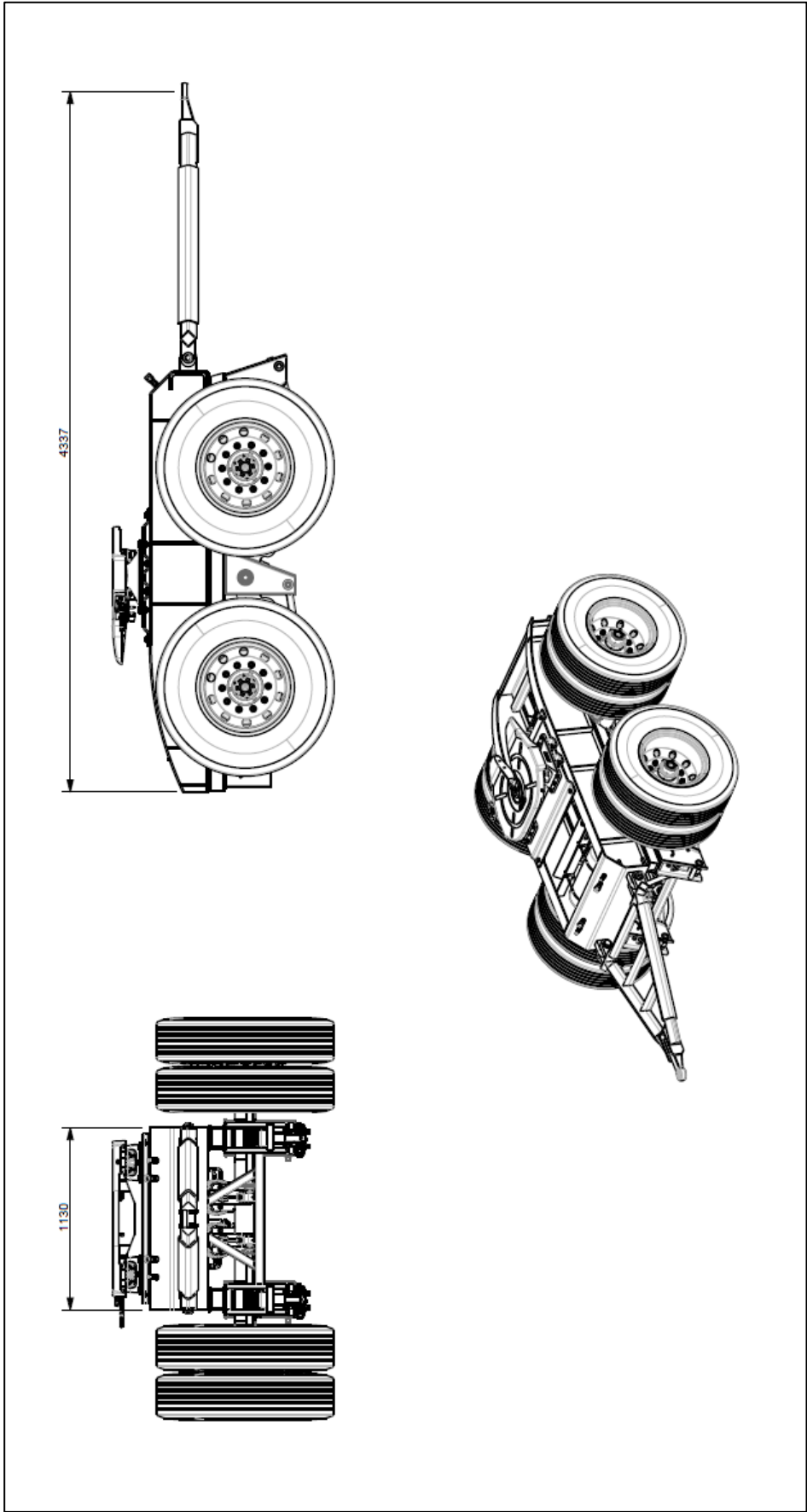


Figure A.3: Converter dolly assembly

Appendix B - Tractive Effort Calculations

For the Kalmar TR626i tractor:

Maximum engine torque (Volvo TAD1360VE Stage 3B) = 1740 Nm

Total speed reduction at wheels due to gearbox and differential = 109.386

Maximum theoretical wheel torque = $1740 \times 109.386 = 190.33 \text{ kNm}$

Wheel radius = 535 mm

Maximum theoretical wheel tractive effort = $190.33/0.535 = 355.76 \text{ kN}$

Transmission efficiency = 0.9

Axle efficiency = 0.87

Maximum wheel tractive effort considering losses = $355.76 \times 0.9 \times 0.87 = 278.56 \text{ kN}$

Maximum coupler force on the leading semi-trailer's kingpin:

$$F_{\text{tractive}} = (m_{\text{mts+tractor}}) (a_{\text{system}})$$

$$278560 = (14000+156370) (a_{\text{system}})$$

$$F_{\text{kingpin}} = m_{\text{mts}} \cdot a_{\text{system}} = 156370 (a_{\text{system}}) = 256 \text{ kN}$$

Maximum coupler force on the converter dolly towing eye:

$$F_{\text{towing eye}} = (m_{\text{semi-trailer+converter dolly}}) (a_{\text{system}})$$

$$F_{\text{towing eye}} = (743948) (256000/156370) = 120 \text{ kN}$$

NOTE: Rolling resistance of the wheels were neglected due to it being much smaller in magnitude than the other forces on the system.

Appendix C – Critical Weld & D-Value Calculations

Note: All weld calculations assume zero-to-maximum cyclic loading.

C.1.1) Fillet welds joining the skid plate to the underneath of the lower flanges:

Force on weld: $F_{max} = 250 \text{ kN}$

Area of the weld bead: $A_{weld} = 1.414hd = 1.67h \text{ m}^2$

Fatigue shear stress concentration factor: $K_{fs} = 2.7$

$$\tau_{max} = \frac{F_{max} \cdot K_{fs}}{A_{weld}} = 404.19h^{-1} \times 10^3 \text{ Pa}$$

$$\tau_{mean} = \tau_{alternating} = \tau_{max} / 2 = 202.09h^{-1} \times 10^3 \text{ Pa}$$

Using ER70S-6 welding wire, the limiting strength of the weld is based on the parent material properties since S355 steel has a lower yield and ultimate tensile strength.

$$S_y = 355 \text{ MPa}$$

$$S_u = 510 \text{ MPa}$$

Ultimate shear strength: $S_{us} = 0.65S_u = 306 \text{ MPa}$

Endurance limit in shear: $S_{se} = 87.13 \text{ MPa}$

Using Goodman's equation for fatigue:

$$\tau_{alternating} = \frac{S_a}{RF} \left[1 - \frac{\tau_{mean} \cdot RF}{S_{us}} \right]; \text{ for infinite life: } RF = 1 \text{ and } S_a = S_{se}$$

Using data above, $h = 2.97 \text{ mm}$ for infinite life. For manufacturing purposes, $h \geq 5 \text{ mm}$

C.1.2) Fillet welds connecting the channels to the towing hitch plate:

Force on weld: $F_{max} = \frac{120}{2} = 60 \text{ kN}$

Area of the weld bead: $A_{weld} = 0.707hd = 0.1414h \text{ m}^2$

$$\sigma_{max} = \frac{F_{max}}{A_{weld}} = 424.32h^{-1} \times 10^3 \text{ Pa}$$

$$\sigma_{mean} = \sigma_{alternating} = \sigma_{max} / 2 = 202.09h^{-1} \times 10^3 \text{ Pa}$$

Endurance limit: $S_e = 145 \text{ MPa}$

Ultimate tensile strength: $S_u = 510 \text{ MPa}$

Using Goodman's equation for fatigue:

$$\sigma_{alternating} = \frac{S_a}{RF} \left[1 - \frac{\sigma_{mean} \cdot RF}{S_u} \right]; \text{ for infinite life: } RF = 1 \text{ and } S_a = S_e$$

Using data above, $h = 1.87 \text{ mm}$ for infinite life. For manufacturing purposes, $h \geq 5 \text{ mm}$

C.1.3) Fillet weld connecting the towing eye to the drawbar

$$\text{Force on weld: } F_{max} = \frac{120}{2} = 60 \text{ kN}$$

$$\text{Area of the weld bead: } A_{weld} = 1.414hd = 0.309h \text{ m}^2$$

$$\text{Fatigue shear stress concentration factor: } K_{fs} = 2.7$$

$$\tau_{max} = \frac{F_{max} \cdot K_{fs}}{A_{weld}} = 524.27h^{-1} \times 10^3 \text{ Pa}$$

$$\tau_{mean} = \tau_{alternating} = \tau_{max} / 2 = 262.135h^{-1} \times 10^3 \text{ Pa}$$

$$S_y = 355 \text{ MPa}$$

$$S_u = 510 \text{ MPa}$$

$$\text{Ultimate shear strength: } S_{us} = 0.65S_u = 306 \text{ MPa}$$

$$\text{Endurance limit in shear: } S_{se} = 87.13 \text{ MPa}$$

Using Goodman's equation for fatigue:

$$\tau_{alternating} = \frac{S_a}{RF} \left[1 - \frac{\tau_{mean} \cdot RF}{S_{us}} \right]; \text{ for infinite life: } RF = 1 \text{ and } S_a = S_{se}$$

Using data above, $h = 3.86 \text{ mm}$ for infinite life. For manufacturing purposes, $h \geq 5 \text{ mm}$

C.2.1) Kingpin D-value

$$D = 0.5g \frac{(B+U_T)(T+0.08B)}{T+B-U_T}$$

$$= 0.5(9.81) \frac{(117275+25198)(39198+0.08(117275))}{39198+117275-25198} = 225.97 \text{ kN}$$

C.2.2) Towing hitch / Towing eye D-Value

$$D = 0.65g \frac{(T+R_{1b})(C_d+R_{2b})}{(T+R_{1b})+(C_d+R_{2b})}$$

$$= 0.65(9.81) \frac{(39198+43674)(43737+29864)}{(39198+43674)+(43737+29864)} = 248.56 \text{ kN}$$

C.2.3) Fifth wheel D-value

$$D = 0.5g \frac{(T+R_{1b}+W_d)(U_d+R_{2b}+0.08(T+R_{1b}+W_d))}{T+R_{1b}+W_d+R_{2b}}$$

$$= 0.5(9.81) \frac{(87497)(68977+0.08(87497))}{87497+68977-25239} = 248.47 \text{ kN}$$

Appendix D – MTS Coupling Specifications

D.1) Semi-trailer kingpin (KZ 1116)

Order No. King pin, complete	D value (kN)	Dimensions (mm)							Approval EC	Starting torque Nm
		A	B	C	D	E	F	G		
KZ 1108		8	52							
KZ 1110	152	10	50	∅ 100	∅ 115	84	2"	219	e1 00-0146	1200
KZ 1112		12	48							
KZ 1116	260	16	80	∅ 140	∅ 160	74	3 1/2"	228	e1 00-0151	1500
KZ 1120	300	20	76	∅ 160	∅ 180	74	3 1/2"	228	-	1500

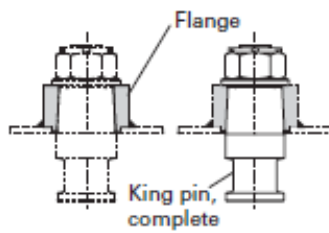


Figure D.1: KZ 1116 specifications [104]

D.2) Semi-trailer towing hitch (RO 50 Flex)

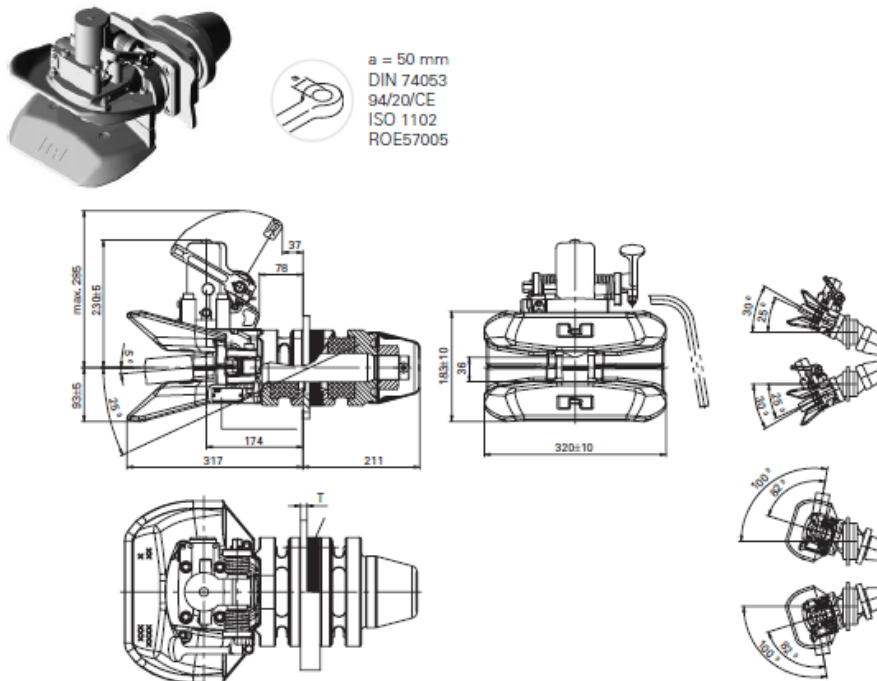


Figure D.2: RO 50 flex specifications [104]

D.3) Towing eye

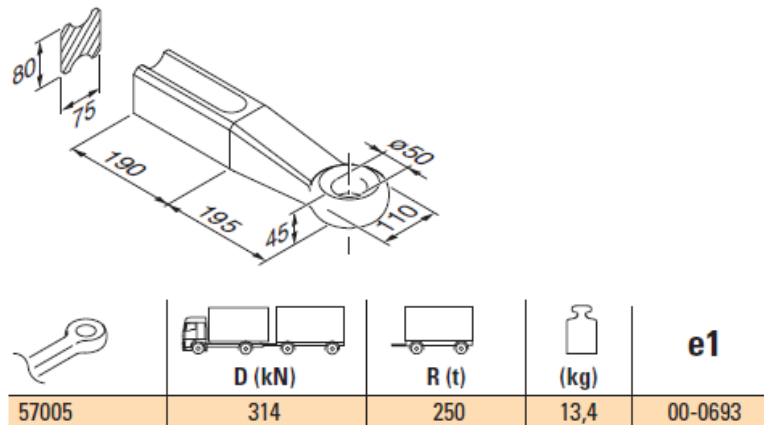


Figure D.3: Converter dolly towing eye specifications [104]

D.4) Fifth wheel

Technical Specification

Rubber bearing, hole pattern as per ISO 3842. JOST heavy duty fifth wheel couplings comply with dimensions as per DIN 74081 or DIN 74084, for plate mounting with hole patterns as per DIN 74081, 74084 and ISO 3842. Suitable for 2" king pins (50) as per DIN 74080, ISO 337 or 3 1/2" king pins (90) as per DIN 74083, ISO 4086 and steering wedges as per DIN 74085 or 94/20/EC. Fitted on a mounting plate.

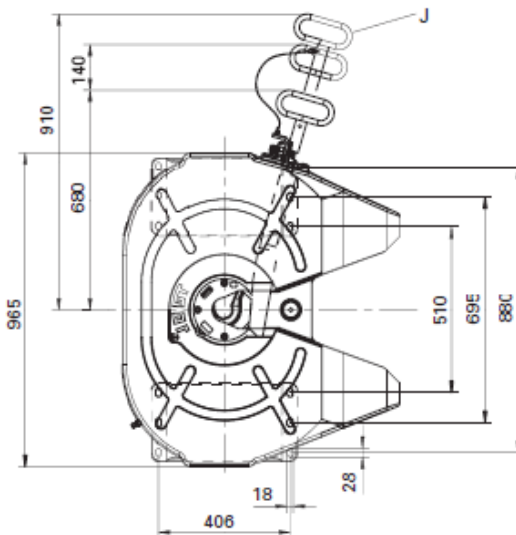
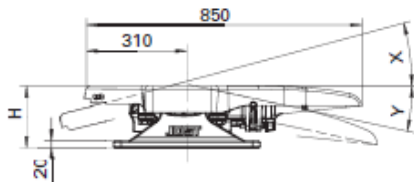


Figure D.4: JSK 36C fifth wheel specifications [104]

Appendix E - Cost Breakdown

Table C.1: New and existing semi-trailer product material cost breakdown

New Semi-trailer					
	Chassis	R 22 823.61	per ton	4.326	R 98 734.94
	Total				R 98 734.94
Auxillary Systems					
				Quantity	
	Kingpin	R 7 670.00	each	1	R 7 670.00
	Landing gear	R 13 540.00	per pair	1	R 13 540.00
	Hitch	R 10 477.00	each	1	R 10 477.00
	Bogie	R 128 302.00	each	1	R 128 302.00
	Tyre&Rims	R 10 573.00	each	8	R 84 584.00
	Total				R 244 573.00
Steel items fabrication cost					
	% of steel cost	R 98 734.94	total	50%	R 49 367.47
Product Material Cost					
	Total				R 392 675.41
Existing Semi-trailer					
	Chassis	R 22 823.61	per ton	6.67	R 152 233.48
	Total				R 152 233.48
Auxillary Systems					
	Kingpin	R 7 670.00	each	1	R 7 670.00
	Hitch	R 10 477.00	each	1	R 10 477.00
	Bogie	R 128 302.00	each	1	R 128 302.00
	Tyre&Rims	R 10 325.00	each	8	R 82 600.00
	Total				R 229 049.00
Steel items fabrication cost					
	% of steel cost	R 152 233.48	total	50%	R 76 116.74
Product Material Cost					
	Total				R 457 399.22

Table C.2: Converter dolly product material cost breakdown

Converter Dolly					
	Chassis	R 22 823.61	per ton	1.045	R 23 850.67
	Total				R 23 850.67
Auxillary Systems					
	Bogie	R 128 302.00	each	1	R 128 302.00
	Tyre&Rims	R 10 573.00	each	8	R 84 584.00
	Fifth wheel + Plate	R 21 912.00	each	1	R 21 912.00
	Towing eye	R 1 376.00	each	1	R 1 376.00
	Total				R 236 174.00
Steel items fabrication cost					
	% of steel cost	R 65 994.00	total	50%	R 32 997.00
Product Material Cost					
	Total				R 293 021.67